MEASUREMENT OF BIOACTIVE TRACE-METALS (Cu AND Zn) IN THE SOUTHERN OCEAN

VALIDATION OF SAMPLING PROTOCOL AND ICP-MS BASED ANALYTICAL METHOD

by

Ryan Cloete

Submitted in fulfillment of the degree of Master of Earth Science

Faculty of Science

Stellenbosch University

Supervisor: Prof. Alakendra N. Roychoudhury

March 2017

Declaration

By submitting this thesis electronically, I declare that the entirety of the work contained therein is my own, original work, that I am the sole author thereof (save to the extent explicitly otherwise stated), that the reproduction and publication thereof by Stellenbosch University will not infringe any third party rights and that I have not previously in its entirety or in part submitted it for obtaining any qualification.

March 2017

Full name:

Signed……

Acknowledgements

I would like to express my most sincere gratitude to my project supervisor, Prof. Alakendra Roychoudhury, for giving me the opportunity to undertake such a project as well as his continuous patience and guidance throughout. To Dr. Susanne Fietz for her mentorship throughout my undergraduate and postgraduate studies as well as her amazing organisational skills ultimately enabling a successful expedition. I would also like to extend my thanks to the members of the Stellenbosch/CSIR SANAE 54 team, in particularly Dr. Thato Mtshali and Dr. Raissa Phillibert, for their patience in teaching me the basics of biogeochemistry and trace metal sampling as well as their friendship. To Riana Rossouw from the CAF laboratory at Stellenbosch University for analysing all my trace metal data.

A massive thank you must be extended to some of my fellow class mates on the cruise. Gillian Trollope, Leigh-ann Palmer and Mari Scott for their essential roles played during the sample collection and sub-sampling process, often for extended periods of time at ungodly hours. To Johan Viljoen for access to phytoplankton community assemblage data from the cruise. To Jean Loock, my friend, housemate and lab partner, for his constant advice, laughs, input and discussion about all things science and non-science related. To the Captain and crew of the SA Agulhas II, thank you for your constant assistance throughout the cruise. Without you this project would not have been possible.

Finally, I would like to thank my parents and sister for their unwavering support throughout my academic career. The nature of this fieldwork meant that holidays, Christmases and birthdays were missed and your understanding in this regard is appreciated. Thank you for affording me the opportunity to pursue my interests.

Table of Contents

List of Abbreviations

Abbreviation	Meaning
AABW	Antarctic bottom water
AASW	Antarctic surface water
ACC	Antarctic circumpolar current
AP	Alkaline phosphatase
APF	Antarctic polar front
BGH	Bonus goodhope line
CA	Carbonic anhydrase
CAF	Central analytical facility
Chl-a	Chlorophyll-a
CI	Confidence interval
CTD	Conductivity, temperature, depth
DCu	Dissolved copper
DTM	Deep trace metal
DZn	Dissolved zinc
EDTriA	Ethylenediaminetriacetic
IDA	Iminodiacetic
HNLC	High nutrient low chlorophyll
ICP-MS	Inductively coupled mass spectrometry
LCDW	Lower circumpolar deepwater
LDPE	Low density polyethylene
LNLC	Low nutrient low chlorophyll
MLD	Mixed layer depth
NADW	North Atlantic deepwater
PFA	Perfluoroalkoxy alkane
PFZ	Polar frontal zone
QC	Quality control
RSD	Relative standard deviation
SAF	Sub-antarctic front
SANAE	South African National Antarctic Expedition
SASW	Sub-antarctic surface water
SAZ	Sub-antarctic zone
SBdY	Southern boundary
SD	Standard deviation
SES	Standard error of skewness
STF	Sub-tropical front
STZ	Sub-tropical zone
SU	Stellenbosch Univeristy
TM	Trace metal
UCDW	Upper circumpolar deepwater
UV	Ultra violet
WG	Weddell gyre

Abstract

A method comprising an improved seawater collection protocol and subsequent Inductively Coupled Plasma Mass Spectrometry (ICP-MS) based analytical technique was validated through an intercalibration exercise performed with the University of Plymouth (UK), multiple cross-over stations and analyses of certified reference materials (SAFe, GEOTRACES and NASS-5). The commercially available seaFAST-pico preconcentration module was employed for the simultaneous extraction of a suite of trace metals (Mn, Fe, Ni, Cu, Zn, Co, Cd and Pb) from their seawater matrix prior to ICP-MS analysis. Extremely low detection limits (< 0.228 nmol/kg) combined with low blank values ensured quantitive recovery on ICP-MS and minimal interferences arising from alkali and alkaline earth metals (Na, K, Mg and Ca) present in the saline matrix. The results of the certified reference materials were in excellent agreement with their corresponding consensus values and validated the methods precision and accuracy. During ICP-MS analysis, repeatability and reproducibility were monitored through analysis of an internal Stellenbosch University (SU) TM4 control and various commercially available quality controls, the results of which further confirmed a high level of precision. The distribution of Dissolved Copper (DCu) and Dissolved Zinc (DZn) was investigated in the Atlantic sector of the Southern Ocean. DCu displayed typical nutrient type behaviour reflected by sub-nanomolar surface concentrations increasing steadily until maximum observed concentrations of 2 – 3 nmol/kg in the Antarctic Bottom Waters (AABW). DZn concentrations ranged between approximately 1 and 12 nmol/kg and exhibited characteristic nutrient-type behaviour although intermediate and deepwater distributions were more conservative compared to DCu. Local subsurface minima coincided with elevated levels of chlorophyll-a (chl-a) indicating biological utilisation by phytoplankton in the euphotic zone. Remineralisation of sinking organic matter, predominantly diatom frustules, from Antarctic Surface Water (AASW) resulted in deeper sub-surface maxima for DZn. The dominant supply of trace metals to surface waters south of the Antarctic Polar Front (APF) was advective upwelling of nutrient rich Upper Circumpolar Deep Water (UCDW) and AABW. Atmospheric inputs and melting ice accounted for minor surface influxes where there was a poor DCu/salinity correlation. Both trace elements displayed significant correlations with the macronutrient silica, evidence of their role in the biological cycle. An overall Cu:Si relationship of Cu (nM) = 0.011 Si (µM) + 0.851 (R^2 = 0.85, n=98) was obtained for this study while the corresponding Zn:Si relationship was Zn (nM) = 0.043 Si (µM) + 1.021 (R^2 = 0.80, n=98). The APF exerted a strong control over nutrient distributions separating low nutrient low

chlorophyll (LNLC) subtropical waters to the north from high nutrient low chlororphyll (HNLC) waters to the south.

Keywords: Southern Ocean, Dissolved Copper, Dissolved Zinc, GEOTRACES, seaFAST, ICP-MS

Opsomming

'N Metode wat bestaan uit 'n verbeterde seewater versameling protokol en die daaropvolgende Inductively Coupled Plasma Mass Spectrometry (ICP-MS) gebaseer analitiese tegniek is bekragtig deur 'n onderlinge oefening uitgevoer met die Universiteit van Plymouth (UK), verskeie 'cross-over' stasies en ontleding van gesertifiseerde verwysingsmateriaal (SAFe, GEOTRACES en NASS-5). Die kommersieel beskikbare seaFAST-pico preconcentration module is aangewend vir die gelyktydige onttrekking van 'n versameling van spoor metale (Mn, Fe, Ni, Cu, Zn, Co, Cd en Pb) van hul seewater matriks voor ICP-MS analise. Uiters lae opsporings perke (<0,228 nmol / kg) gekombineer met 'n lae leegwaardes verseker kwantitatiewe herstel op ICP-MS en minimale inmenging wat voortspruit uit alkalie en alkalie-aard metale (Na, K, Mg en Ca) teenwoordig is in die sout matriks. Die resultate van die gesertifiseerde verwysingsmateriaal was in 'n uitstekende ooreenkoms met hul ooreenstemmende konsensuswaardes en bekragtig die presisie en akkuraatheid van die metodes. Tydens ICP-MS analise, herhaalbaarheid en reproduseerbaarheid is gemonitor deur analise van 'n interne Universiteit Stellenbosch (US) TM4- beheer en verskeie kommersieel beskikbare kwaliteit beheer, die resultate waarvan 'n hoë vlak van akkuraatheid verder bevestig. Die verspreiding van opgeloste Koper (DCu) en opgeloste Zinc (DZn) is ondersoek in die Atlantiese sektor van die Suidelike Yssee. DCu vertoon tipiese tipe voedingstofagtige gedrag weerspieël deur sub-nanomolar oppervlak konsentrasies steeds toenemende tot maksimum waargenome konsentrasies van 2 - 3 nmol / kg in die Antarctic Bottom Waters (AABW). DZn konsentrasies wissel tussen ongeveer 1 en 12 nmol / kg en vertoon voedingstofagtige gedrag hoewel intermediêre- en diepwaterverspreidings meer konserwatief in vergelyking met DCu was. Plaaslike ondergrondse minima saamgeval met verhoogde vlakke van chlorofil-a (Chl-a) dui biologiese benutting deur fitoplankton in die euphotic sone aan. Remineralisasering van sink organiese materiaal, hoofsaaklik diatom frustules van Antarctic Surface Water (AASW) tot gevolg gehad vir 'n dieper sub-oppervlak maksima vir DZn. Die dominante verskaffing van spoor metale om water oppervlak suid van die Antarctic Polar Front (APF) was advektiewe opwelling van voedingstofryke Upper Circumpolar Deep Water (UCDW) en AABW. Atmosferiese insette en smeltingsys is verantwoordelik vir klein oppervlak strome waar daar was 'n swak DCu / soutgehalte korrelasie. Beide spoorelemente vertoon beduidende korrelasies met die makro-silika, bewyse van hul rol in die biologiese siklus. 'N Algehele Cu:Si verhouding van Cu (nM) = 0,011 Si (µm) + 0,851 (R^2 = 0.85, n = 98) is verkry vir hierdie studie, terwyl die ooreenstemmende Zn: Si verhouding was Zn (nM) = 0,043 Si (µM) + 1,021 (R^2 = 0.80, n = 98). Die APF oefen sterk beheer uit oor voedingstof

verspreiding wat low nutrient low chlorophyll (LNLC) subtropiese waters in die noorde skei high nutrient low chlorophyll (HNLC) water na die suide.

Trefwoorde: Suidelike Yssee, opgeloste Koper, opgeloste Zinc, GEOTRACES, seaFAST, ICP-MS

1. Introduction

1.1. Overview

Despite its relatively small size compared to oceans such as the Pacific and Atlantic, the Southern Ocean has been identified as playing a key role in the global carbon cycle due to unique features involving both physical circulation and biological processes. Oceans represent the largest sink of carbon dioxide (CO_2) on Earth by facilitating the downward movement of this greenhouse gas from the atmosphere to the deep ocean via a combination of processes or 'pumps' including the biological pump. The efficiency with which the biological pump operates is dependent, amongst other factors, on the availability of the macronutrients silicic acid ($Si(OH)_4$), nitrate (NO_3^-) and phosphate (PO_4^{3-}) as well as a suite of micronutrients or trace metals (e.g., Fe, Cu, Zn, Mn, Cd, Co, Al, Ni and Pb). The Southern Ocean's uniqueness stems from its high nutrient low chlorophyll (HNLC) status whereby the incomplete utilisation of nutrients by phytoplankton allows the concentration of CO_2 in the atmosphere to be substantially greater than would be the case if nutrients were completely utilised (Le Moigne *et al.*, 2013). A knowledge of the distribution of trace metals will aid in constraining their poorly understood biogeochemical cycles and ultimately yield insights into the underlying reasons behind regions of low primary productivity in the Southern Ocean.

1.2. The Biological Pump

The ability of atmospheric CO_2 to dissolve into ocean surface waters enables the three carbon pumps, namely the biological, solubility (physical) and carbonate pumps, to transfer carbon into the deep ocean. The solubility pump is based on differences in water mass densities resulting in downwelling of surface waters rich in sequestered CO_2 (Reid *et al.*, 2010); whereas the carbonate pump covers the production and dissolution of marine organisms with body parts made up of inorganic calcium carbonate ($CaCO_3$) (Reid *et al.*, 2010). The biological pump is of particular importance in this project due to the involvement of photosynthetic phytoplankton, which convert CO_2 into glucose and oxygen in the presence of light, and transfer the organic carbon to the deep ocean, where it is stored for centuries, primarily via dead organisms, faecal material and carbonate skeletons. This cycling is illustrated in Figure 1. Dissolved bioactive trace metals (particle size < 0.2 µm), such as Cu and Zn, play an important role in catalysing this process by serving as active centres in the enzymes essential for metabolism. The extended Redfield ratio describes the proportions with which phytoplankton utilise major nutrients and is defined as 180C: 23N:

1P: $5x10^{-3}$Fe: $2x10^{-3}$Zn: $1x10^{-3}$Mn: $5x10^{-4}$Ni: $4x10^{-4}$Cd: $2x10^{-4}$Cu: $4x10^{-5}$Co. The efficiency of the biological pump is expressed in terms of export production or the rate at which particulate organic carbon sinks below the base of the euphotic zone (Williams and Follows, 2011). The euphotic zone is loosely defined as the sunlit layer of the surface ocean where primary production takes place. Inputs of dissolved trace metals to the euphotic zone can be supplied through multiple pathways including atmospheric dry and wet deposition, riverine inputs, continental erosion and melting of ice sheets in the polar latitudes (Croot, Baars and Streu, 2011; Klunder *et al.*, 2011; Heller and Croot, 2014). Additional processes such as remineralisation of decaying organic matter, upwelling of nutrient rich deepwaters and inputs from hydrothermal activity serve to increase deepwater trace metal concentrations and can replenish surface inventories (Figure 1). The result of the biological pump is a surface nutrient depletion and subsequent deep water regeneration. This is typical 'nutrient like' behaviour and was the basis upon which scientists concluded the involvement of trace metals in the marine biogeochemical cycle (Frew *et al.*, 2001).

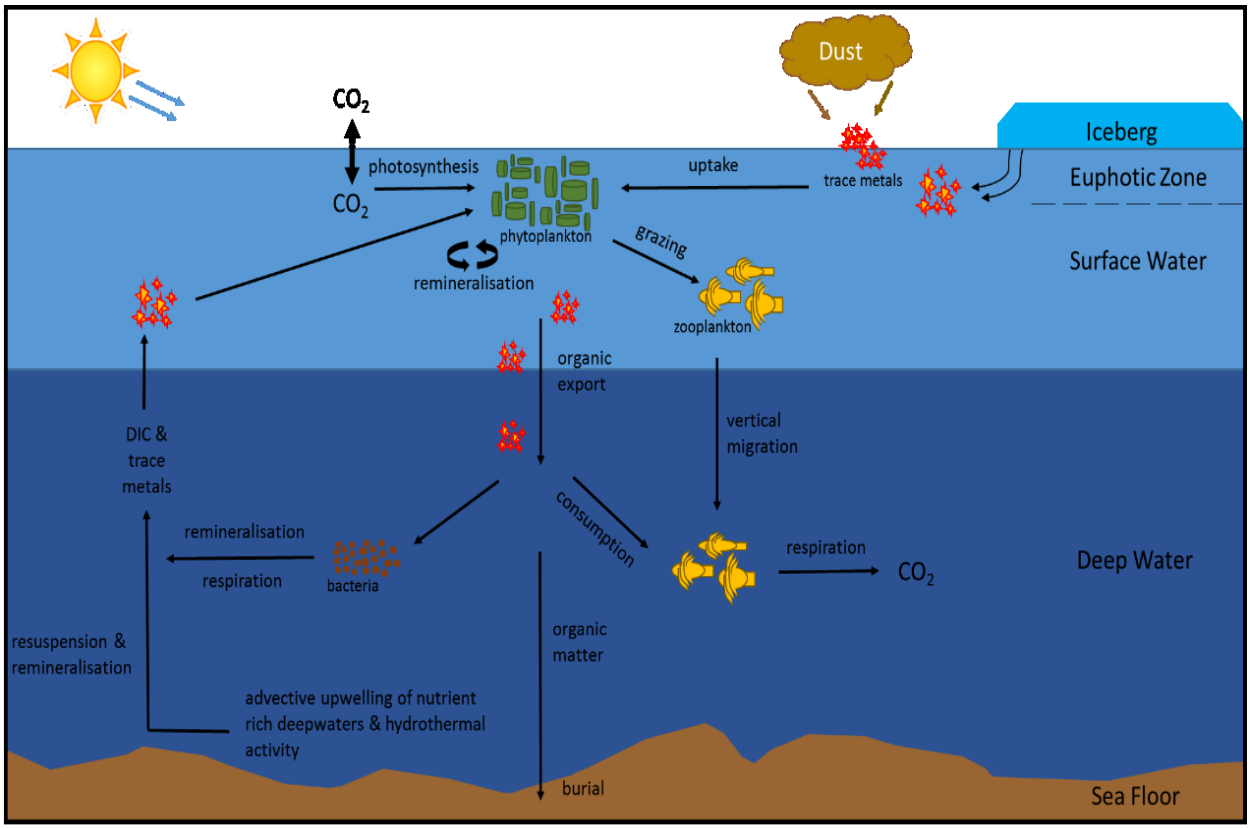

Figure 1 –schematic illustrating the biological carbon pump and cycling of trace metals in the Southern Ocean.

1.3. The Southern Ocean

The Southern Ocean plays a critical role in driving, modifying and regulating global climate change thanks largely to a combination of cold deep water masses and the presence of the world's largest ocean current, the Antarctic Circumpolar Current (ACC), redistributing heat, salt and CO_2. In addition to currents, frontal systems exert a strong control in dividing the Southern Ocean into distinct biogeochemical domains. The Antarctic Polar Front (APF), whose position varies around 50°S (Bown *et al.*, 2011), best exemplifies this control by serving as the boundary between low nutrient low chlorophyll (LNLC)/ oligotrophic subtropical waters to the north and HNLC waters to the south (Hassler *et al.*, 2012). Spring phytoplankton blooms result in near zero surface nutrient concentrations north of the APF which are then replenished by deep mixing and upwelling during the winter. South of the APF, the presence of ample macronutrients yet low phytoplankton abundance is evidence that macronutrients are incompletely utilised by phytoplankton therefore reducing the efficiency of the biological pump. This incomplete utilisation of macronutrients has been suggested to be due to trace metal limitation, with particular emphasis on Fe, while the effect of light limitation in waters with deep surface mixed layers has also been cited (Klunder *et al.*, 2011). The Southern Ocean has been suggested as a major potential source for increasing the biological removal of carbon and therefore lowering atmospheric pCO_2 levels (Popova, Ryabchenko and Fasham, 2000). The Southern Ocean Iron Release Experiment (SOIREE) demonstrated that by fertilizing a 50km^2 site in the Southern Ocean with Fe, a corresponding decrease in pCO_2 was observed (Frew *et al.*, 2001).

The drawdown of CO_2 is also heavily dependent on the resident phytoplankton community structure. Variations in biological requirements, sinking rates and coping strategies link the carbon cycle with other biogeochemical cycles including those of macronutrients and bioactive trace metals. The HNLC waters of the Southern Ocean typically sees flagellates dominating the pico- and nano-plankton size class whereas the micro-plankton class is comprised predominantly of large, heavily silicified diatoms (Smetacek *et al.*, 1997; Gibberd *et al.*, 2013). Episodic algal blooms in this region, due to localised inputs of dissolved trace metals, have been seen to be associated with diatoms and haptophytes which have high nutrient requirements and growth rates (Arrigo, 1999).

Research by (Brand, Sunda and Guillard, 1986; Sunda, 1991; Saito and Moffett, 2002; Croot, Baars and Streu, 2011; Heller and Croot, 2014) has begun to reveal the exact functions of certain trace metals in algal physiology. Cu serves as a carrier for both photosynthetic and mitochondrial electron transport via the enzymes Plastocyanin and Cytochrome c oxidase respectively (Heller & Croot 2014). Despite being a requirement for phytoplankton reproduction, Cu is considered toxic if its free ion concentration ($[Cu^{2+}_f]$) exceeds species specific thresholds. Cyanobacteria are the most sensitive to Cu toxicity showing reduced growth rates when exposed to $[Cu^{2+}_f]$ > 1 pM, while other species such as coccolithophores and dinoflagellates exhibit intermediate sensitives while diatoms are the least sensitive to elevated $[Cu^{2+}_f]$ concentrations (Brand, Sunda and Guillard, 1986). Organic complexation of metals in seawater is an important determinant of their chemical and biological reactivity. This is particularly true for copper as organic complexation may lower Cu toxicity in phytoplankton (Moffett and Dupont, 2007). In seawater there are two classes of organic ligands, namely L1 and L2. L1 ligands are very strong and have conditional stability constants of $K=10^{12.5}\ M^{-1}$ while the L2 class represents weak ligands with a conditional stability constant range of $K=10^{10}$ to $10^{12}\ M^{-1}$ (Heller and Croot, 2014). Usually ligand concentrations exceed ambient Cu concentrations however in some regions their concentration is lower (Moffett and Ho, 1996). Under the initial condition, the organic complexation of Cu by L1 ligands serve to decrease $[Cu^{2+}_f]$ to below $1x10^{-12}$ M (1pM) in most open ocean waters. As mentioned previously, this value is important as $[Cu^{2+}_f]$ > 1pM results in copper becoming toxic and reducing phytoplankton reproduction rates. In the latter case the $[Cu^{2+}_f]$ increases as ligands are saturated with respect to Cu concentration and Cu is complexed by the L1 and weaker L2 ligand classes. It follows that the toxicity of Cu is dependent on $[Cu^{2+}_f]$ and not the total Cu concentration. Furthermore, increased $[Cu^{2+}_f]$ in seawater can inhibit the uptake of other essential trace metals such as Mn (Heller and Croot, 2014). On the other hand, $[Cu^{2+}_f] < 10^{-14}$M may limit Fe acquisition due to the involvement of copper oxidases in Fe uptake within phytoplankton cells (Coale and Bruland, 1990).

Zn is utilized for both nucleic acid transcription and repair proteins in the enzyme alkaline phosphate and for the uptake of CO_2 via the enzyme carbonic anhydrase (CA). The 'Zn hypothesis' was formulated by (F. M. M. Morel *et al.*, 1994) when studying processes that control carbon uptake by marine phytoplankton. The Zn hypothesis suggests that dissolved Zn concentrations in oceanic surface waters may be low enough to limit the growth rate of phytoplankton and ultimately limit the uptake of CO_2 via an absence of the enzyme CA. It is important to understand that trace metals are bio-limiting and that

reduced primary production cannot be solely attributed to one element. The extent to which Zn limitation affects primary production has however been shown to be minimal with only small changes in the composition of the phytoplankton community observed. In the Sub-Antarctic zone, additions of Zn to surface waters resulted in a shift in the diatom community composition from large colonial pennate (*Pseudonitzchia sp*.) to smaller less silicified pennate (*Cylindrotheca closterium*) (Croot, Baars and Streu, 2011). Like Cu, Zn is toxic to phytoplankton and bacteria at high concentrations. The complexation of Zn by organic ligands, which acts to lower the free metal concentration of Zn, is therefore very important in identifying the toxicity of Zn to primary producers. Another important consequence of Zn distribution is the control it exerts on the uptake mechanism of other trace metals. Culture experiments have indicated that there are two transport systems of Cd in marine diatoms, a low-zinc induced system and a Mn-uptake system at high zinc concentrations (Boye *et al.*, 2012). This highlights the delicate interplay between trace metal biogeochemical cycling.

1.4. Analytical Methods

One of the primary difficulties associated with trace metal research in the marine environment is the contamination of samples throughout the collection, filtration, storage, preconcentration and analysis stages. Due to the extremely low trace metal concentrations being dealt with and the ubiquitous presence of metals during all stages of research, results are extremely susceptible to the unwanted external introduction of contaminants rendering results unreliable (Achterberg and Braungardt, 1999). It wasn't until the late 1970's that scientists discovered that trace metals are present in seawater at much lower concentrations than previously believed (Bruland *et al.*, 1979). This was most likely the result of improper techniques which failed to isolate the sample from contamination. As a result, a resurgence in the field of trace metal geo-chemistry was sparked with research focused on developing new methods with which to accurately quantify trace metal concentrations. Furthermore, justifying trace metal concentration datasets is very difficult due to the dynamic nature of oceanic water masses and differences in the sample collection period. In order to overcome this challenge, international collaborations such as the international GEOTRACES program, have been launched. In addition to better understanding the processes controlling the distribution of trace metals in the marine environment, these programs distribute reference samples to laboratories globally in order to compile consensus values. Comparison of the reference standard results and the consensus values for these reference standards renders a much better method of assessing the accuracy of the experimental setup.

Numerous methods are employed to detect dissolved trace metals in seawater. The analysis of trace metals in seawater differs from the analysis of fresh water samples in that seawater requires a pre-treatment step in order to elevate trace metal concentrations above analytical detection limits whereas freshwater samples contain much higher trace metal concentrations. Open ocean seawater samples are characterised by low trace metal concentrations and high salinity concentrations. This makes direct sample injection impractical as salt precipitation and deposition decreases the flow rate through the ICP-MS machine and causes interference with the analyte signal through the formation of isobaric interferences (Milne *et al.*, 2010). Pre-treatment is therefore necessary to remove the high salinity matrix. This is achieved by either dilution of the sample or by employing a preconcentration step which involves the separation and extraction of trace metals from the major ions and dissolved organic matter. Dilution is not recommended as the saline matrix (composed of elements such as Na, K, Mg and Ca) contributes to instrumental drift and sensitivity decreases due to ionization suppression even after several dilutions of the sample (Rahmi *et al.*, 2007; Jerez Veguería *et al.*, 2013). Instruments employed in the detection of trace metals have evolved to include Inductively Coupled Plasma Atomic Emission Spectroscopy (ICP-AES) (Mclaren *et al.*, 1985), Inductively Coupled Plasma Mass Spectrometry (ICP-MS) (Biller and Bruland, 2012), Graphite Furnace Atomic Absorption Spectrometry (GFAAS) (Kingston *et al.*, 1978) with lesser employed chemiluminescence, spectrophotometric colorimetry and adsorptive Cathodic Stripping Voltammetry (CSV) methods (Saito and Moffett, 2001). The major disadvantage of technique such as CSV, Flow Injection analysis (FIA) and GFAAS is the restriction to single element analysis at a time (Achterberg and Braungardt, 1999)

Recently, preconcentration - both online and offline - using chelating resins coupled with a subsequent ICP-MS detection step have proven to be an extremely accurate technique for multi-element analysis over a wide range of seawater concentrations. The chelating resin is very important as it contains functional groups which are directly responsible for separating the metal ions from the seawater matrix. This is the most critical step in the quantification process. Multiple chelating resins, each containing various functional groups, are in use by scientists worldwide. Some of these resins, such as the silica-immobilized 8-hydroxyquinoline (8-HQ) must be synthesized from scratch and are therefore not commercially available making it undesirable (Mclaren *et al.*, 1985). Resins containing the Nitriloacetate (NTA)-type chelating resin beads have proven effective however isotope dilution was necessary to

account for non-quantitive recovery (Lee *et al.*, 2011). Furthermore, the method was a single element determination method. The Toyopearl AF-Chelate-650M (Milne *et al.*, 2010) and Dionex MetPac CC-1 (Ho *et al.*, 2010) resins are commercially available chelating resins containing an iminodiacetic acid (IDA) functional group and has been successfully used in the offline preconcentration of seawater samples prior to quantification of a suite of trace metals, similar to those quantified in this study, by ICP-MS. Studies using a chelating resin containing both ethylenediaminetriacetic acid (EDTriA) and IDA functional groups, such as the resin used for this study, have demonstrated the resins excellent affinity to trace metal ions (Sohrin *et al.*, 2008).(Biller and Bruland, 2012) present an offline preconcentration procedure similar to the one presented in this study. It must be noted that ultra-violet (UV)-oxidation was determined necessary in order to calculate the total dissolved concentrations of Cu and Co. Organic molecules in seawater have an affinity to bond with metals making them immune to the chelating resin therefore passing through the system without being extracted.

1.5. Aims and Objectives

The knowledge of the spatial distribution, speciation and role of bioactive trace metals in the Southern Ocean is ever increasing. Improvements in sample collection and analytical techniques have enabled the creation of a more complete database. This project served the dual purpose of method development for the collection and analyses of trace metal samples, together with constraining the controls of bioactive trace metals on phytoplankton productivity. The objectives are as follows:

Objective one: Assess the effectiveness of employing vertical profile sampling using GEOTRACES CTD, GO-FLO bottles and clean lab, in collecting contamination free seawater samples.

Objective two: Validate a preconcentration coupled ICP-MS trace metal quantification technique through an intercalibration effort and analysis of certified reference standards according to GEOTRACES requirements.

Objective three: To determine the trace metal concentrations, specifically Cu and Zn, at various locations along the Good Hope Line in the Southern Ocean during the austral summer.

- Hypothesis 1: Copper exhibits properties of nutrient type behaviour.
- Hypothesis 2: Zinc exhibits properties of nutrient type behaviour.

Objective four: Report on the biological factors controlling the distribution of Cu and Zn in the Southern Ocean.

1.6. Thesis Structure

In this thesis, the process involving the collection and analysis of seawater samples is described in chapter 2, the results for an in-lab validation process for the measurement of trace metals using reference standards, a joint intercalibration exercise with the University of Plymouth (UK) and use of a cross-over station as per GEOTRACES protocol is outlined in chapter 3 and finally, the distribution of the trace metals copper and zinc in the Southern Ocean, has been presented and discussed in its entirety with connections to numerous oceanographic parameters in chapter 4. The dataset generated for the complete trace metal suite along with protocols for cleaning of equipment and sub-sampling procedures are included in the appendix (chapter 5). Collection of uncontaminated trace metals has proven extremely difficult in past attempts with several past cruises returning contaminated results. Thus, proving uncontaminated sample collection was possible, utilizing the method adapted from the GEOTRACES cookbook (Andersson *et al.*, 2014), would be a major milestone. Further, the development of a multi-elemental analysis method was needed for the accurate and precise quantification of trace metals. Presented in this study is a method that utilizes the seaFAST pico offline pre-concentration and matrix removal module coupled with modern, high resolution, magnetic sector inductively coupled plasma mass spectrometry (ICP-MS), as a tool in the simultaneous quantification of up to 10 trace metals. The development of the method is ongoing. The results of the GEOTRACES SAFe and NASS-5 standards are used as reference samples to provide evidence for accurate quantification. Moreover, it's understood that bioactive trace metals play a key role in the growth of marine plankton; illustrated by the control of marine phytoplankton on the distribution, speciation and bioavailability of these elements. The interaction between micronutrients Cu and Zn and phytoplankton will receive substantial discussion in this study; focusing on the spatial and temporal characteristics as well as their biogeochemical cycling.

2. Methodology

The purpose of this chapter is to describe the protocols and methods followed during the collection, pre-treatment and ICP-MS analysis of seawater for its trace metal concentrations. This method has subsequently been employed on multiple cruises and has ultimately aided in the creation of valuable trace metal datasets to the data-scarce Southern Ocean. This method has established South Africa as a key contributor to the global biogeochemistry community. In addition, the ability to conduct this research coupled with the geographic location of Cape Town harbour in relation to the Southern Ocean and Antarctica, makes our research group attractive for international collaborators.

2.1. Study area

Seawater samples were collected at multiple locations in the Southern Ocean along a transect known as the Bonus Goodhope Line (BGH) between Cape Town and Antarctica via the Zero Meridian (Figure 2). The voyage took place during the 2014/2015 austral summer (04/12/2014 – 17/02/2015) on-board the S.A. Agulhas II polar research vessel as part of the SANAE 54 voyage. The locations of the sampling stations were pre-determined to coincide with cross-over stations from previous expeditions as a means of comparison for a sample collection protocol under validation.

The transect crossed the Subtropical Zone (STZ), the Antarctic Circumpolar current (ACC) and entered the Weddell Gyre (WG). In addition, several fronts including the Sub-Tropical (STF), Sub-Antarctic (SAF) and Antarctic Polar Front (APF) were crossed. The presence of deep reaching frontal systems serve as the boundary between these distinct biogeochemical domains and directly influences the distribution of trace metals in the Southern Ocean. Having strategically located sampling stations is therefore crucial to quantifying these influences. Sampling stations were comprised of three Deep Trace Metal (DTM) and four Trace Metal (TM) stations. Up to 23 depths representing the whole water column were sampled at DTM stations whereas 15 depths to a maximum of 1000 metres was sampled at TM stations. A GO-FLO conditioning station was performed in the ACC on the downward leg of the expedition. DTM3 was chosen as an intercalibration station with the University of Plymouth.

2.2. Vertical profile sampling

A vertical profile sampling method was employed at all sampling stations. Seawater samples were collected using 24 internally Teflon-coated PVC 12 litre GO-FLO bottles (General Oceanics Inc.) modified

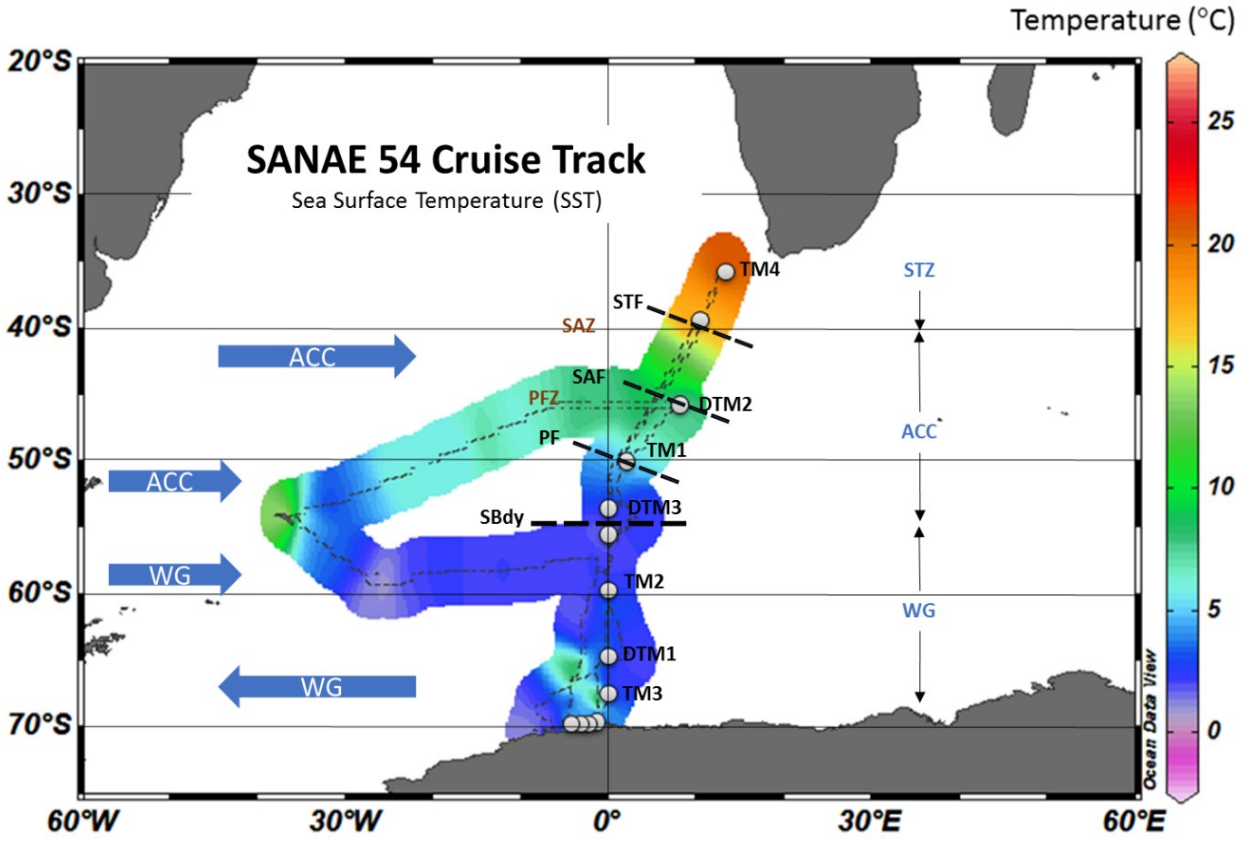

Figure 2 – SANAE 54 cruise track indicating locations of sample stations along the BGH Line. Fronts and zones are included and underlain by sea surface temperature (SST) data collected throughout the cruise. Abbreviations in alphabetical order: ACC: Antarctic Circumpolar Current; APF: Antarctic Polar Front; DTM: Deep Trace Metal station, PFZ: Polar Frontal Zone; SBdy: Southern Boundary, SAF: Sub-Antarctic Front; SAZ: Sub-Antarctic Zone; STF: Sub-Tropical Front; STZ; Sub-Tropical Zone; TM: Trace Metal station; WG: Weddell Gyre. Diagram compiled on Ocean Data View (ODV).

with Viton O-rings. The GO-FLO bottles were mounted on a Seabird aluminium rosette coated in a trace metal clean polyurethane powder (Figure 3A). The rosette housed a Seabird 9+ Conductivity Temperature Depth (CTD) recorder in an anodized aluminium casing, eliminating the need for a sacrificial zinc anode, a possible contamination source. A Kevlar hydrowire with internal signal cables was utilised for transferring of data between the on-board CTD control room as well as triggering the GO-FLO bottles at the various depths during the upcast. GO-FLO bottles were loaded onto the rosette prior to station occupation. As part of the protocol, transporters wore sterile nitrile gloves and sleeves while the GO-FLO bottles were covered in a plastic wrap, their ends covered in plastic shower caps and spigot sealed with a ziplock bag (Figure 3B). While the plastic wrap was removed prior to loading, it was only at the last moment before deployment that the shower caps and ziplock bags were removed. Directly upon recovery, the above process was repeated and the GO-FLO's were transported into a class 100 (ISO 5 equivalent) clean lab for sub-sampling. Samples to be analysed for the total dissolved fraction were collected from the GO-FLO

bottles through polytetrafluoroethylene (PTFE) tubing, unfiltered, in acid-cleaned 125 ml perfluoroalkoxy (PFA) bottles (Figure 3C) while samples collected for the determination of the dissolved fraction were collected in low density polyethylene (LDPE) bottles (Nalgene) after online filtration using a 0.2 µm Acropak (500 Supor Membrane) filter connected to PTFE tubing and under a pure nitrogen (N_2) assisted pressure (99.99% N_2, BIP Technology) of 2 bar (Figure 3D). Each LDPE sample was then acidified to a pH of 1.7 on-board under a laminar flowhood with hydrochloric acid (ultrapure HCL, Merck) and stored in double ziplock bags at ambient temperature in the dark until the samples were analysed, 6 months later, in a land-based laboratory.

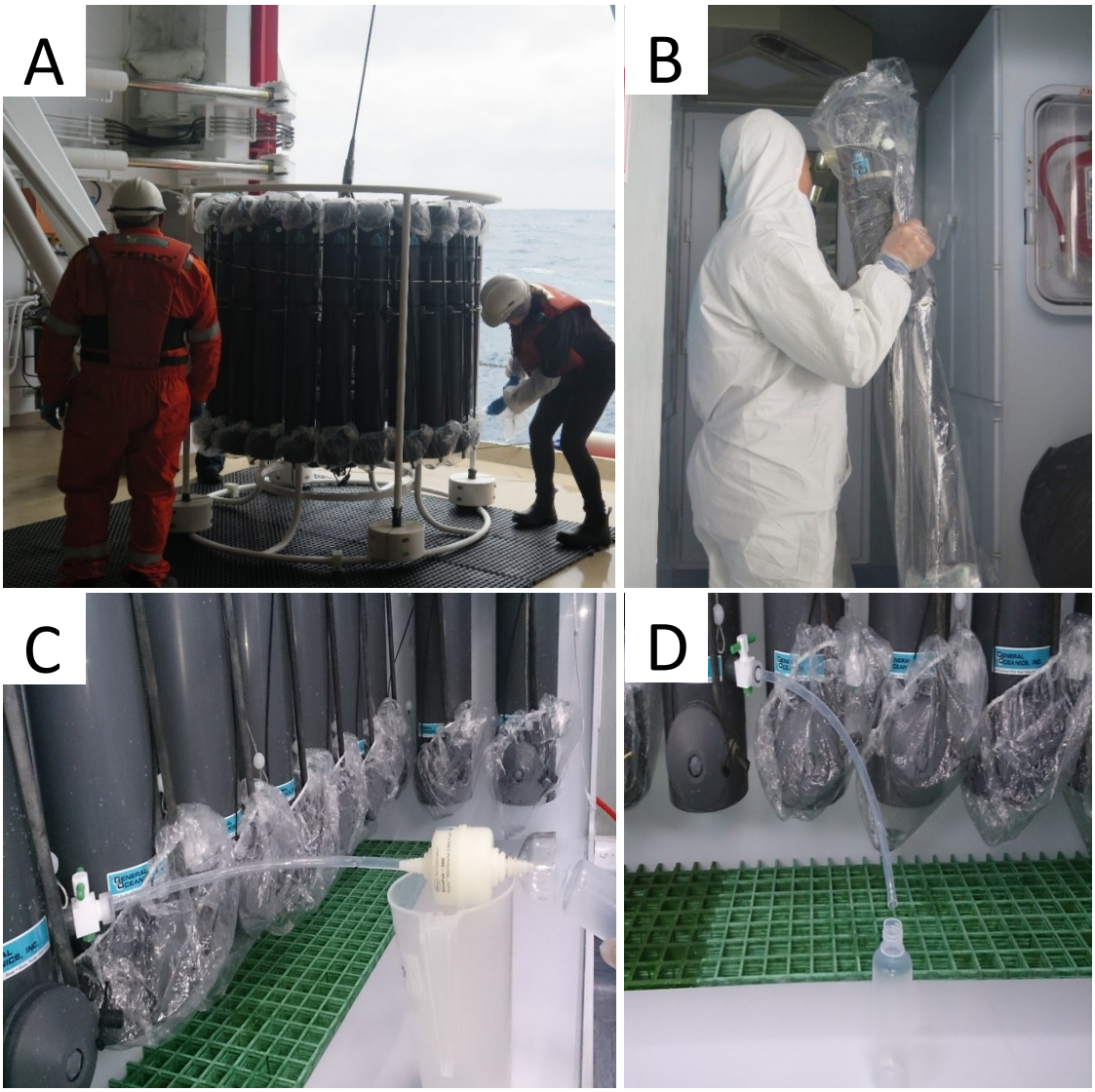

Figure 3 – A: removal of shower caps from GO-FLO bottles before the rosette is launched. B: transportation of GO-FLO bottles to and from the on-board class 100 clean lab. Note the PVC lining enclosing the GO-FLO bottles. C: filtering (0.2µm) seawater for the determination of the dissolved fraction. D: apparatus used for the collection of seawater for the total dissolved fraction determination. Note samples are collected unfiltered.

2.3. Reagents and Materials

Ultrapure deionized water purified with the Milli-Q Advantage A10 system was used for the dilution of all solutions. Analytical grade Hydrochloric acid (32 % HCl) was used for acid washing sample bottles as well as storage acid inside 125ml sample bottles. Ultrapur Hydrochloric acid (30% HCl) was used to acidify seawater samples to a pH of 1.7 before storage. The buffer solution used in the preconcentration step was prepared with Ammonium Hydroxide Solution (25% NH_4OH), which was diluted to 22% NH_4OH using deionized water, and Glacial Acetic Acid (100% CH_3COOH) until a final pH of 6.0 ± 0.2 was attained. The Eluent for the preconcentration step was prepared using Ultrapur Nitric Acid (60% HNO_3). All reagents used were sourced from Merck Millipore. Iso-2-propanol was used in the initial clean of the GO-FLO bottles. Sample bottles used in the collection of seawater for the total and dissolved fraction quantification were perfluoroalkoxy (PFA) and low density polyethylene (LDPE) respectively. Falcon tubes were polypropylene (PP).

2.4. Sample Pre-Treatment

Certain trace metals, most notably Fe, Cu and Co, exhibit strong complexation with organic ligands present in ocean surface waters (Lohan *et al.*, 2005). Organic complexation removes the trace metal ions from the bioavailable source pool. Sample acidification, to a pH of 1.7 on this cruise, is performed to ensure dissociation from organic complexes and stabilize the metal ions as labile inorganic forms. Acidification however has been shown to be insufficient in releasing Co, and to a lesser extent Cu, ions from organics. A subsequent underestimation of these two trace metals results from the chelating resin used in the preconcentration process being effectively blind to organic complexes. Ultra-violet (UV) oxidation has been previously employed to destroy the Co and Cu complexes (Ellwood and Van den Berg, 2001). UV oxidation was not performed on samples in this study. Reasons for this are discussed in section 3.5.2.

2.5. Analytical Methods

2.5.1. Sample Preconcentration by Solid Phase Extraction

The analysis of seawater for trace metals requires that elements typically present at pmol kg^{-1} to nmol kg^{-1} concentrations be determined in a matrix dominated by major seawater ions present at much higher (mmol kg^{-1}) concentrations. Preconcentration is required to separate the trace metals from the major ions and dissolved organic matter and furthermore to increase the signal to blank ratio (Lagerstrom *et al.*, 2013). The net effect of preconcentration is an effective increase in trace metal concentrations to values in excess of ICP-MS detection limits.

The seaFAST-pico SC-4 DX (Elemental Scientific Inc.) is a preconcentration module which applies a solid phase resin extraction method in order to separate the targeted metal ions from their seawater matrix. This system is an ultra-clean, automated, low pressure ion chromatography system capable of single digit picogram per litre detection limits. The manifold setup comprises a syringe pump (S400V-111) consisting of four syringes (rinse, carrier, diluent and internal standard), TRIO valve module (VM3-P6P6SSV11), 12 port valve (V12), 11 port valve (V11), 5 port valve (A5e), fluoropolymer flow paths, a seawater preconcentration column (CF-N-0200), trace metal clean up column and a nitrogen gas line (Figure 4A). The resin contained within the seawater preconcentration column comprises both ethylenediaminetriacetic acid (EDTriA) and iminodiacetic (IDA) functional groups which are immobilized on a hydrophilic methacrylate polymer with a bead diameter of 60 µm. This enables the resin to act as a high affinity metal chelator, extracting the solid phase metal ions from the seawater matrix. The system has a resin bed volume of 200 µL with a column capacity of 20 µEq/column. Column materials are as follows: PFA body and caps, polytetrafluoroethylene (PTFE) frits and chlorotrifluoroethylene (CTFE) plugs. The entire system was kept under 2 bar pure air pressure. Solvents used in the preconcentration process were prepared as follows: the buffer consisted of glacial acetic acid and ammonium solution, adjusted to a pH of 6.0 ± 0.2 as suggested by the Elemental Scientific method guide. The eluent and eluent Internal Standard (IS) consisted of 53 ml of nitric acid (2M) diluted to 500 ml with ultrapure deionized water.

The preconcentration procedure was carried out under trace clean conditions in a class 100 laboratory at the Department of Earth Sciences, Stellenbosch University. The system was operated in the prepFAST offline configuration. This automated setting vacuum loads 14 ml of acidified seawater into the injection valve where it is buffered. The buffered solution is then loaded onto the chelating resin column where the solid phase extraction takes place (Figure 4B). Finally, the chelated metal ions are eluted resulting in a low volume (270 µL) of concentrated sample (Figure 4C & D). The pH of the buffer solution in the column is vital for the proper recovery of the trace metal ions. Prior to preconcentration, the probe was soaked overnight in a 1 M HCl bath before being thoroughly rinsed with milli-Q. Furthermore, two sodium chloride (NaCl) blanks and a large volume seawater standard were preconcentrated at the start of each analysis in order to condition the resin column. A simple decant method was used to transfer the seawater samples into falcon tubes for preconcentration. Samples were preconcentrated in order of increasing depth. For each depth, one PFA (total trace element concentration) and two LDPE bottles (dissolved trace element concentration) were decanted into three separate falcon tubes and placed in the sample rack. Correspondingly, empty vials were placed on the destination rack ready to receive the preconcentrated sample. Upon completion of the

preconcentration, vials from the destination rack were capped, labelled and placed in double ziplocked bags for analysis by ICP-MS in the Central Analytical Facility (CAF) at Stellenbosch University. A preconcentration factor of 40 ensured quantitive recovery at the pico-molar range.

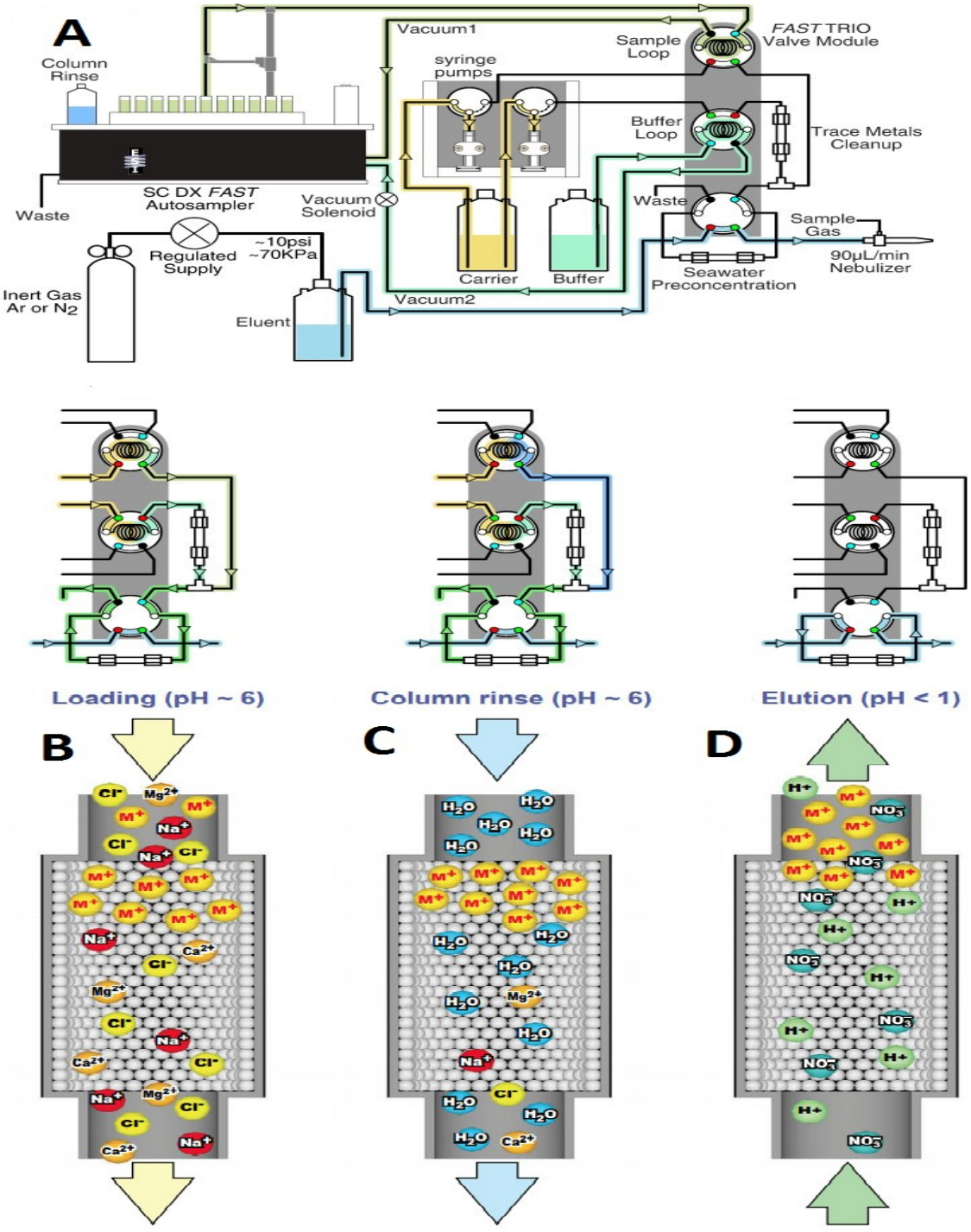

Figure 4 – Schematic of the seaFAST SC-DX preconcentration module set up illustrating the offline step wise flow injection paths during A) the filling of the sample and buffer loops, B) loading of the chelation column with the buffered sample, C) rinsing the column of the matrix elements whilst retaining the metal ions and D) elution of the trace metals from the chelation column into the sample vial. Schematic adapted from (Lagerstrom *et al.*, 2013).

The preconcentration procedure for each sample takes roughly 15 minutes. A vertical depth profile sampled at 15 different depths in triplicate would therefore take approximately 11 to 12 hours to complete. It is not practical to be present during the procedure for this length of time however to leave the procedure completely unattended would result in potential evaporation of samples in the uncapped falcon tubes. Evaporation of samples may be significant, particularly in the destination vials, due to the low volumes of preconcentrated samples (270 µL) and will serve to alter trace metal concentrations yielding unreliable results. As a separate experiment, a control test was performed to assess the effect of evaporation on the concentration of the various trace metals in a vial left uncapped for 4 hours. The results for the suite of trace metals are shown below in Figure 5. The results (n=1) showed little variation for all trace elements except Fe which showed an increase in concentration with time. Cu and Zn showed negligible differences. The trace elements Co and Pb are not shown due to their higher inherent concentrations distorting the graph axis. Results for these two metals were unchanged at 20.00 and 10.00 pmol kg^{-1} respectively. To minimise this effect as much as possible, and keeping in mind the practicality of entering and exiting the clean lab, it was decided to leave a maximum of 6 vials uncapped at any given time. This means that vials will be uncapped for a maximum of 90 minutes.

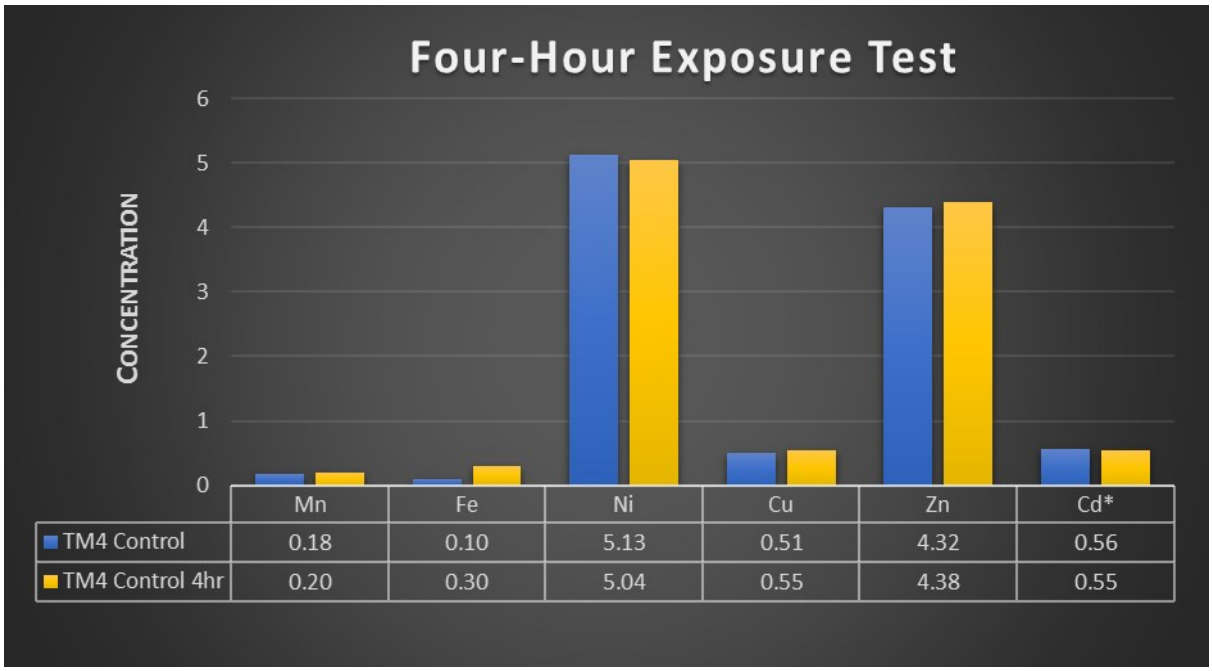

	Mn	Fe	Ni	Cu	Zn	Cd*
TM4 Control	0.18	0.10	5.13	0.51	4.32	0.56
TM4 Control 4hr	0.20	0.30	5.04	0.55	4.38	0.55

*Figure 5 –results showing the effect of evaporation on trace metal concentrations after a four-hour exposure test. All values in nmol kg^{-1}. * denotes pmol kg^{-1}.*

2.5.2. Measurement of Elemental Concentrations by ICP-MS

The pre-concentrated seawater samples were analysed on an Agilent 7900 ICP-MS, using the standard configuration of quartz spray chamber and torch, and Ni-plated sampling and skimmer cones.

A 0.2 ml/min PFA nebulizer was used to auto-aspirate the sample using a 0.3 mm ID PTFE sample line connected to the autosampler probe. The sample introduction line was made as short as possible due to the small volume of sample (400µl) available. The instrument was optimized for best sensitivity and low oxide ratios (< 0.3%). Samples were introduced using a low flow self-aspirating PFA nebulizer with a flow rate of ~ 0.2 µl/min. Isotopes of 27Al, 51V, 55Mn, 56Fe, 59Co, 60Ni, 63Cu, 66Zn, 111Cd and 208Pb was measured using the ORS in He collision mode to eliminate plasma and matrix based interferences, which was extensively reduced by using the ESI SeaFast system to remove the seawater matrix. Internal standards 45Sc and 89Y were used to compensate for instrument drift as well as matrix differences between samples and standards. The instrument was calibrated using a multi-element standard from Inorganic Ventures Inc (Christiansburg Virginia), and the calibration verified with a multi-element standard supplied by Merck Millipore (Merck KGaA, Darmstadt, Germany). Continuous check standards were analysed throughout the run to monitor instrument drift. Data was processed using the Agilent Mass Hunter software. The instrument was housed at the CAF at Stellenbosch University (SU).

Instrument parameters were set as follows:

Table 1- ICP-MS setup parameters

Parameter	Unit	Value
RF Power	W	1600.00
Carrier gas	L min^{-1}	0.90
Sample depth	mm	10.00
Make-up gas	L min^{-1}	0.25
He flow	ml min^{-1}	4.50
H2 flow	ml min^{-1}	6.00

Analysis parameters for each element were set to measure 1 point per peak, 3 replicate measurements per isotope under the following conditions:

Table 2 – Elemental analysis parameters

Element	Isotope	Cell Gas	Integration Time (sec)
Mn	55	He	0.6
Fe	56	H2	1.0
Co	59	He	1.0
Ni	60	He	0.6
Cu	63	He	0.6
Zn	66	He	0.6
Cd	111	He	1.0
Pb	208	He	1.0

3. Protocol validation and Intercalibration Station

3.1. Introduction

Since the construction of Africa's first metal-free trace clean facility at the Department of Earth Science, Stellenbosch University, the opportunity to conduct ocean based trace metal research entirely within South Africa's borders has arisen. At the centre for Trace and Experimental Biogeochemistry, Stellenbosch University, one of the primary objectives of this research has been to establish and validate a protocol for the quantification of trace elements in seawater. The second primary objective is to implement this protocol in creating trace metal datasets for the data-scarce Southern Ocean. This task has proved extremely difficult and unsuccessful in recent attempts largely due to contamination issues which are commonly associated with this type of work. As such, several changes were made in order to eliminate the contamination issues and, a method validation exercise was conducted. Changes include a more stringent sample bottle cleaning process and alterations made to GO-FLO bottles (Appendix C). This chapter serves to outline the in-lab validation process for the measurement of trace metals using reference standards, a joint intercalibration exercise with the University of Plymouth (UK) and the use of a cross-over station as per GEOTRACES protocol (GEOTRACES Cookbook).

Method validation is the process of establishing documented evidence that provides a high degree of assurance that a specific method, and all ancillary instruments involved, will consistently yield results that accurately reflect the quality of the method under development. Results from such validations can be used to judge the quality, reliability and consistency of analytical results and play an integral part in any good analytical practice. Analytical methods need to be validated or re-validated for a number of reasons. In this case, the method adopted for this study follows the established sampling and sample-handling protocols outlined by the international GEOTRACES program; however, this does not suffice as adequate proof that our experimental setup will produce the same reliable results. Factors such as equipment specification, equipment calibration and operator competency vary between laboratories and thus the need for a new validation is warranted. Parameters for the method validation are defined in Appendix E.

In order to gain accreditation from the GEOTRACES Standards and Intercalibration (S&I) Committee, a number of items need to be considered. Firstly, where possible, every cruise must occupy at least one cross-over station from another cruise in order to affect an intercalibration for sampling and subsequent analysis. Secondly, nutrient and salinity samples should be taken along with

all trace element samples in order to verify hydrographical parameters against those established with the conventional CTD (refer to chapter 4). Lastly, because ultra-low concentration seawater standards are not available, appropriate certified reference materials (i.e. SAFe or GEOTRACES) must be processed to assess analytical accuracy (GEOTRACES Cookbook).

3.2. Methods

The analytical method can be divided into two separate but related procedures, namely the seawater sample collection procedure and the ICP-MS based trace element quantification procedure. As a result of these two steps being conducted in different environments and following different protocols, it introduces new pathways for contamination and so it is necessary to validate each step separately.

3.2.1. Sample Collection

In order to validate the effectiveness of the vertical profile sampling technique in collecting representative seawater samples, a laboratory based intercalibration station as well as multiple cross-over stations were performed. Together with the University of Plymouth (UK), sampling station DTM3 (54°S; 0°) was predetermined as the intercalibration station. Samples for the analysis of the dissolved phase were collected, in triplicate, in 125 ml LDPE (Nalgene) bottles from 23 depths, between surface and 2400 metres, after filtration through a 0.2 µm filter attached to the GO-FLO bottles. Seawater samples from DTM3 were sent to the University of Plymouth (UK) to be analysed for their Dissolved Iron (DFe) concentration using a flow-injection analyser to detect contamination issues at the time of collection and preservation of samples on-board the ship. This laboratory has an established, validated trace element quantification procedure and therefore results from this analysis can be assumed to be reliable. The Plymouth data was further used for intercalibration of an ICP-MS based analytical technique set-up at Stellenbosch University. Based on previous trace metal work in the Southern Ocean by Klunder et al. 2011, the concentration ranges of DFe at the cross-over stations are reasonably well constrained. If the results received fell within the observed concentration range, it would confirm the samples were uncontaminated and were the result of an effective implementation of the sample collection protocol and analyses. Sampling depths mimicked those in the study to allow for a direct comparison between the results obtained from this study and those obtained by Klunder et al. 2011. The intercalibration process followed thus allowed for the direct comparison of analytical results between the two laboratories using two different analytical techniques and for comparison of previously measured data at the same site.

3.2.2. Analytical Methods

3.2.2.1. Preconcentration by Solid Phase Resin Extraction

The seaFAST-pico SC-4 DX (Elemental Scientific Inc.) is a preconcentration module which applies a solid phase resin extraction method in order to separate the targeted metal ions from their seawater matrix. This serves to remove major constituents in seawater, such as alkali and alkaline earth metals, which interfere with ICP-MS determination as well as ensure concentrations are above the systems detection limits. The seaFAST system utilises a resin column upon which both ethylenediaminetriacetic (EDTA) acid and iminodiacetic (IDA) acid functional groups are immobilized. The polyaminocarboxylic acid functional group acts as a high affinity metal chelator and dominates the adsorption behaviour of elements. This resin is commercially available and so it must be emphasized that the purpose here is not to assess the recovery of the resin under varying conditions (e.g. changing buffer pH), but rather to validate the implementation of the preconcentration protocols in our laboratory. The preconcentration procedure was carried out under trace clean conditions in a class 100 laboratory at the Department of Earth Sciences, Stellenbosch University. The reader is referred to chapter 2 for additional information about the preconcentration module as well as the methods and protocols employed during this procedure.

3.2.2.2. Certified Reference Material

Due to the extremely low concentrations of trace elements displayed by oceans globally, there are no commercially available seawater standards with which to validate the accuracy and precision of the ICP-MS at these trace concentration ranges. Scientists recognised this problem and, through several global intercalibration efforts, consensus standards such as SAFe (D2), GEOTRACES (GSC-1-19 and GSP 62) and NASS were produced and distributed to the scientific community. The comparison with consensus standards allowed for the determination of accuracy and reproducibility of the ICP-MS analytical method and the effectiveness of the coupled pre-concentration step.

One SAFe standard, two GEOTRACES standards and the NASS-5 standard were analysed in order to validate the sensitivity of the ICP-MS machine. The SAFe standard (SAFe D2) represents seawater samples collected from the North Pacific Ocean in 2004. It is a deepwater (1000 metres) sample collected with multiple four-bottle casts using a Teflon coated GO-FLO bottle (30 L volume) deployed using a Kevlar hyrdroline. The GEOTRACES intercalibration comprises the GSC 1-19, a coastal seawater sample, and GSC 62, a surface seawater sample. The two GEOTRACES standards were collected at 2 metres depth, outside the ship's area of influence, by a "GeoFish" towed sampling system. The NASS-5 reference material represents the 5th series of ocean water certified reference

material for trace metals. The seawater was collected in the North Atlantic Ocean at a depth of 10 metres. Large volumes of the surface and deep seawater were collected, filtered and homogenised to create these standards.

3.2.2.3. Internal Control Standards

Due to the limited volume of SAFe D2 standard available to us, the expiry of the NASS-5 standard and subsequent release of the NASS-6 reference material and the lack of consensus data available for the GEOTRACES standards, it was decided to create our own internal control standard – the Stellenbosch University (SU) TM4 control. Seawater used for the creation of this control standard was collected in a large volume (20L) from multiple surface depths between 15 and 50 metres at 36°S; 13°E. The seawater was subsequently filtered for the dissolved fraction (0.2µm) and stored in an acid cleaned 20 L carboy. Ten SU TM4 control standards were subjected to preconcentration and ICP-MS analysis at the CAF in order to create our own consensus values for the suite of trace metals. In addition, creating this internal control standard served the purpose of monitoring the repeatability of the ICP-MS during sample analysis. The nature of ICP-MS means it is very sensitive to instrumental drift, amongst other factors, which results in decreased sensitivity throughout the analysis process. To counter this, SU TM4 control samples are inserted into the sample queue at regular intervals. Two are inserted at the start of each analysis and thereafter after every 12 seawater samples analysed. The results were then compared to the consensus values mentioned previously. As this internal control is repeatedly analysed at different time intervals it allows a measure of system stability to be quantified. In addition to the SU TM4 control, various quality control (QC) standards (Inorganic Ventures Inc.) were analysed after every 6 seawater samples (~ 12 minutes) to assess accuracy. The QC standards were not preconcentrated.

3.2.2.4. ICP-MS Analysis

The pre-concentrated seawater samples were analysed on an Agilent 7900 ICP-MS at the CAF laboratory at Stellenbosch University. The reader is referred to chapter 2 for further information regarding the ICP-MS setup.

3.2.2.5. ICP-MS Calibration

The instrument was calibrated using NIST traceable standards purchased from Inorganic Ventures, and the accuracy of the calibration validated by a separate standard from the same supplier. Calibration curves were calculated by analysing 3 standards, namely a blank, 1 ppb and 10 ppb

standards. As a precautionary measure a 20 ppb standard was also analysed in the event that a sample concentration fell outside the concentration range of the calibration.

3.2.2.6. Blank Measurements and Detection Limits

Procedural blank measurements are designed to quantify any additional contributions to elemental signals during the preconcentration and analysis process. The predominant blanks are sourced from a combination of the ammonium acetate (NH_4Ac) solution used to buffer the pH of the samples, the rinse/conditioning solution, the preconcentration manifold itself and the ICP-MS instrument. As the preconcentration module is commercially available, we can assume this effect to be negligible when operated under the conditions specified in the manual. Analysing preconcentrated ultra-high purity (UHP) milli-Q water would not suffice as a viable blank as it contains no seawater matrix. Two sodium chloride (NaCl) blanks were preconcentrated prior to each station in order to condition the resin column. An un-preconcentrated procedural blank (Inorganic Ventures) was analysed after every 6 seawater samples (~ 12 minutes), and used to correct for any instrument drift over the analysis time.

Detection limits were calculated as three times the standard deviation of the blank. In other words, the concentration of analyte required to give a signal equal to background/blank noise plus three times the standard deviation of the blank. Values lower than the detection limit mean that we cannot confidently say whether or not the analyte is present.

3.3. Results

3.3.1. Intercalibration Station

The Dissolved Iron (DFe) concentrations received from the University of Plymouth and taken from the study by Klunder et al. 2011 are compared to the results obtained by this study in Table 3 and Figures 6 and 7 respectively. There was no value available for DFe at 152 metres depth in the Klunder et al. 2011 dataset. As a result of some GO-FLO bottles returning not completely fill, 16 of the 23 depths intended for intercalibration were collected and sent to the University of Plymouth for analysis. Data from these two datasets represents the average of 3 analyses (n=3) whereas samples were analysed twice (n=2) for this study. Values highlighted in red indicate a result where the Relative Standard Deviation (%RSD) between the duplicate samples was greater than 15% and was therefore rejected. In these cases, the criteria for which of the two values was to be rejected was based simply on which value least conformed to the general trend of the profile.

3.3.1.1. Laboratory Based Intercalibration with University of Plymouth

It is important to note that the difference in sample resolution between the DFe profile in this study and that of the University of Plymouth has played a major factor in altering the shape of the curve, especially in the surface waters. The concentration of DFe in the water column ranged from a minimum of 0.08 nmol/kg in the sub-surface to a maximum of 1.82 nmol/kg in the intermediate waters. Profiles mimic each other well in the mixed layer depth (MLD), both showing a local sub-surface DFe maximum at approximately 50 metres depth. Although data suggests a much higher DFe average in the upper 500 metres of the water column for this study (Table 3), this is due to a distinct peak in concentrations between 250 and 450 metres depth (Figure 6). Crucially, data points at 300 and 350 metres depth are not available which highlights the role sample resolution plays in this comparison. Based on the fact that values at 250 and 450 metres depth compare very well, we can assume that this peak would in fact be present had these depths been analysed. In the intermediate waters, profiles mirror each other remarkably well, the only noticeable difference being a 0.3 nmol/kg deviation at 1000 metres depth.

3.3.1.2. Cross-over Station with Klunder et al, 2011

The values from the dataset of Klunder et al. 2011 represent samples collected during 2008 and so observations made between these two profiles must be made tentatively as a result of an approximate 8-year difference in sample collection period. Nevertheless, this comparison would still provide a good indication as to whether or not contamination was an issue during sample collection. Despite having similar DFe concentration ranges, there are significant differences between these two profiles. In the MLD, the profile of Klunder et al. 2011 displays a surface concentration of 0.51 nmol/kg which is more than double the corresponding value obtained in this study. Furthermore, the lack of a local sub-surface maxima in the Klunder et al. 2011 profile at 50 metres depth is another significant difference between the datasets. The previously mentioned DFe peak displayed in this study between 250 and 450 metres depth is not present in the results of Klunder et al. 2011. Instead, concentrations remain relatively constant at approximately 0.4 nmol/kg. The other significant difference between the datasets occurs in the Intermediate waters where the DFe concentrations of this study remain between 0.4 and 0.6 nmol/kg. The corresponding data points from Klunder et al. 2011 however show concentrations ranging between 0.38 and 1.87 nmol/kg with a clear peak at 1750 metres depth (Figure 7).

Table 3 - Comparison between three datasets containing the Dissolved Iron (DFe) concentrations for an intercalibration station at 54°S;0°. The three datasets include that of Klunder et al. 2011, this study (SANAE 54) and the results of an intercalibration with the University of Plymouth (UK). Values highlighted in red indicate results of which one of the duplicate samples was removed due to the %RSD being greater than 15%. The MLD was calculated at 58 metres. Surface water is defined as <500 metres. Intermediate waters are defined as 500 - 2500 metres. (*) denotes average value.

	Klunder et al. 2011		This study		Plymouth (UK)	
Depth (m)	**DFe [nmol/kg]**	**std dev**	**DFe [nmol/kg]**	**std dev**	**DFe [nmol/kg]**	**std dev**
15	0.51	0.000	0.24	0.021	-	-
25	0.14	0.004	0.12	0.006	0.08	0.000
51	0.25	0.000	0.49	0.151	0.19	0.033
76	0.26	0.011	0.38	0.080	0.3	0.000
101	0.25	0.011	0.18	0.038	0.09	0.010
152	-	-	0.22	0.055	0.24	0.018
251	0.31	0.010	0.41	0.039	0.38	0.008
301	0.35	0.009	1.22	0.004	-	-
350	0.46	0.012	1.82	0.021	-	-
401	0.37	0.018	0.92	0.011	1.05	0.028
450	0.39	0.015	0.44	0.059	0.33	0.013
500	0.51	0.019	0.45	2.979	-	-
552	0.43	0.007	0.94	0.014	-	-
600	0.38	0.000	0.55	0.020	0.38	0.000
649	0.52	0.013	0.53	0.021	0.47	0.015
750	0.35	0.007	0.46	0.021	0.48	0.005
999	0.66	0.003	0.64	0.000	0.34	0.020
1249	0.38	0.000	0.43	0.006	0.37	0.015
1499	1.17	0.001	0.42	0.075	0.44	0.003
1749	2.16	0.004	0.48	0.011	-	-
2000	1.51	0.000	0.57	0.008	-	-
2248	1.59	0.010	0.56	0.018	0.63	0.003
2398	1.87	0.017	0.59	0.013	0.52	0.000
Min	0.14		0.12		0.08	
Max	2.16		1.82		1.05	
MLD*	0.30	0.001	0.29	0.059	0.14	0.017
Surface*	0.35	0.010	0.61	0.023	0.33	0.014
>Intermediate*	1.00	0.006	0.56	0.019	0.45	0.008

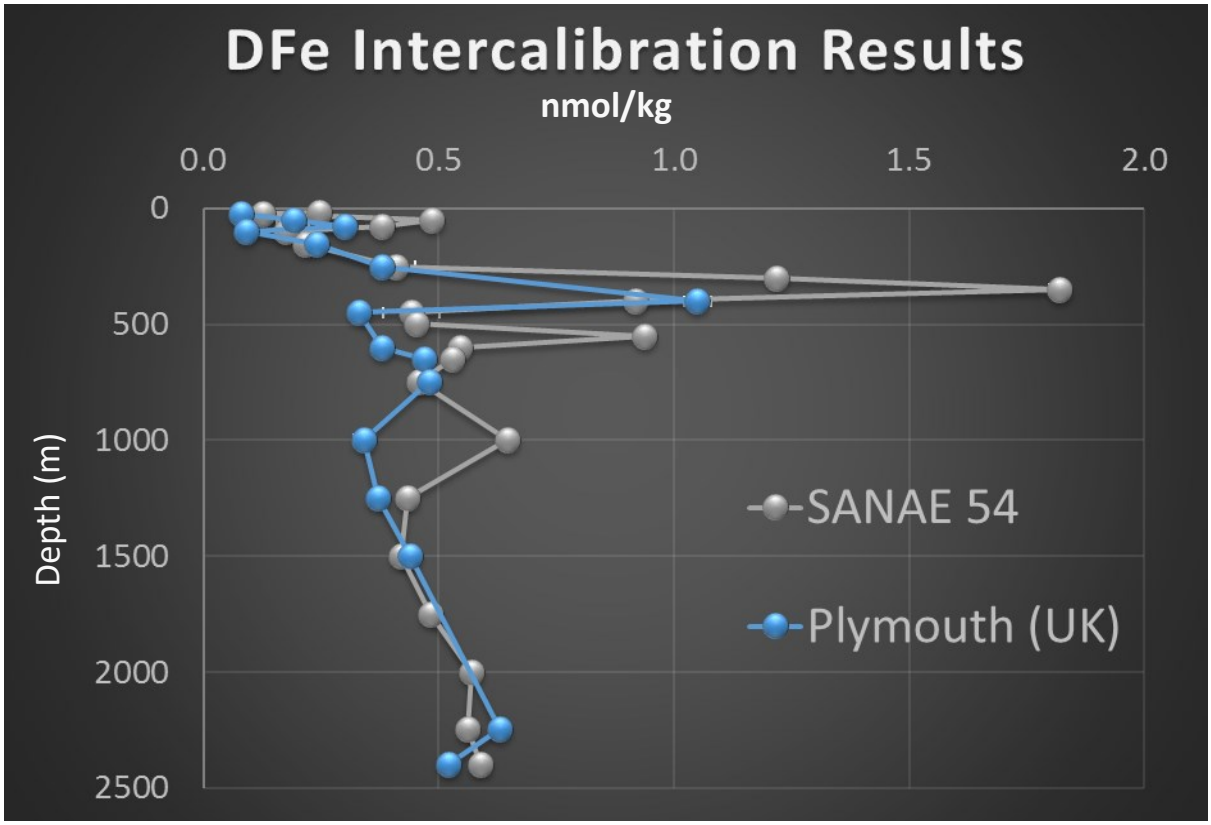

Figure 6 – Laboratory based Intercalibration station results comparing Dissolved iron (DFe) profiles obtained from this study (SANAE 54) and the University of Plymouth (UK).

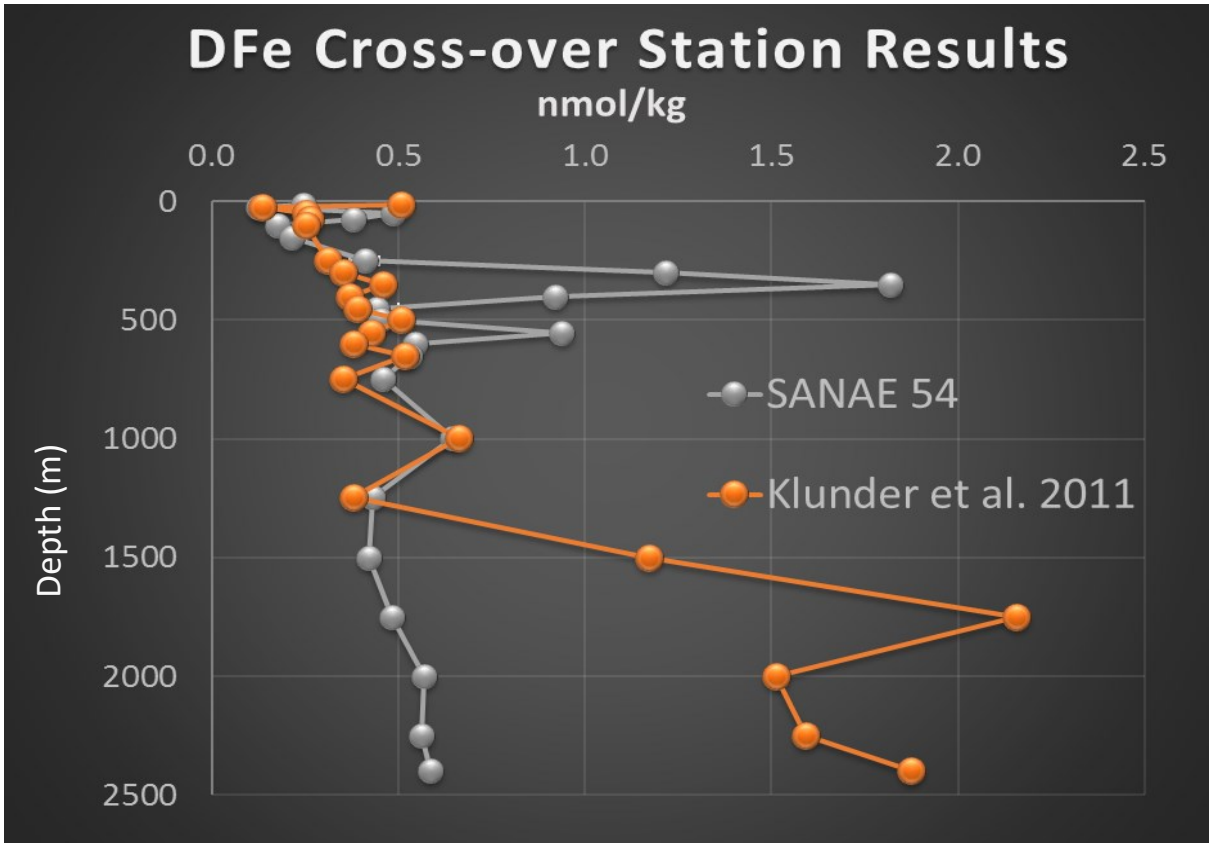

Figure 7 – Cross-over station results comparing Dissolved iron (DFe) profiles obtained from this study (SANAE 54) and the dataset published by Klunder et al. 2011.

3.3.2. Certified Reference Material

Table 4 - Results of the ICP-MS analysis of three sets of certified seawater standards namely SAFe (SAFe D2), GEOTRACES (GSP 62 and GSC 1-19) and NASS-5 are displayed alongside their respective consensus values. Consensus values for the SAFe standards as of May 2013 (www.geotraces.org). Consensus values for the NASS-5 standard as of 1998 (www.gbcpolska.pl/me/crm/pdf/certyf_woda_morska_nass_5.pdf). (-) means data is not available.

SAFE D2	**Mn**		**Fe**		**Co**		**Ni**		**Cu**		**Zn**		**Cd**		**Pb**	
	nmol/kg	*SD*	*nmol/kg*	*SD*	*pmol/kg*	*SD*	*nmol/kg*	*SD*	*nmol/kg*	*SD*	*nmol/kg*	*SD*	*pmol/kg*	*SD*	*pmol/kg*	*SD*
Consensus	0.35	0.05	0.93	0.02	45.70	2.90	8.63	0.25	2.28	0.15	7.43	0.25	986.00	23.00	27.70	1.50
Measured (n=5)	0.40	0.04	0.96	0.03	32.72	0.44	8.05	0.11	2.04	0.03	7.23	0.25	955.28	59.68	28.48	1.19

GSC 1-19	**Mn**		**Fe**		**Co**		**Ni**		**Cu**		**Zn**		**Cd**		**Pb**	
	nmol/kg	*SD*	*nmol/kg*	*SD*	*pmol/kg*	*SD*	*nmol/kg*	*SD*	*nmol/kg*	*SD*	*nmol/kg*	*SD*	*pmol/kg*	*SD*	*pmol/kg*	*SD*
Consensus	-		-		-		-		-		-		-		-	
Measured (n=5)	1.96	0.18	1.51	0.08	81.71	4.06	3.91	0.16	1.14	0.04	1.41	0.10	345.40	21.42	39.54	1.89

GSP 62	**Mn**		**Fe**		**Co**		**Ni**		**Cu**		**Zn**		**Cd**		**Pb**	
	nmol/kg	*SD*	*nmol/kg*	*SD*	*pmol/kg*	*SD*	*nmol/kg*	*SD*	*nmol/kg*	*SD*	*nmol/kg*	*SD*	*pmol/kg*	*SD*	*pmol/kg*	*SD*
Consensus	-		-		-		-		-		-		-		-	
Measured (n=5)	0.69	0.07	0.38	0.02	5.11	0.54	2.37	0.11	0.56	0.02	0.16	0.05	4.66	1.13	64.69	2.46

NASS-5	**Mn**		**Fe**		**Co**		**Ni**		**Cu**		**Zn**		**Cd**		**Pb**	
	nmol/kg	*SD*	*nmol/kg*	*SD*	*pmol/kg*	*SD*	*nmol/kg*	*SD*	*nmol/kg*	*SD*	*nmol/kg*	*SD*	*pmol/kg*	*SD*	*pmol/kg*	*SD*
Consensus	16.32	1.01	3.62	0.61	182.10	0.05	4.21	0.47	4.56	0.71	1.52	0.58	199.62	0.03	37.67	0.02
Measured (n=3)	15.49	0.82	3.70	0.13	182.14	8.86	7.66	0.26	4.40	0.23	1.63	0.04	180.62	9.43	33.14	1.49

The results of the analysis of the three sets of certified seawater reference material are displayed in Table 4.

The elemental composition obtained from the analysis of the SAFe D2 standard compared well with their respective consensus values. This was most notable for Fe, showing only a 0.03 nmol/kg difference between the measured and consensus values. Measured Zn values of 7.23 ± 0.25 nmol/kg were very similar to the consensus measurements of 7.43 ± 0.25 nmol/kg. Values of 32.72 ± 0.44 pmol/kg for Co and 2.04 ± 0.03 nmol/kg for Cu were lower than their corresponding consensus values of 45.70 ± 2.90 pmol/kg and 2.28 ± 0.15 nmol/kg.

As can be seen from Table 4, there are currently no consensus valued published for the two GEOTRACES reference standards. By analysing these standards, we hope to contribute to the creation of these consensus values.

The results of the analysis of the NASS-5 reference material are in good agreement with the published consensus data. Measured Fe, 3.70 ± 0.13 nmol/kg, displayed remarkable accuracy and much better repeatability compared to the corresponding 3.62 ± 0.61 nmol/kg. A similar relationship was observed between measured Zn, 1.63 ± 0.04 nmol/kg, and the relevant consensus value of 1.52. ± 0.58 nmol/kg. Unlike the SAFe D2 results, Co and Cu did not show the slight underestimation with respect to their individual consensus values.

3.3.3. Internal Control Standards

3.3.3.1. SU TM4 Control

The TM4 large volume seawater was not acidified after collection. The SU TM4 control standards were hence preconcentrated and analysed as such. The results, compiled in Table B1 (appendix B) and summarised in table 5, returned from this standard showed good precision for each element with the exception of Fe. Concentrations for Fe ranged between 0.03 nmol/kg and 0.44 nmol/kg which demonstrates a lack of repeatability with respect to this element. The large error bar seen in figure 8 for Pb resulted from an anomalously high value of 17.80 pmol/kg obtained during the 2016 std analysis 1, more than double the concentration of the mean Pb content of the seawater. In an attempt to increase the stability of the Fe values, and further increase precision among the other elements, it was decided to acidify the SU TM4 control. In an acid cleaned LDPE container, we decanted 1L of the large volume SU TM4 control and spiked it with ultrapure HCl for a final pH of 1.7, the same pH as the seawater samples preserved for their dissolved phase quantification. Prior to incorporating the acidified SU TM4 control standard into the sample analysis runs, we

preconcentrated and analysed 10 simultaneously in order to establish our own consensus value and for subsequent comparisons. The results of this analysis and those inserted into the subsequent sample analyses are compiled in Table B2 (appendix B) and summarised in table 6. As expected, all elements showed higher concentrations when compared to their corresponding un-acidified samples (Figure 8). Differences in average concentration ranged from ~ 10% for Co to ~ 69% for Cu. There is a marked improvement in the precision of the analysis for all elements, as seen by the decrease in the deviation from the mean. This as most notable for Fe which showed a considerably smaller concentration range of 0.23 nmol/kg – 0.37nmol/kg. Cu and Zn were among the elements displaying the highest degree of repeatability having approximately 80% of the results within 1 S.D. of the mean and 96% within 2 S.D of the mean.

Outliers were identified as values plotting outside 3 S.D of the mean. These values were excluded from all statistical analyses (Table 5 & 6) however they were not omitted from the datasets (Appendix B). For the unacidifed TM4 control, two outliers were identified while for the acidified standards, 9 outliers were identified. No relationship was observed between outliers in the unacidifed control dataset while in the acidified standard dataset, eight of the nine outliers were sourced from either TM1 or TM1-Winter analyses. These values showed no affinity for a specific element.

The distribution of the results around the mean for each element was calculated to ascertain whether or not the data was positively or negatively skewed. Skewness was calculated according to the formula:

$$\nu = \frac{1}{n}\sum_{i=1}^{n}\left(\frac{x_i - \bar{x}}{\sigma}\right)^3$$

Where n is the population size; $\bar{x}$ is the mean and σ is the standard deviation of the population.

To test whether the skewness was significant or not, a standard error of skewness (SES) test was performed whereby the skewness value was compared to the SES value derived from the equation: $\sqrt{\frac{6}{n}}$. Skewness is deemed significant if the absolute value of the skewness is greater than 2 times the SES value (Tabachnick and Fidell, 2007). All elements whose data did not display this relationship were assumed to display a normal distribution. Fe and Pb (un-acidified control) were the only two elements to display a skewed distribution. Both elements were positively skewed meaning results were unevenly distributed toward concentrations less than the mean.

Ascertaining whether the elemental distributions were normal or skewed is important for the calculation of Confidence Intervals (C.I.). For normal distributions, i.e. all elements except Fe and Pb, the 95% C.I. was calculated as follows:

$$\bar{x} \pm z^* \left(\frac{\sigma}{\sqrt{n}}\right)$$

Where z^* is the critical value which is 1.96 for the 95% C.I.

The excel function, CONFIDENCE.T, was used to calculate the 95% C.I. for Fe and Pb (acidified and un-acidified standards) and Cu (acidified standard). This function takes into account the skewness of the distribution and computes the C.I. accordingly.

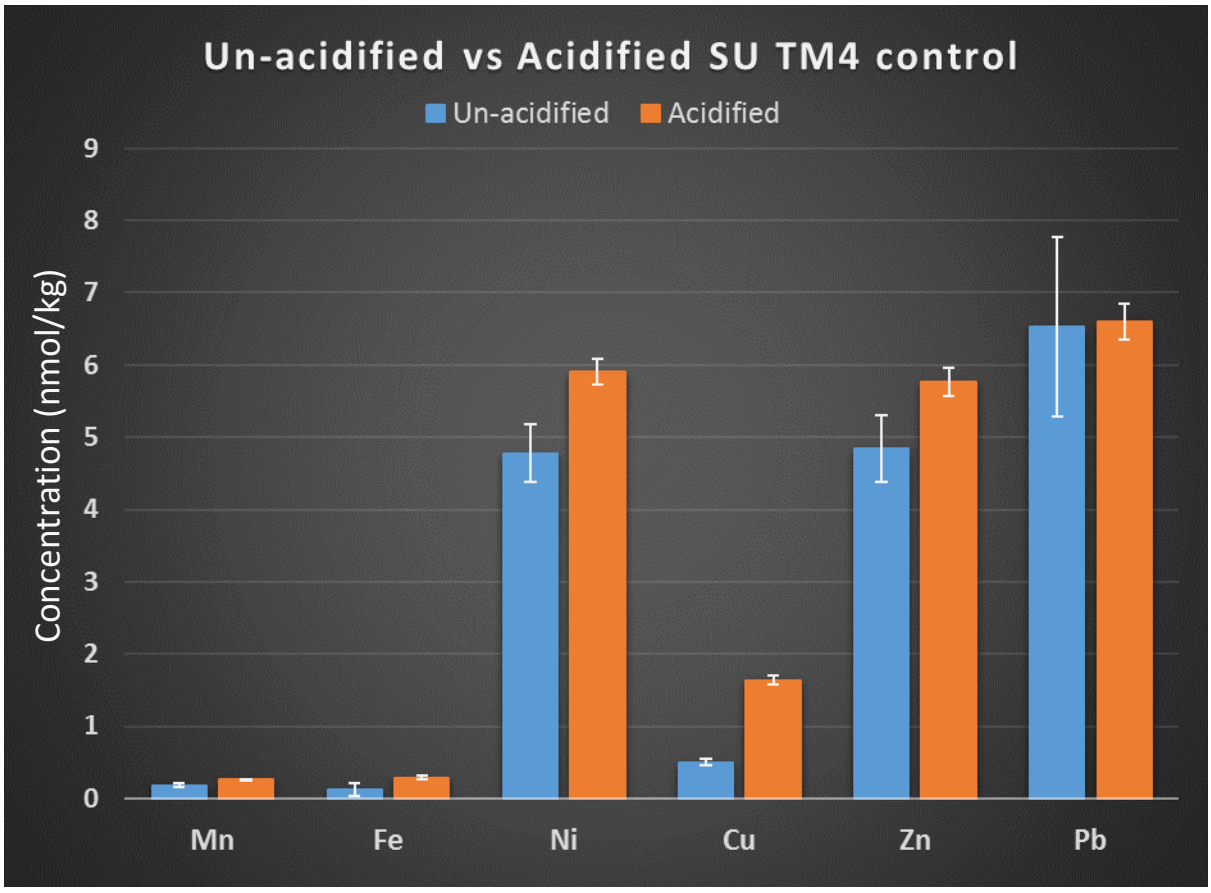

Figure 8 - differences in overall mean and precision for all analyses of both acidified and un-acidified SU TM4 control standards. The elements Cd and Co has been purposefully omitted due to their typical concentration ranges being an order of magnitude greater compared to the rest of the trace element suite.

Table 5 - Summary of the results for separate analyses of the SU TM4 un-acidified internal control. Errors expressed at the 95% confidence interval. Outliers have been excluded from all descriptive statistics calculated.

SU TM4 control - unacidified	***n***	**Mn**	**Fe**	**Co**	**Ni**	**Cu**	**Zn**	**Cd**	**Pb**
		nmol/kg	*nmol/kg*	*pmol/kg*	*nmol/kg*	*nmol/kg*	*nmol/kg*	*pmol/kg*	*pmol/kg*
2015 avg	2	0.18	0.11	17.68	5.13	0.51	4.29	560.83	6.35
DTM1	2	0.20	0.28	16.09	4.33	0.45	4.91	525.08	7.16
DTM2	4	0.22	0.23	18.42	5.13	0.58	4.38	618.19	8.90
2016 avg	4	0.18	0.13	14.22	4.28	0.52	4.62	531.31	6.21
2016 std analysis (1)	4	0.16	0.12	13.84	4.59	0.49	4.74	544.66	8.85
2016 std analysis (2)	5	0.20	0.19	15.51	4.86	0.50	5.06	598.84	5.75
DTM3	7	0.17	0.07	14.76	4.93	0.49	5.30	618.03	6.07
	28	0.19 ± 0.01	0.14 ± 0.03	15.51 ± 0.70	4.78 ± 0.15	0.50 ± 0.02	4.85 ± 0.17	581.03 ± 17.82	6.93 ± 0.49
total runs		28	28	28	28	28	28	28	28
outliers		0	1	0	0	0	0	0	1
max		0.23	0.44	20.59	5.49	0.63	5.74	690.91	9.20
min		0.15	0.03	12.45	4.01	0.39	4.03	479.91	4.73
mean		0.19	0.13	15.51	4.78	0.50	4.85	581.03	6.53
median		0.18	0.10	15.35	4.82	0.51	4.85	588.60	6.04
S.D.		0.02	0.09	1.90	0.40	0.05	0.46	48.11	1.24
% within 1 S.D.		75	89	64	71	79	68	68	96
% within 2 S.D.		89	93	96	100	93	100	93	96
skew		0.76	1.87	0.80	-0.16	-0.06	-0.05	0.09	3.16
SES		0.93	0.94	0.93	0.93	0.93	0.93	0.93	0.94
significant		N	Y	N	N	N	N	N	Y

Table 6 -Summary of the results for separate analyses of the SU TM4 acidified internal control. Errors expressed at the 95% confidence interval. Outliers have been excluded from all descriptive statistics calculated.

SU TM4 control - acidified	***n***	**Mn**	**Fe**	**Co**	**Ni**	**Cu**	**Zn**	**Cd**	**Pb**
		nmol/kg	*nmol/kg*	*pmol/kg*	*nmol/kg*	*nmol/kg*	*nmol/kg*	*nmol/kg*	*pmol/kg*
2016 avg	10	0.26	0.34	18.23	5.80	1.57	5.83	625.08	6.78
DTM3 Winter	8	0.26	0.27	20.33	5.96	1.65	5.72	640.90	6.62
TM1	6	0.23	0.29	18.69	5.84	1.64	6.03	614.58	6.38
DTM2 Winter	5	0.25	0.30	22.40	5.94	1.65	5.69	628.61	6.36
TM1 Winter	8	0.26	0.30	23.20	6.13	1.68	6.02	657.28	6.90
DTM1 Soluble	4	0.26	0.25	17.31	5.84	1.65	5.66	646.42	6.61
DTM2 Soluble	4	0.26	0.26	16.57	5.86	1.64	5.57	636.96	6.52
DTM3 Soluble	5	0.26	0.26	17.60	5.96	1.68	5.80	648.52	6.60
	50	0.26 ± 0.003	0.29 ± 0.01	19.56 ± 0.69	5.90 ± 0.05	1.63 ± 0.02	5.77 ± 0.06	635.35 ± 4.96	6.61 ± 0.07
total runs		50	50	50	50	50	50	50	50
outliers		2	1	0	1	1	2	1	1
max		0.29	0.37	24.34	6.34	1.85	6.35	674.22	7.33
min		0.23	0.23	15.95	5.57	1.50	5.40	598.77	5.97
mean		0.26	0.29	19.56	5.90	1.63	5.77	635.35	6.61
median		0.26	0.29	18.99	5.90	1.64	5.75	633.62	6.65
S.D.		0.01	0.03	2.48	0.18	0.06	0.19	17.70	0.25
% within 1 S.D.		80	70	56	76	78	84	72	82
% within 2 S.D.		94	96	100	98	96	96	98	94
skew		0.27	0.23	0.37	0.16	0.69	0.49	0.05	-0.18
SES		0.71	0.70	0.69	0.70	0.70	0.71	0.70	0.70
significant		N	N	N	N	N	N	N	N

3.3.3.2. Quality Control Standards

The results of the Quality Control (QC) standards are shown in Figure 9. The QC were analysed after every 6 seawater samples standards were designed to test the ICP-MS sensitivity over a wide concentration range as can be seen by the range of certified QC values (0.97 – 9.70 µg/L). DTM3 displayed remarkable accuracy for all trace elements. A high degree of repeatability was also evident across the suite of trace metals.

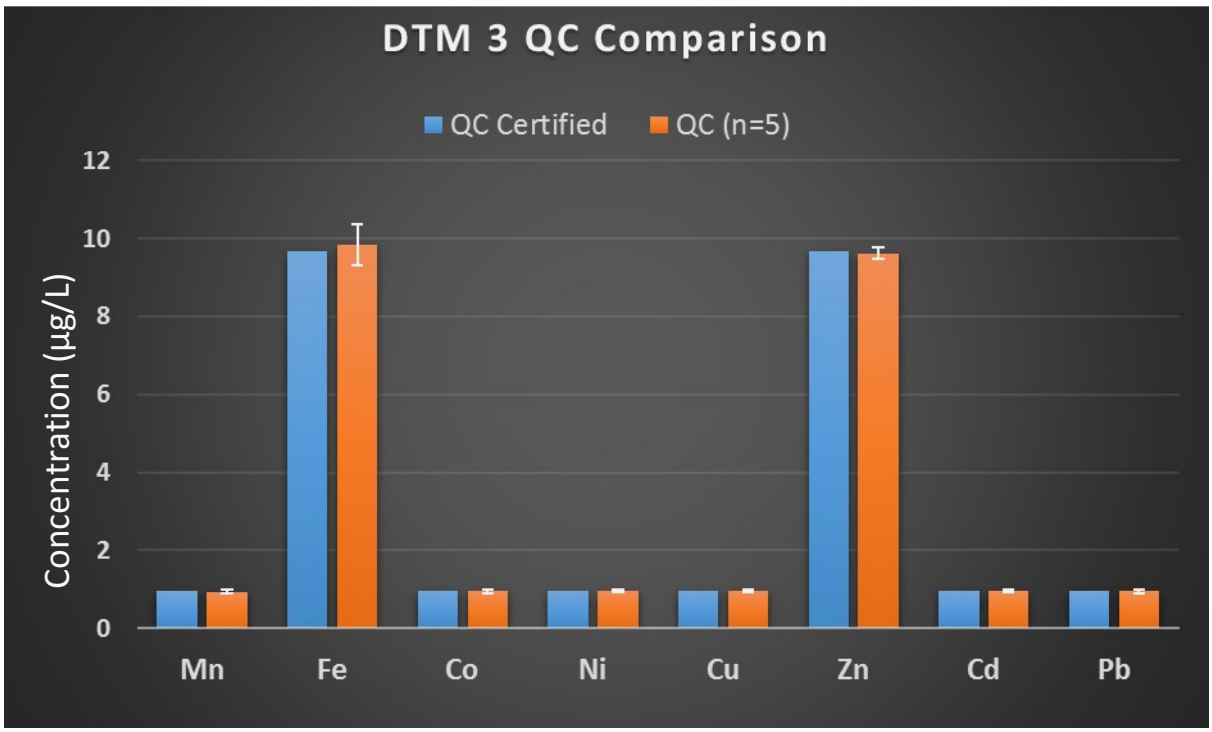

Figure 9 –Selected Quality Control (QC) results from each sample station compared with their respective certified values. Error bars represent 1 SD on either side of the mean.

3.3.4. Calibration Curves

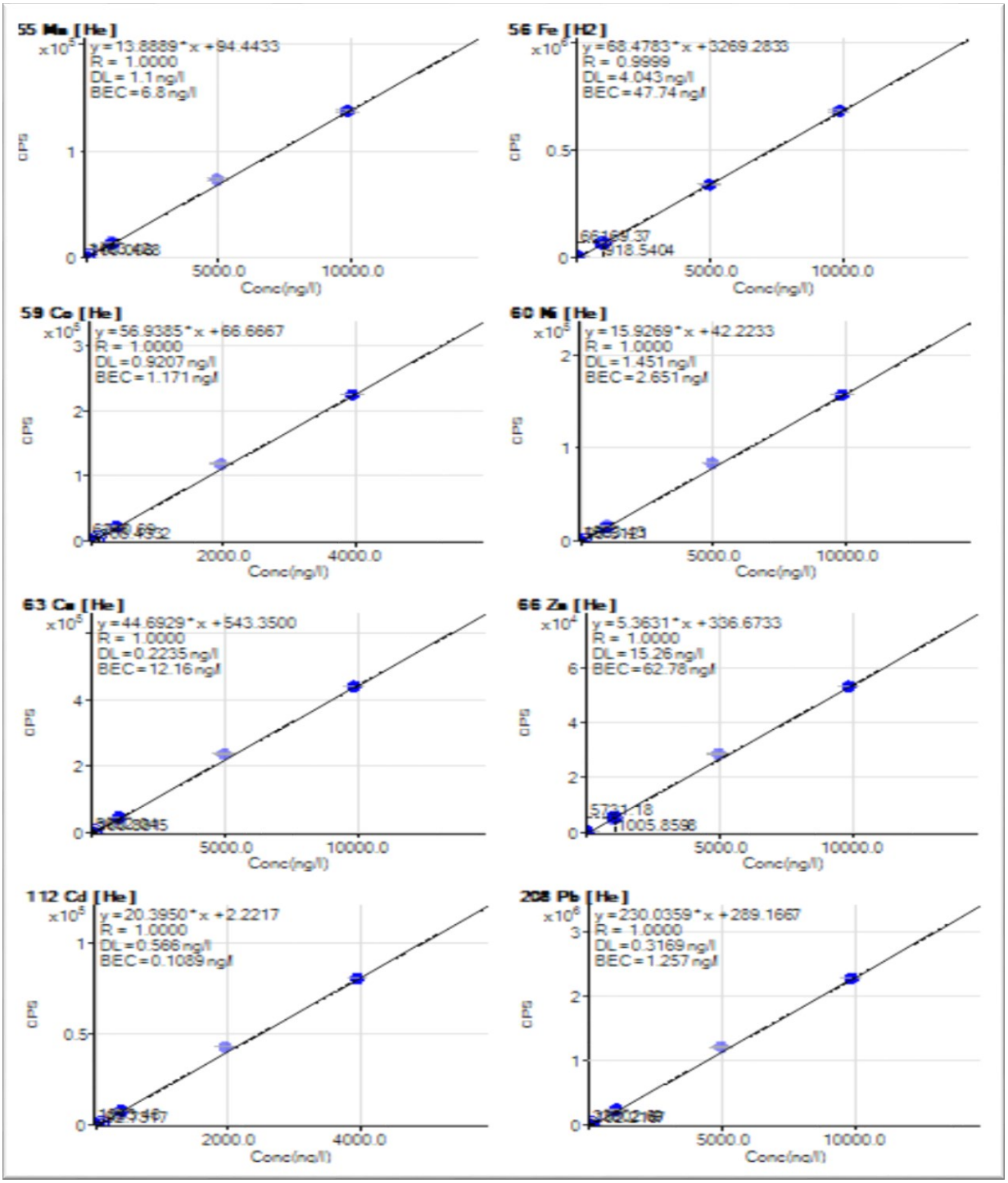

Figure 10 - calibration curves calculated prior to analysis of the intercalibration station.

Figure 10 represents the calibrations curves generated for each trace element during the analysis of seawater samples from the intercalibration station. All calibration curves displayed a linear relationship ($R^2 \cong 1$) between the instrument response and the known concentration of the calibration standard.

3.3.4.1. Calibration Effect

Despite achieving good precision in general for each separate analysis, it was evident from Figure 11 that there existed a significant lack of inter-analysis precision. This also points towards a lack of instrument stability. Prior to the ICP-MS analysis phase, all samples underwent the same processes according to the standardised protocols carried out by the same people under the same conditions. Differences in elemental concentrations observed between analyses can therefore assumed to be due to variations in the ICP-MS calibration. In an attempt to quantify the so called 'calibration effect', the standard deviation (SD) and relative standard deviation (RSD) of each element have been calculated from the mean for each analysis, and compared with the overall combined mean. Averaging the RSD over all the analyses gives an indication of the ICP-MS error induced as a result of re-calibrating the machine before each analysis. Figure 11 shows the summarised results of the calculation for the un-acidified and acidified SU TM4 control respectively. The results show that the calibration contributed between 3.46% (Mn) and 28.05% (Fe) error for the un-acidified standards and between 2.00% (Cd) and 7.16 % (Fe) error for the acidified standards, element dependant. Fe was most affected by re-calibration for both acidified and un-acidified standards. Unfortunately, the ICP-MS is not dedicated to trace metal work and therefore re-calibration is required prior to the analysis of each sample station. These results highlight the importance of attaining similar calibration curves for each re-calibration so as to control all variables contributing to the experimental error.

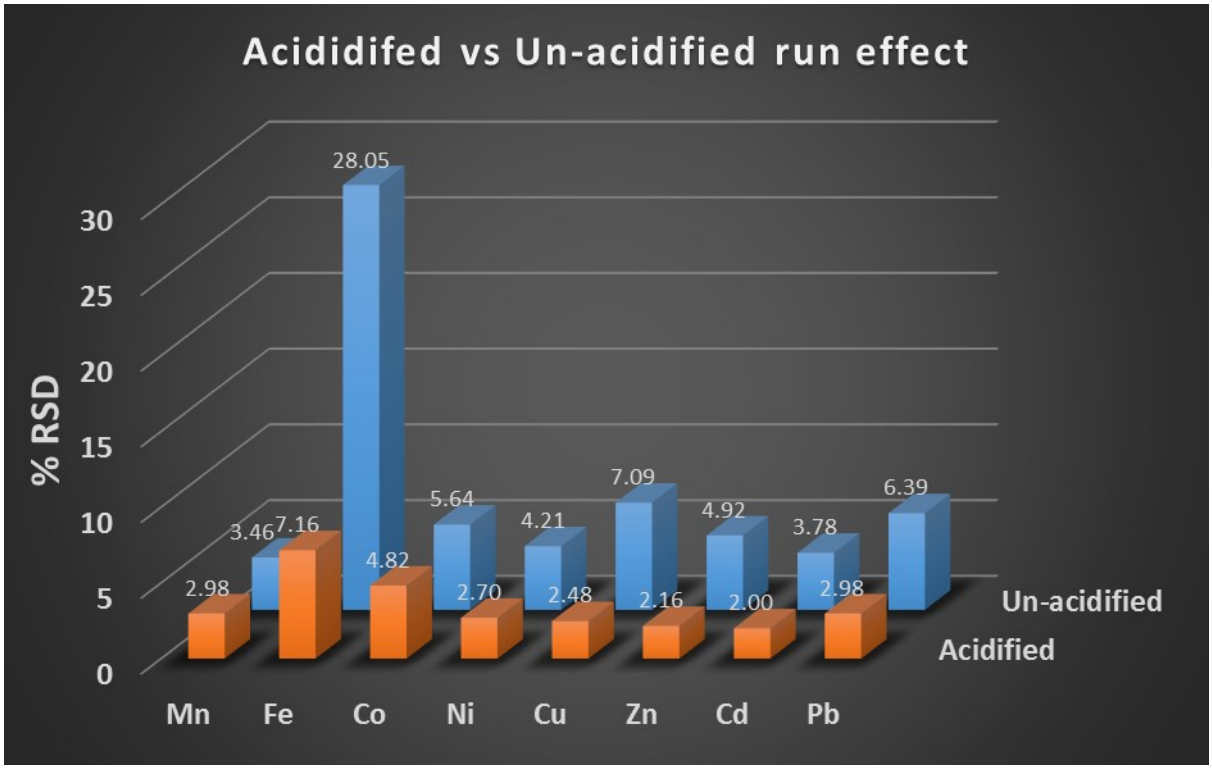

Figure 11 - graphically displaying the contribution that ICP-MS calibration made to the overall precision between analyses.

3.3.5. Blank Measurements and Detection Limits

Calculated detection limits and procedural blank results were compared to those published in four recent studies (Sohrin *et al.*, 2008; Quéroué *et al.*, 2014; Wang, Lee and Ho, 2014; Minami *et al.*, 2015) (Table 7). All four studies described similar analytical methods to this study utilising a commercially available resin, containing the same functional groups, and ICP-MS based quantification step. With the exception of Mn, the detection limits calculated for all trace elements were within the comparative studies ranges. Despite this, Mn was still well below open ocean concentrations. The detection limit calculated for Cu was the lowest of all the studies. Barring the significant blanks for Mn, Fe and Co, all elements showed comparable blanks with Zn showing the lowest blank concentrations by some margin.

The detection limit for ICP-MS without preconcentration was evaluated as three times the standard deviation of the calibration blank and is shown in Table 7 (third column) below. Global ocean mean values (Table 7, fourth column), sourced from Sohrin et al. 2008 for each element are also shown to illustrate the importance of sample preconcentration prior to ICP-MS analysis. Global mean ocean trace element concentrations are notably higher than the corresponding detection limits with the exception of Co, which is bordering on the calculated ICP-MS detection limit. The Southern Ocean mean trace element concentrations are significantly lower than the global mean further emphasizing the importance of preconcentration. After applying a preconcentration factor of 40 to the global ocean mean (Table 7, fifth column), we can confidently say that all trace element concentrations were well above their respective detection limits and were quantitively recovered. Procedural blanks were analysed after every 6 seawater samples throughout the analysis. The procedural blank for each element was less than 0.52% of the mean open ocean concentration but was significant for Mn (13.86%), Fe (54.53%) and Co (28.56%).

*Table 7 - Detection limits and procedural blanks for the Intercalibration station. * Units are pmol/kg. [a] 3SD of calibration blank. [b] data sourced from Sohrin et al. 2008. [c] 40 times preconcentration. [d] not detected. [e] not analysed*

element	measured isotope	detection limit without preconc.[a] (nmol/kg)	Mean conc. in the open ocean[b] (nmol/kg)	mean conc. after preconc.[c] (nmol/kg)	Detection limit comparisons				procedural blank [d]		Blank comparisons			
					Minami et al.	Sohrin et al.	Quéroué et al.	Wang et al.	n	avg. ± SD	Minami et al.	Sohrin et al.	Quéroué et al.	Wang et al.
Mn	55	0.020	0.364	14.56	0.003	0.010	0.002	0.01	6	0.05 ± 0.03	0.001	< 0.01	0.004	0.005
Fe	56	0.071	0.537	21.49	0.090	0.040	0.090	0.19	6	0.29 ± 0.12	0.032	0.033	0.250	0.070
Co*	59	15.241	16.969	678.74	2.000	2.000	0.700	1.00	6	4.85 ± 3.31	0.500	< 2	1.700	1.000
Ni	60	0.024	8.519	340.76	0.070	0.010	0.003	0.03	6	0.04 ± 0.01	0.017	< 0.01	0.013	0.040
Cu	63	0.003	3.147	125.89	0.020	0.005	0.030	0.19	6	0.02 ± 0.01	0.017	< 0.005	0.053	0.020
Zn	66	0.228	4.589	183.54	0.100	0.060	n.a.[e]	0.21	6	0.02 ± 0.00	0.120	0.071	n.a.[e]	0.090
Cd*	112	4.913	622.721	24908.82	2.000	9.000	0.120	0.50	6	0.85 ± 0.57	< 2	< 9	0.190	1.000
Pb*	208	1.492	9.653	386.10	0.900	1.000	0.200	1.00	6	n.d. [d]	0.300	1.600	0.720	1.000

3.4. Discussion

3.4.1. Validation of Sampling Protocol

3.4.1.1. Laboratory Based Intercalibration with University of Plymouth

It is evident from Figure 6 that the vertical DFe profiles constructed from analysis during this study and the results received from an intercalibration with the University of Plymouth (UK) mirror each other very closely. The exception to this observation is an apparent deviation of the two profiles from each other between the 250 and 450 metres depth. Results from this study show a distinct peak between these depths with a peak concentration of 1.82 nmol/kg at 350 metres depth. On the other hand, the intercalibration data received displays a less prominent peak concentration of 1.05 nmol/kg at 400 metres depth. This difference can be attributed to a difference in sample resolution. 16 of the 23 depths sampled were sent to the University of Plymouth. Crucially samples from depths 300 and 350 metres were not included in the 16 samples sent for analysis as seawater from the respective GO-FLO bottles ran out before sub-sampling for the intercalibration exercise could begin. Comments regarding the distinct concentration peak at 350 metres depths are therefore limited. The fact that the comparative concentrations at 250, 400 and 450 metres are very similar and highlights the analytical accuracy achieved for this intercalibration. It is important to note that despite this successful comparison, precision was a slight issue at multiple depths. A number of results (6) were rejected as the %RSD was greater than 15%. Indeed, throughout the study, Fe was the least precisely measured element. Although sensitivity issues with respect to the ICP-MS can be cited this is unlikely. This lack of precision indicates a possible contamination of the sample during the collection, sub-sampling or preconcentration process. Fe is arguably the most prone element to contamination which can arise from a number of situations, the most likely being the fact that the ICP-MS unit is not housed in a class 100 clean lab. Despite following stringent trace clean protocols, the possibility of Fe particulate being deposited into the sample while it is exposed on the analysis rack is a possibility. With the exception of these issues, these results are very significant as this intercalibration station provided sufficient evidence for us to conclude that our vertical profile sampling sample collection protocol is validated in facilitating the collection of contamination free seawater samples.

3.4.1.2. Cross-over Station with Klunder et al. 2011

The results of the cross-over station at 54°S were also compared to data reported in a study conducted by Klunder et al. 2011 at the same location in 2008 . The depths sampled and reported in this study were pre-determined to coincide with those of Klunder et al. 2011 and allowed for direct DFe comparisons throughout the water column. The difference in sampling period between these two

studies plays a major role in explaining differences between the vertical profiles shown in Figure 7. Samples analysed by Klunder et al. 2011 were collected between 10 February and 14 April (2008) compared to DTM3 sample which were collected on the 15 January (2015). Due to the natural short term variability of the ocean, trace metal concentrations are constantly changing. A recent deposition of aeolian dust originating from the Patagonia Desert in South America was suggested to be the reason for the abnormally high surface concentration of 0.51 nmol/kg for DFe (Klunder *et al.*, 2011). This value is more than double the concentration of 0.24 nmol/kg reported for this study and suggests no such depositional event took place prior to our occupation of this location. Collecting seawater samples later into the Summer, as in the case of Klunder, meant that the effects of the Summer phytoplankton blooms were dissipating resulting in the settling out of dissolved trace metals, via dead sinking organic material, thereby increasing deepwater concentrations. Hydrothermal activity, a known source of dissolved trace metals to deepwaters (Heller and Croot, 2014), is a likely possibility for the comparatively elevated deepwater DFe concentrations published by Klunder et al. 2011 who noted a strong hydrothermal plume rich in dissolved Fe and Mn between 52°S and 56°. Analysis of the dissolved Fe and Mn profiles obtained at 54°S in this study reveal no such elevated characteristics and suggests hydrothermal activity was less prominent during the time of this study. It is interesting to note the lack of a DFe peak between 250 and 450 metres in the data reported by Klunder et al. 2011 when compared to the data reported from this study. There is a large seamount present at 54°S which extends to within 1000 metres of the sea surface (figure 12 and 13). It is possible that during our occupation of this location, upwelling currents re-suspended Fe containing silt from the sides of this seamount thereby elevating concentrations of dissolved iron above it. Similar concentration peaks were observed for Mn, Co, Pb, Cd and Zn further justifying the re-suspended material as a result of upwelling currents. In figure 12, a cross-section of DFe distribution along the Bonus Goodhope Line sourced from the GEOTRACES website, this is clearly visible as a localised area of high (1.00 - 1.25 nmol/kg) DFe concentrations situated above the seamount and coincides very well with our observations (Figure 13 top cross section). Interestingly however, we did not observe deepwater concentrations as high as observed in Figure 12 at 54°S. Comparing both datasets reveals a good agreement between DFe concentrations observed at the other cross-over stations. Both datasets agree on an approximate DFe range of 0.1 -1.8 nmol/kg showing similarities in areas of local enrichments and depletions. A lower sample resolution for this study resulted in these areas being less defined. Comparing the results of measured DCu with previous work in the Southern Ocean (Boye *et al.*, 2012; Heller and Croot, 2014) and for DZn by (Croot, Baars and Streu, 2011; Wyatt *et al.*, 2014) reveals similarly well correlated datasets. See chapter 4 for a more in depth comparison. Taking into consideration the difference in sample collection period and the variable nature of ocean waters, the

sample collection protocol is effective in collecting variable nature of ocean waters, the sample collection protocol is effective in collecting contamination free seawater samples.

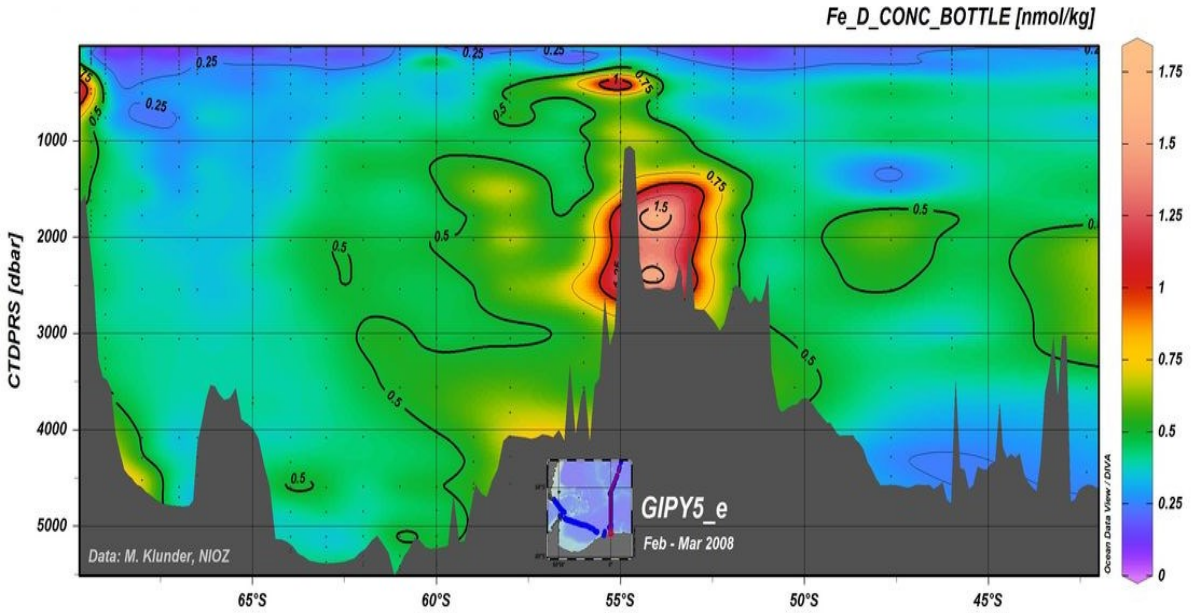

Figure 12 - Dissolved Fe along the Bonus Goodhope Line. Section taken from www.geotraces.org.

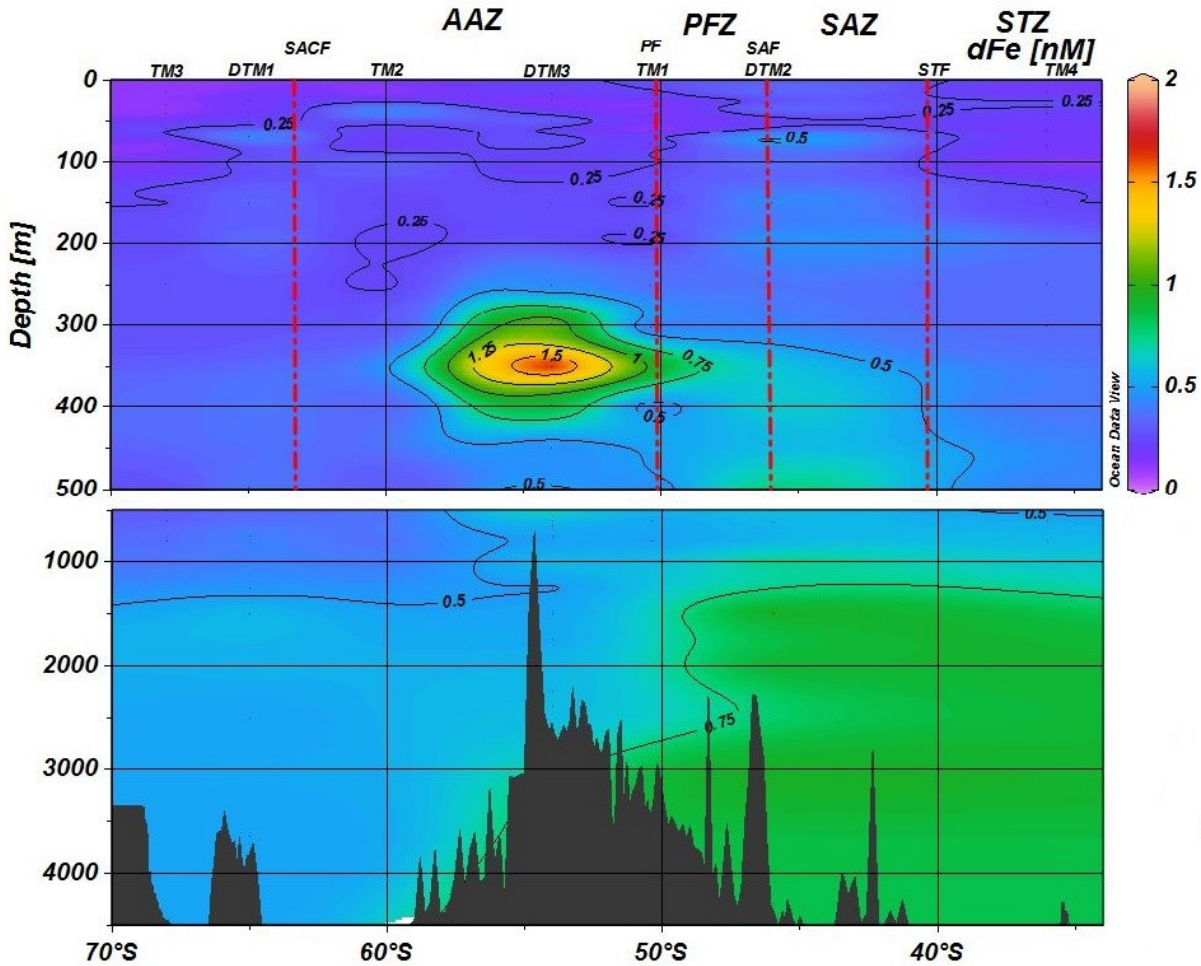

Figure 13 – Dissolved Fe measured along the Bonus Goodhope Line during this study. Figure compiled using Ocean Data View (ODV).

3.4.2. Certified Reference Material

The comparison of the SAFe standards with their corresponding certified values reveals a good general agreement with all results, except Cu and Co, falling within the stipulated upper and lower limits (Table 4). Measured Zn (7.23 ± 0.25 nmol/kg) was in excellent agreement with the consensus value of 7.43 ± 0.25 nmol/kg. Measure Fe against consensus also warrants mentioning with only a 0.03 nmol/kg difference between the two.

Concentrations for Co, and to a lesser extent Cu, for the SAFe D2 standard was slightly lower than the respective consensus value. The under-estimation of these trace metal quantities was 29% for Co and 11% for Cu. The reason for this can be explained by differences in the seawater chemistry when the standards undergo Ultra Violet (UV) oxidation prior to ICP-MS analysis. UV oxidation was performed on all reference samples whose results contributed to the determination of SAFe consensus values. This process is critical in quantifying the total dissolved trace metal fraction (free and organically bound metal ions combined). It has been demonstrated that a large fraction of trace metals present in seawater, in particularly the bioactive trace metals Fe, Zn, Cu, Co and Cd, are present as chelates with a strong tendency to bind themselves to organic matter inherently present in the water column (Milne *et al.*, 2010). It is therefore necessary to solubilise these metal-organic complexes prior to the determination of the total dissolved metal concentration as, without solubilisation, these complexed ions pass through the chelating resin contained within the pre-concentration module without being extracted. This results in the underestimation of the total dissolved trace metal fraction. Solubilisation is achieved by sample acidification directly after the sample collection however it has been shown that acidification is not adequate to release all organically bound Co and Cu metal ions specifically as these metals display very strong complexation (Biller and Bruland, 2012). To account for this, UV oxidation, which is a strong enough treatment to break the remaining Co and Cu metal-organic bonds, is prescribed. UV oxidation was not performed on samples prior to analysis which explains the reason why the SAFe concentrations for Cu and Co are lower compared to their respective consensus values. UV oxidation was not performed on seawater samples contributing the NASS-5 consensus values and hence we do not see the underestimation of Co and Cu. The results of the certified reference material validate the accuracy and reproducibility of the offline preconcentration coupled ICP-MS analytical technique.

3.4.3. Internal Standard

3.4.3.1. SU TM4 Control

The variability seen in the Fe concentrations of the SU TM4 un-acidified control was first thought to have been due to contamination of the sample during either the preconcentration or the ICP-MS analysis stage. One would expect a contamination signal to show as a distinct spike in one of the Fe values however the results appear to show a more consistent deviation (0.03 nmol/kg) from the mean (Table 5). Bearing the typical contamination signal in mind, it is possible that the spike in Pb concentration obtained during the 2016 std analysis is as a result of contamination (Appendix B). To alleviate the inconsistencies for Fe, and in an attempt to increase precision for the rest of the elements, it was decided to acidify the SU TM4 control. Acidification destroys the bonds between organic ligands and the metal ions which, if left un-acidified, will pass through the preconcentration process without being extracted. The combination of un-acidified seawater and decanting from a large volume sample meant that the possibility of having varying amounts of organically bound metal ions in each sample vial was possible. The fact that the acidified TM4 control results were higher for all elements, between 9% for Cd and 69% for Cu, proved the contribution of the organically bound fraction to be significant although precipitation of these trace metals at seawater pH may also be contributing to the lower observed values for the un-acidified controls. According to (Ellwood and Van den Berg, 2001; Lohan *et al.*, 2005), trace metals exhibiting the strongest tendency to complex with organic ligands are Fe, Zn, Cu, Co and Cd. In theory, these trace metals should show the highest increase in concentration after acidification. Comparison of the mean trace metal values in tables 5 and 6 shows our observations to be only partly aligned with this theory, with some elements such as Zn and Co showing relatively small increases. In such cases it is important to consider the strength of complexation for each element. For elements such as these, the complexation out competes the acidification which is why UV oxidation is a necessary pre-treatment step prior to analysis of total dissolved fraction (Achterberg *et al.*, 2001). The seemingly small concentration increases displayed by these elements is therefore justified by the fact that samples in this study were not UV oxidised prior to preconcentration and ICP-MS analysis. Acidification of the standard proved successful in not only increasing the precision of Fe concentrations but all metals analysed. In addition to this, the smaller volume of the acidified standard and the fact that we shook the sample prior to decanting, meant increased homogeneity in the sample vial.

The fact that the acidified standards yielded more outliers than the un-acidified standard seems counter-intuitive. This is however as a result of the overall standard deviation for the unacidified standard being greater than the acidified standard. The upper and lower bounds defining

acceptable results is therefore smaller for the acidified standard. A sample which may not be classified as an outlier for the un-acidified standard may be classified as an outlier for the acidified standard. In addition, the two outliers in the un-acidified standard contribute a disproportionate amount to skewing the mean as they are anomalously high. If statistical analysis were to be performed on the dataset with the original outliers omitted, there would likely be an increase in the number of outliers owing to a decrease in the interval defining 3 S.D. This suggests that the number of outliers is not a good indication of how precise the data is. All elements except two, namely Fe and Pb from the un-acidified SU TM4 control dataset, displayed normal distributions. Results which are spread evenly around the mean are encouraging in this study as it suggests there is no relationship between analysis time and decreased sensitivity on ICP-MS. For Fe and Pb, analysis of their distribution plots reveals that the results of DTM3 and the 2016 stds analysis (2) respectively have had a disproportionate effect on the shape of the distributions owing to their comparatively low concentrations relative to the rest of the analyses (Figure 15). The resulting positive skewness is visible from the left side of Figures 14 and 15 where the sample points are concentrated to the left of the mean. Removal of the data from these stations results in a normal distribution for both elements as seen by the right hand side of Figures 14 and 15. It is not coincidental that Fe and Pb were the two elements whose results were most affected by the 'calibration effect' explained earlier (Figure 11) and again highlights the importance of accurate calibration prior to analysis.

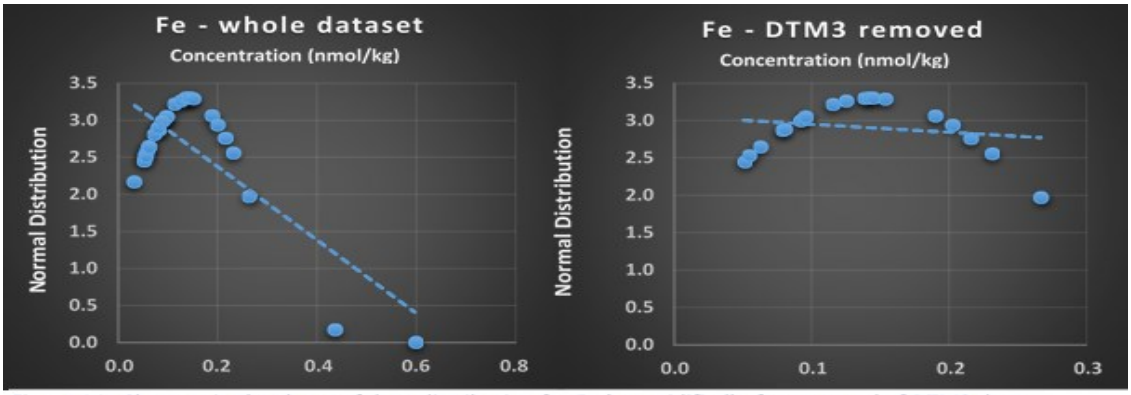

Figure 14 - Changes in the shape of data distribution for Fe (un-acidified) after removal of DTM3 data.

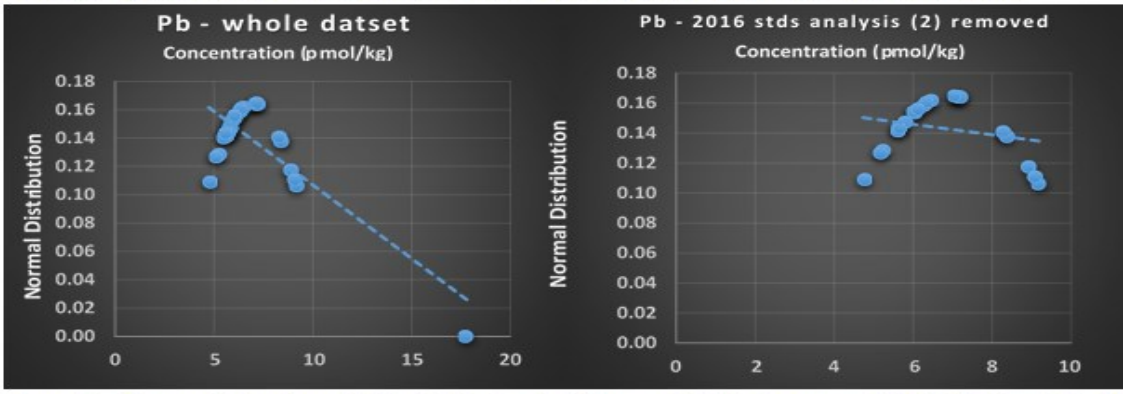

Figure 15 - Changes in the shape of data distribution for Pb (un-acidified) after removal of 2016 stds analysis (2) data.

3.4.3.2. Quality Control Standard

Assuming the certified QC values are in fact correct and no contamination has ruined the integrity of the standards, the persistent underestimation of all trace element concentrations within a single analysis tends to suggest a decrease in the sensitivity of the ICP-MS. This is however only marginally true for the DTM2 (46°S; 0°) analysis run. Upon closer inspection of each individual QC measurement, there is a small yet consistent decrease in elemental concentrations, with the exception of Zn which displayed no apparent trend, between the first and last QC standard analysed. The fact that no other analysis showed such a relationship and that results from the DTM3 analysis run proved remarkably accurate and precise, discounts any issues regarding decreased in-run ICP-MS sensitivity. The labelling of the obtained elemental data as 'underestimated' according to the certified value may be brought into question. For stations DTM1 (with the exception of Fe as already noted), DTM2 and TM1 the 'underestimation' appears relatively uniform at roughly 1 SD. This brings into question the integrity of the quality control standard and an error during the preparation of the standard cannot be ruled out. The consistently elevated Fe values obtained during the DTM1 analysis may be as a result of possible contamination of the standard either by Fe rich atmospheric fallout or during the preparation process.

Taking into account the intercalibration station comparisons, certified reference material results as well as the SU TM4 and QC internal control results, the seaFAST-pico SC-4 DX preconcentration modules ability to preconcentrate multiple elements simultaneously from a single 14 ml aliquot has ultimately been proved. The use of a polyaminocarboxylic acid, containing EDTA and IDA, as a functional group immobilized on the resin, has allowed the separation of trace metals from their seawater matrix while removing potential sources of ICP-MS interference such as alkali and alkaline earth metals (Na, K, Mg, Ca and Sr). This exclusion ability for alkali and alkaline earth metals is particularly attractive to the analyses of seawater due to the high concentrations of these metals inherent in the seawater matrix (Kagaya et al., 2009). Previous studies utilising a resin containing the same functional groups as this study reported removal of >99.998% of these elements from seawater (Minami *et al.*, 2015). Furthermore, the presence of two functional groups on the resin has expanded the range of pH within which trace metals can be adsorbed. Sohrin et al. 2008 showed the effects of sample pH on individual trace element recovery and concluded that a pH range between 6-7 is optimal for all target metals. The sample buffer range employed in this study was 6.0 ± 0.2, as recommended, which is well within the optimal range and also minimises the collection percentage of alkaline earth metals which was seen to be significant at pH > 7 (Sohrin *et al.*, 2008). As new reagents and buffer solution, and hence a new buffer pH, had to be prepared before each preconcentration session, it

provides a measure of the robustness of the method. The columns ability to produce quantitive results despite these variations is evidence of this validation parameter.

3.4.4. Blank Measurements and Detection Limits

Significant blanks were observed for Mn, Fe and Co during the analysis of seawater samples from the intercalibration station. This usually suggests decreased ICP-MS sensitivity due to a number a reasons e.g. alkali and alkaline earth metals causing interferences in trace element signal. Significant blanks are not desirable as it means the trace metal concentrations could be overestimated. Inspection of the individual blank measurements however reveals a general trend of insignificant blanks at the beginning of the ICP-MS analysis which increase to significant blanks toward the end of the analysis session (Figure 16). The vial containing the procedural blank solution is left uncapped in the rack during analysis (approx. 2 hours) therefore exposing it to contamination sources such as atmospheric deposition. Despite adhering to strict trace clean protocols, the ICP-MS machine is not housed in a class-100 clean lab and so the air is not filtered for particulate. Vials containing seawater samples are uncapped 3 at a time (6 mins) therefore any risk of external contamination of the sample can be deemed negligible.

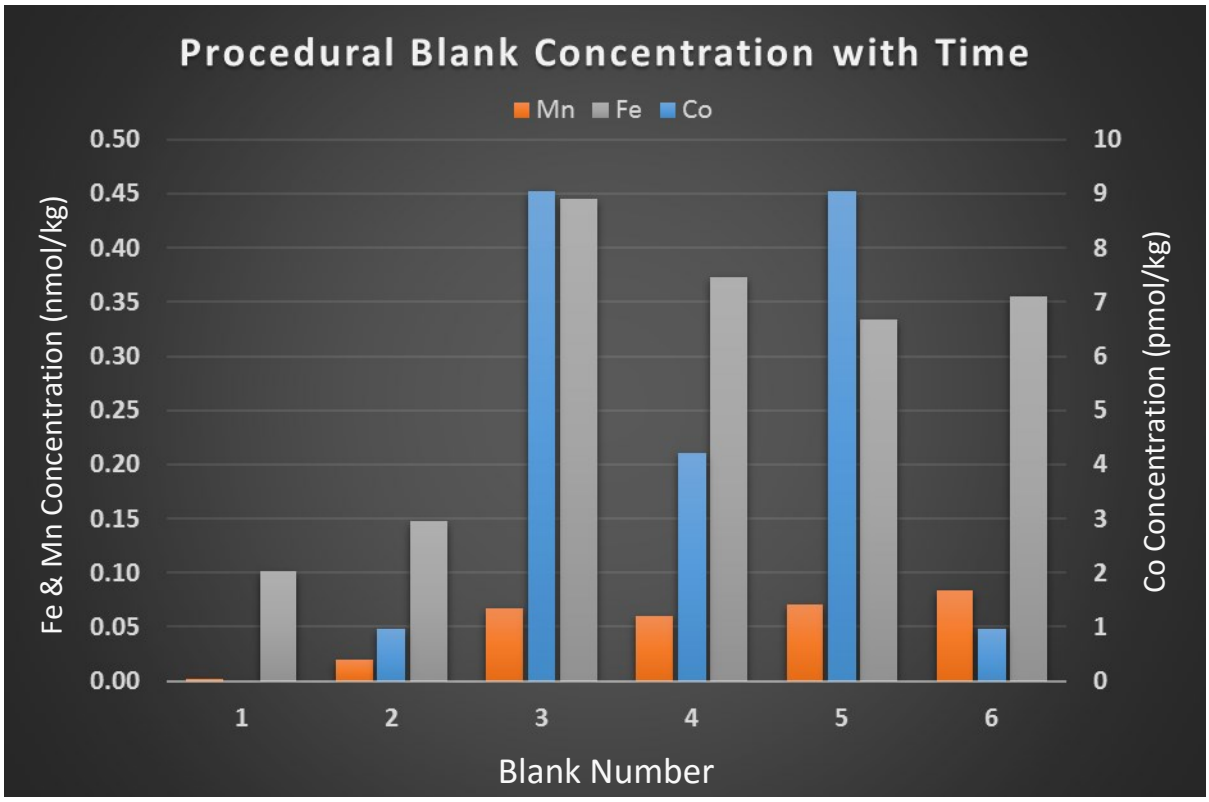

Figure 16 –increasing Mn, Fe and Co procedural blank concentrations over the ICP-MS analysis period.

The detection limits and procedural blanks obtained from this study were compared to those published in four recent studies. Despite analytical methods being consistent throughout all studies, equipment specification and operating conditions vary. Whereas Sohrin et al. 2008 used an ICP-MS for trace element determination, as in this study, Quéroué et al. 2014 and Wang et al. 2014 both utilised a sector field ICP-MS while Minami et al. 2015 employed a high resolution ICP-MS. This combined with different optimization conditions, see chapter 2, can explain the slight variations in analytical sensitivity observed in Table 7. The ICP-MS machine used in this study has proven to produce extremely low detection limits and comparatively low procedural blanks for suite of trace elements.

4. Total and Dissolved Copper and Zinc in the Southern Ocean

4.1. Results

4.1.1. Hydrographic setting

4.1.1.1. Frontal systems and biogeochemical domains

The Southern Ocean is not a singular biogeochemical system. Distinct biogeochemical domains exist which are characterised by unique salinity and temperature signatures as well as macronutrient and chlorophyll-a (chl-a) concentrations (Gladyshev *et al.*, 2008). The presence of deep reaching frontal systems, which serve as the boundary between these domains, directly influences the physical and biological distribution of trace metals along this transect and highlights the importance of having sample stations strategically located around these frontal zones. It is important to note that in reality, the positions of the fronts vary greatly in time. This is most notable for the Subtropical Front (STF) as a response to large variations in the wind stress field.

The transect crossed the Subtropical zone (STZ), the Antarctic Circumpolar Current (ACC) and entered the Weddell Gyre (WG) (Figure 2). The STZ southwest of Africa extends to the Subtropical Front (STF) which was located at 40°54'S during the cruise. The STF forms the northern boundary of the ACC which extends until the Southern Boundary (SBdy), located at 55°54'S (Bown *et al.*, 2011; Le Moigne *et al.*, 2013). The Weddell Gyre (WG) forms the southernmost domain of the transect and extends until the Antarctic ice shelf at ~ 69°S. Within the ACC, the Subantarctic Zone (SAZ) is bounded in the south by the Subantarctic Front (SAF) at 46°38'S while the Polar Frontal Zone (PFZ) is bounded to the south by the Antarctic Polar Front (APF) at 50°37'S (Figure 2).

4.1.1.2. Water masses

In addition to the biogeochemical domains outlined prior, water masses also define the horizontal and vertical hydrographical regime throughout the transect. These water masses are identified by unique temperature and salinity signatures which ultimately control the water masses position in the water column based on its density relative to other water masses.

Surface waters at TM4 (36'S) are characterised by a very high surface temperature (± 20 °C) and salinity (35.4 ppt) signature compared to the stations further South. Surface water stratification in this region is controlled predominantly by temperature (Croot, Baars and Streu, 2011) whereas sub surface stratification south of 50°S sees salinity dominating as a result of fresh melt water influxes (Figure 17) (Pollard, Lucas and Read, 2002). Stations located within the PFZ (DTM2 and TM1) have Sub-Antarctic Surface Water (SASW) characterizing the upper 200 metres of the water column. Surface

waters south of the APF (DTM3, TM2, DTM1 and TM3), and extending all the way to the Antarctic shelf, are classified as Antarctic Surface Waters (AASW) (S < 34.40; Θ < 0.5°C) and occupy the upper 300 metres of the water column. Antarctic Intermediate Water (AAIW) (S ~ 34.20; 2.9°C < Θ < 0.5°C) is found below surface waters throughout the PFZ as it subducts northwards to depths of between 300 and 600 metres near the SAF (Le Moigne *et al.*, 2013). Below the AAIW, at depths between 1500 – 3000 metres, is Upper Circumpolar Deep Water (UCDW). This water mass flows southwards while simultaneously shallowing. UCDW is in turn underlain by North Atlantic Deep Water (NADW). Further south, NADW is replaced by the saltier (S < 34.70) Lower Circumpolar Deep Water (LCDW). Bottom waters in the Weddell Gyre are identified as Antarctic Bottom Waters (AABW) and have characteristic temperature minimums (Boye et al, 2012) (Figure 18).

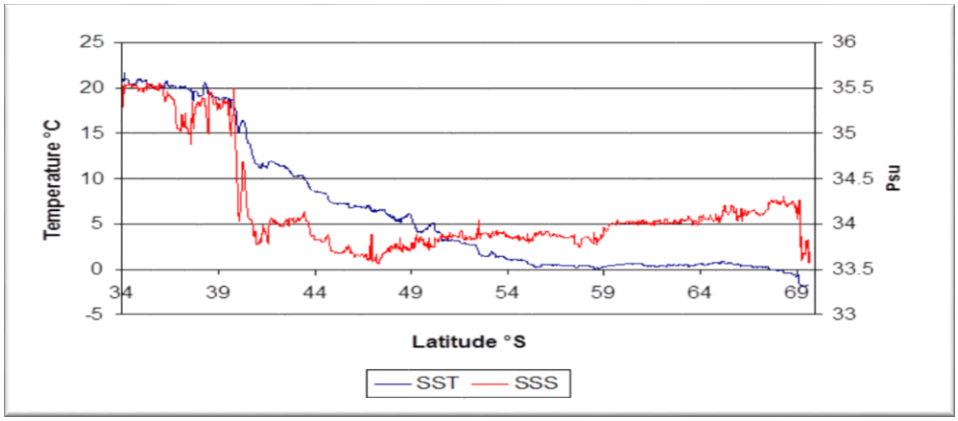

Figure 17 - thermosalinograph illustrating temperature (north of 50°S) and salinity (south of 50°S) controlling sub-surface stratification. Salinity defined as practical salinity units (psu) equivalent to per thousand.

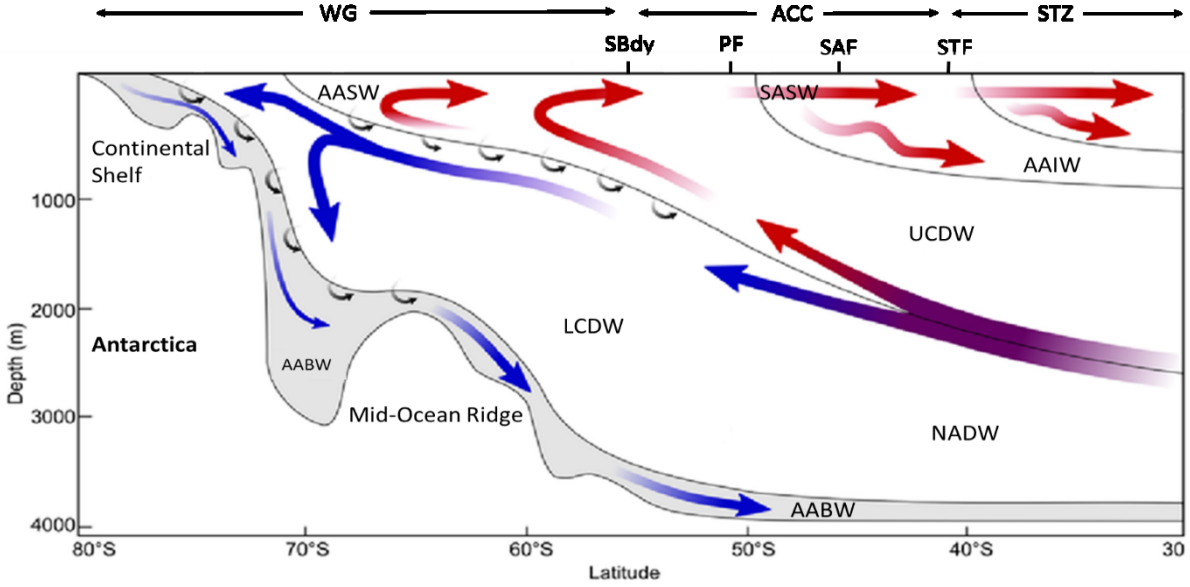

Figure 18 - summary of the hydrographic regimes encountered during the expedition. Abbreviations in alphabetical order: AASW: Antarctic Surface Water; AAIW; Antarctic Intermediate Water; AABW: Antarctic Bottom Water; ACC: Antarctic Circumpolar Current; LCDW: Lower Circumpolar Deepwater; NADW: North Atlantic Deepwater; PF: Polar Front; SAF: Sub Antarctic Front; SASW: Sub Antarctic Surface Water: SBdy: Southern Boundary; STF: Sub Tropical Front; STZ: Sub Tropical Zone; UCDW: Upper Circumpolar Deepwater; WG: Weddell Gyre. Schematic adapted from (Alberto C. Nav, 2012).

4.1.2. Biogeochemical features along the transect

Contrasting biogeochemical provinces were crossed along the transect, generally characterised by a southward increase in Mixed Layer Depth (MLD) macronutrient (NO_3^-, $Si(OH)_4$ and PO_4^{3-}) concentrations. The STZ was characterised by extremely low - sub-nanomolar - concentrations of all three macronutrients (figure 19). Depleted $Si(OH)_4$ concentrations persisted in surface waters (< 500 metres) until the APF whereas NO_3^- and PO_4^{3-} increased steadily southward through the SAZ and PFZ where maximum concentrations of 2 µM and 20 µM respectively were observed. Surface (10 metres) chl-a concentrations were lowest (0.03 µg L^{-1}) in the STZ where the phytoplankton community assemblage was >90% cyanobacteria (Figure 20. Viljoen, 2016).

In the vicinity of the SAF, surface chl-a, dominated by a combination of diatoms and haptophytes (Figure 20. Viljoen, 2016), was low at < 0.2 µg L^{-1} and remained low (< 0.5 µg L^{-1}) throughout the MLD of 100 metres. The PFZ had a MLD depth of ~ 112 metres, the deepest observed along the transect, coinciding with the centre of the ACC. At the APF, Haptophytes were the major phytoplankton species while diatoms were also in relative abundance contributing 40% and 32% to the total assemblage respectively. Productivity within the MLD in this region was high with chl-a > 1.0 µg L^{-1} despite lower surface chl-a concentrations of ~0.1 µg L^{-1} (Figure 20. Viljoen, 2016). In the PFZ between 400 and 1500 metres, a localised lens of high (< 3 µM) PO_4^{3-} was observed (Figure 19 middle). The influence of a diatom based community structure is most evident in the ACC where silicate concentrations were low (< 5.0 µM) in the late austral summer while nitrate and phosphate levels were in comparative abundance. Conversely, the southern side of the ACC was marked by increased silicate levels (< 125 µM), and high nitrate and phosphate, in the surface waters. Early spring blooms of large diatoms have been reported in the PFZ, the result of which is the depletion of silicate in the Polar Frontal Zone over the productive season, hence resulting in the southward migration of the sharp gradient of silicate observed in late summer (Le Moigne et al. 2013). The flourishing diatoms are heavy silicified due to iron limitation, whereas their biological uptake of nitrate can decrease. This causes a strong depletion of silicate relative to nitrate (Baars et al. 2014). The southern extent of the ACC exhibited low productivity from a predominantly diatom phytoplankton assemblage with lesser amounts of dinoflagellates and haptophytes.

In the WG, PO_4^{3-} concentrations displayed both a vertical and meridional homogeneity of ~2 µM. In the WG, north of 64°S, both $Si(OH)_4$ and NO_3^- displayed a tongue of elevated concentrations, 150 µM and 35 µM respectively, between 200 and 1000 metres (Figure 19). Further south, strong vertical gradients were observed for both macronutrients which displayed their highest

concentrations in the AABW near the Antarctic shelf. Productivity appeared higher in the WG where diatoms and haptophytes contributed between 45 – 55% and 40 – 50% to the assemblage respectively. At 65°S a very distinct sub-surface chl-a maximum was observed with values peaking at 3.81 µg L^{-1} at 40 metres depth before decreasing rapidly to values of <1 µg L^{-1} at 69 metres depth roughly coinciding with the MLD. Interestingly, 0.57 µg L^{-1}, the highest surface chl-a concentration observed during the transect was found at 68°S. These values did not persist throughout the MLD (95 metres) resulting in this location being the least productive in the WG.

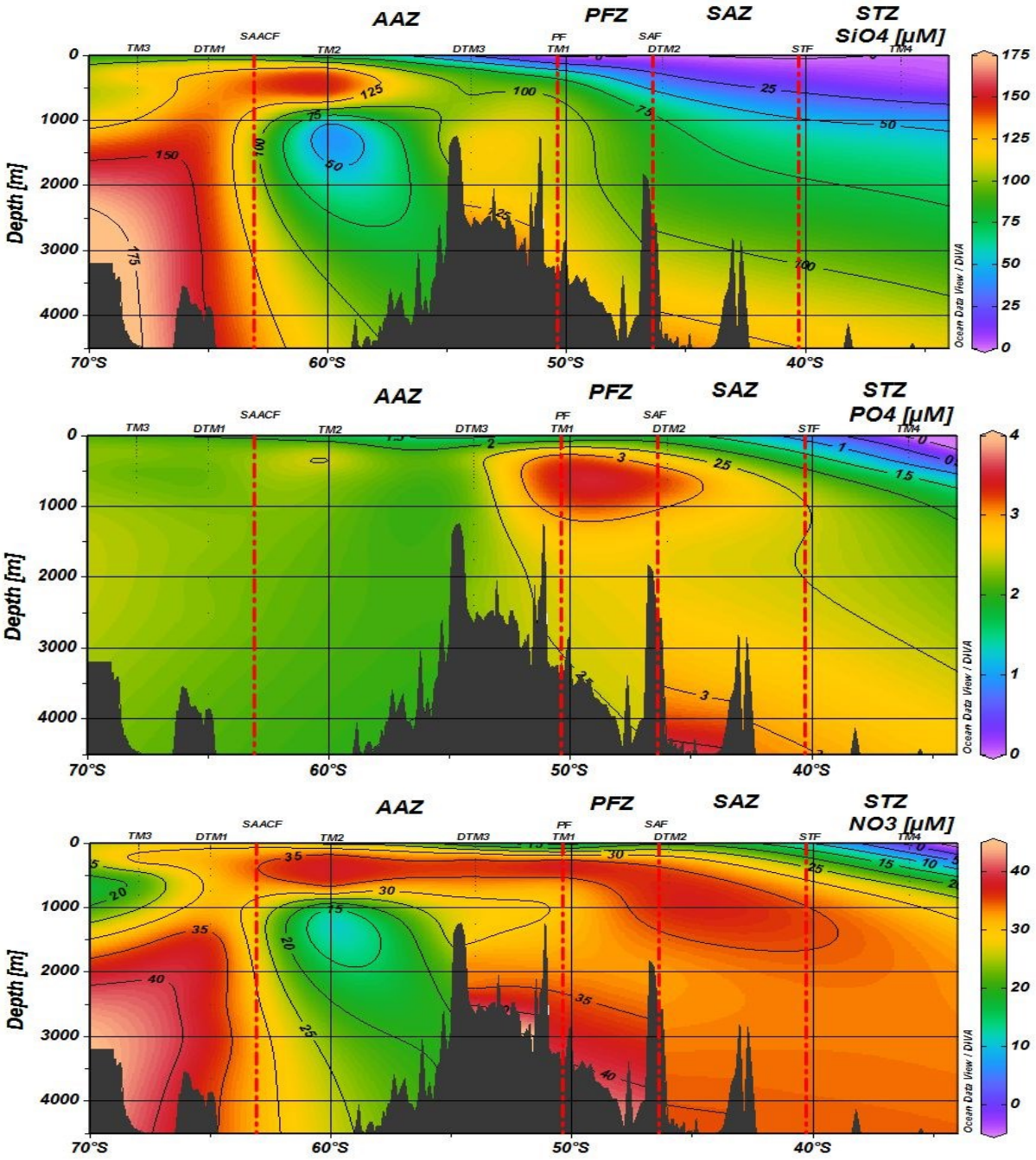

Figure 19 – Figures show colour and contour plots for the concentrations of the macronutrients silicate (top), phosphate (middle) and nitrate (bottom) along the transect. Dots indicate datapoints. Sampling station locations are shown relative to the position of major fronts encountered. Figure compiled using Ocean Data View (ODV).

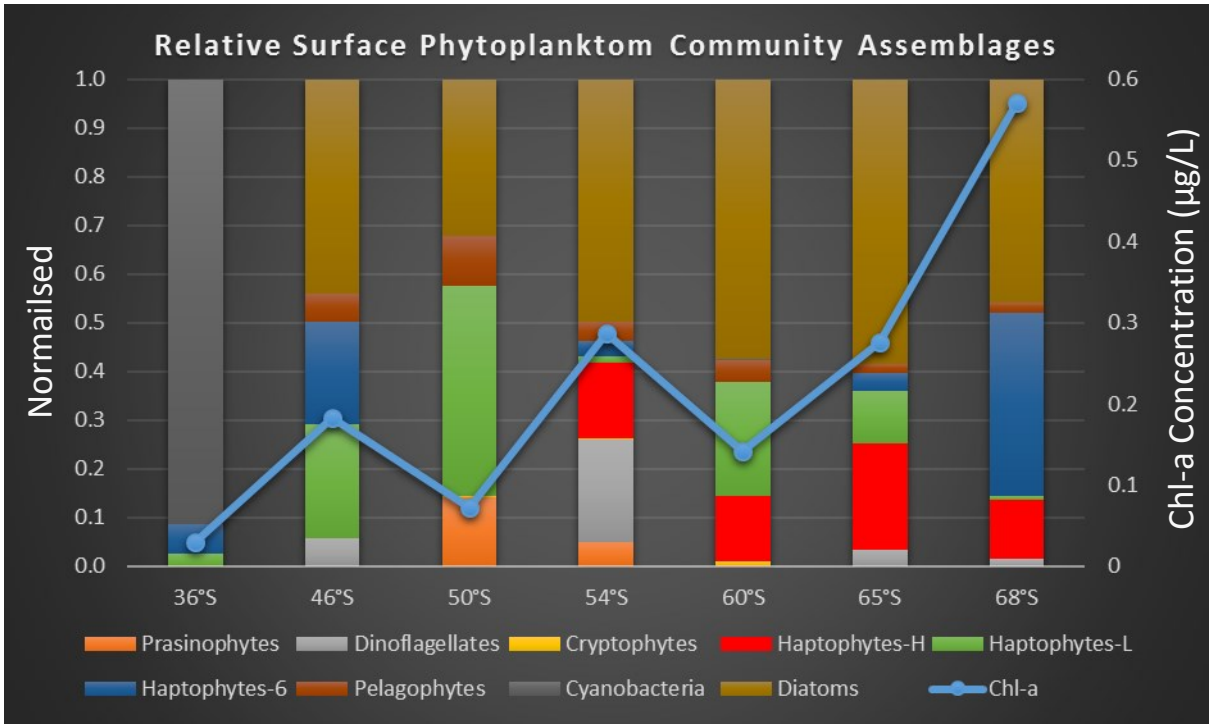

Figure 20 –normalised surface (10 m) phytoplankton community assemblages with corresponding chl-a concentrations. Data sourced from (Viljoen, 2016)

4.1.3. Meridional and Vertical distribution of Total Copper (TCu) and Zinc (TZn)

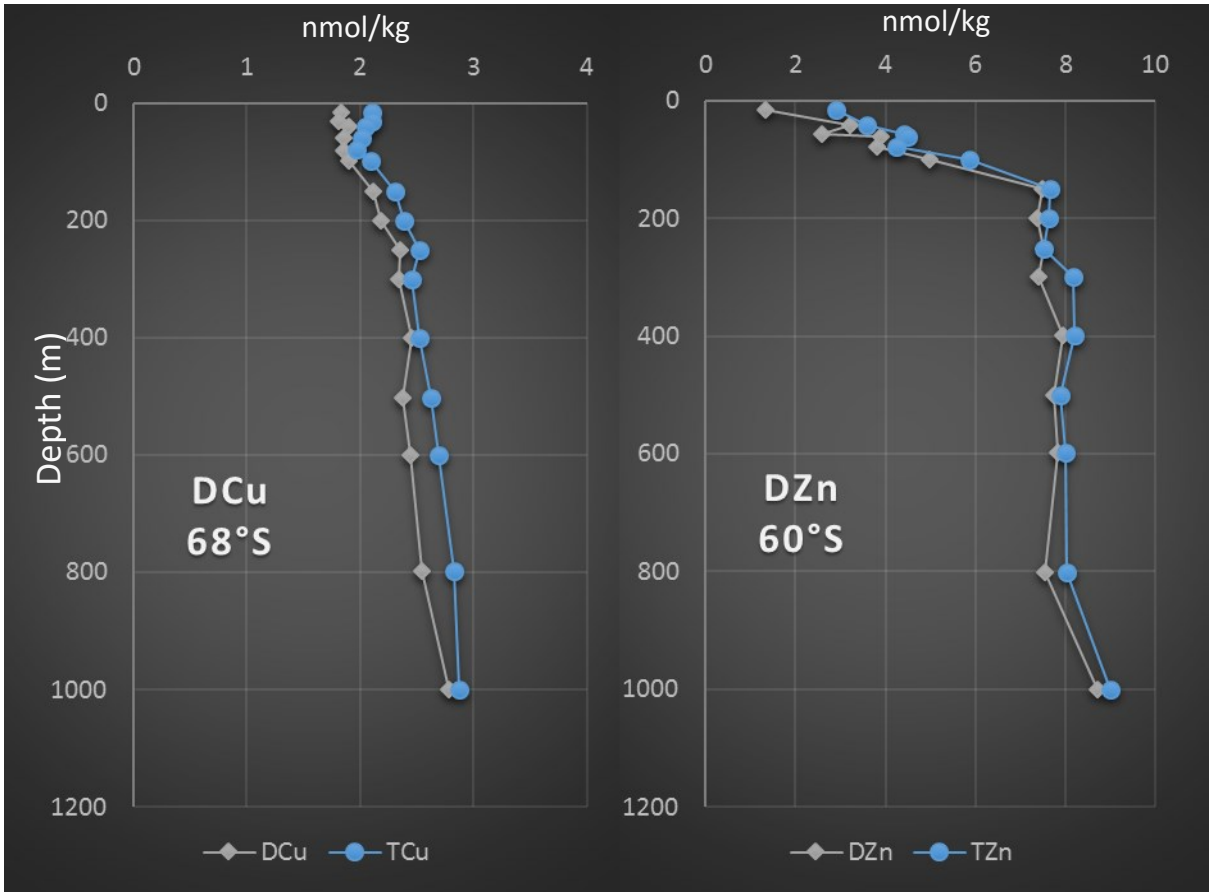

Figure 21 – representative depth profiles of DCu vs TCu (left) and DZn vs TZn (right) at 68°S and 60°S respectively showing the large proportion which the dissolved fraction contributes to the total fraction.

The relationship between the Total and Dissolved fractions of Cu and Zn is shown in Figure 21. (refer to appendix A for the complete dataset). Samples collected for the determination of the total trace metal concentration were collected unfiltered while samples for the dissolved phase were filtered through a 0.2 µm filter. For Cu and Zn, the total and dissolved fraction profiles mimic each other throughout the water column with perhaps the dissolved fraction contributing slightly less to the total fraction in the upper 100 metres. The figure show that for both elements the dissolved fraction represents approximately 95% of the total fraction, a characteristic reported previously during the Southern Ocean Iron Release Experiment (SOIREE) (Frew *et al.*, 2001). This suggests very low amounts of Cu and Zn are associated with particulates (> 0.2 µm).

4.1.4. Meridional and Vertical distribution of Dissolved Copper (DCu) and Zinc (DZn)

The vertical concentration profiles for DCu and DZn obtained from the seven sampling stations are compiled in figures 22 and 23 respectively using Ocean Data View (ODV). The complete dataset is compiled in Table 8 and appendix A for the entire trace element suite. The figures represent a cross-sectional view of the transect from the African continental shelf (~34°S) to the Antarctic continental shelf (~69°S) and includes ocean bathymetry as well as the location of the sampling stations relative to the frontal zones encountered. Each data point represents the mean concentration obtained from the analysis of duplicate sample bottles. Statistical analysis was performed on all results in order to identify possible outliers. Outliers were identified as those values having an %RSD > 15%. The value rejected was then decided as the value which least fitted the general trend of the curve. It must be noted that stations located at 36°S, 50°S, 60°S and 68°S, the maximum depth sampled was 1000 metres. Concentrations below 1000 metres have been extrapolated by ODV. At all other stations (46°S, 54°S and 65°S) depths to within a few hundred metres of the ocean floor were sampled.

DCu and DZn profiles displayed a general nutrient-type behaviour across all stations. This is consistent with depleted (sub-nanomolar) surface concentrations which proceed to increase with depth. At 54°S, DCu showed a deviation from the typical nutrient profile in the upper 100 metres with concentrations decreasing from 1.45 nmol/kg to 1.33 nmol/kg before increasing with depth as expected. DCu concentrations ranged from a minimum of 0.43 nmol/kg in the surface waters of the STZ to a maximum of 3.15 nmol/kg in bottom waters of the northern ACC. DZn concentrations ranged between 0.58 nmol/kg, in the surface waters of the PFZ, and 12.51 nmol/kg observed in the bottom waters of the STZ. The WG was the only domain where DCu and salinity were significantly correlated ($p < 0.05$) in the MLD (Figure 24) and suggests an external atmospheric input to surface waters in the

STZ and ACC. DZn was significantly ($p < 0.05$) correlated with Salinity in all domains except the STZ which infers a water mass control over its vertical distributions.

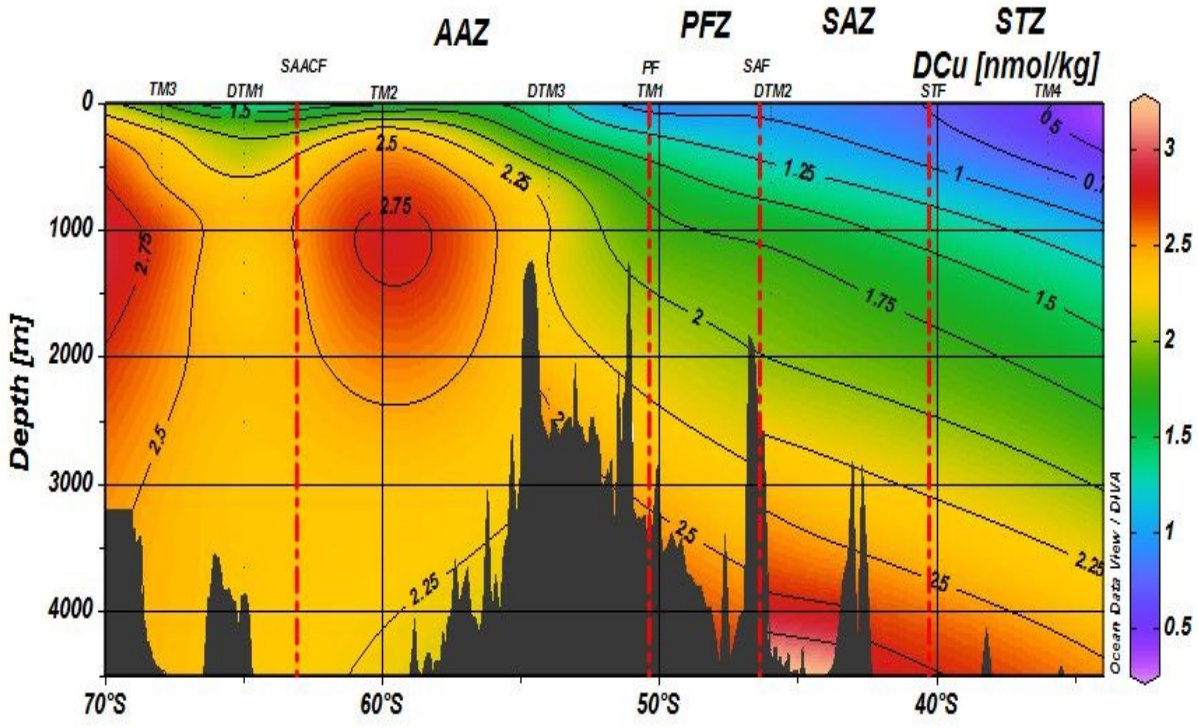

Figure 22 –colour and contour plots of the concentration of dissolved Cu (nmol/kg) for the transect. Dots indicate data points. Sampling station locations are shown relative to the position of major fronts encountered. Figure compiled using Ocean Data View (ODV).

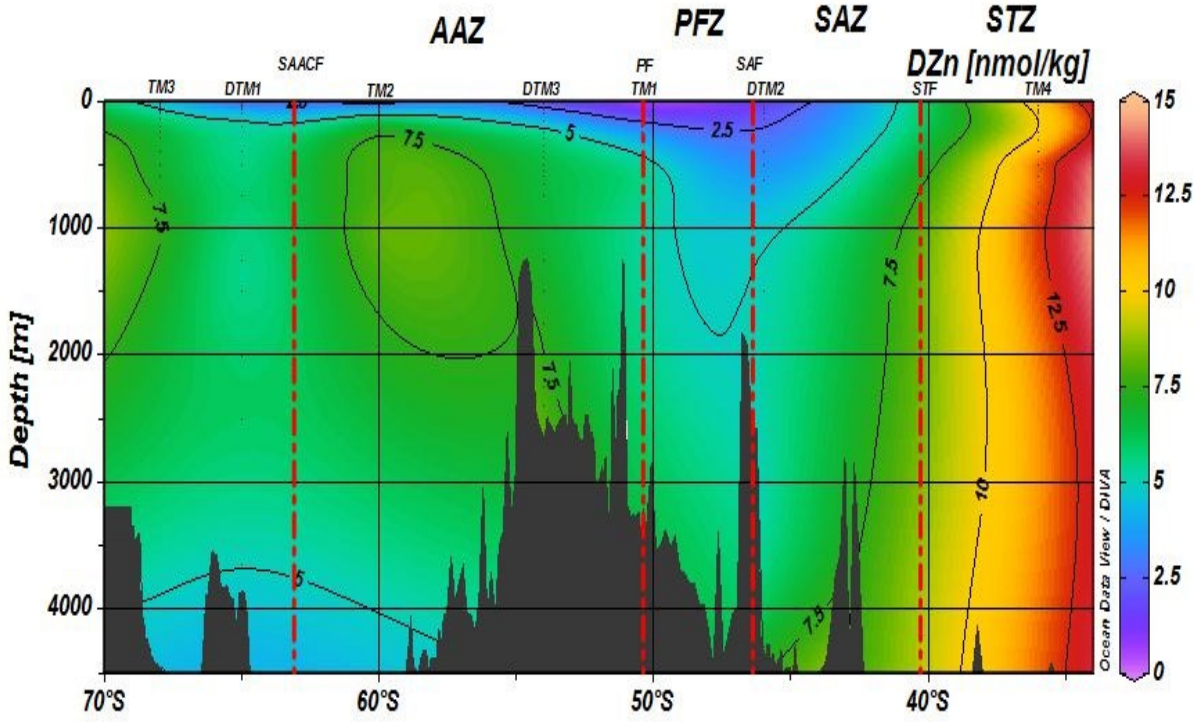

Figure 23 - colour and contour plots of the concentration of dissolved Cu (nmol/kg) for the transect. Dots indicate data points. Sampling station locations are shown relative to the position of major fronts encountered. Figure compiled using Ocean Data View (ODV).

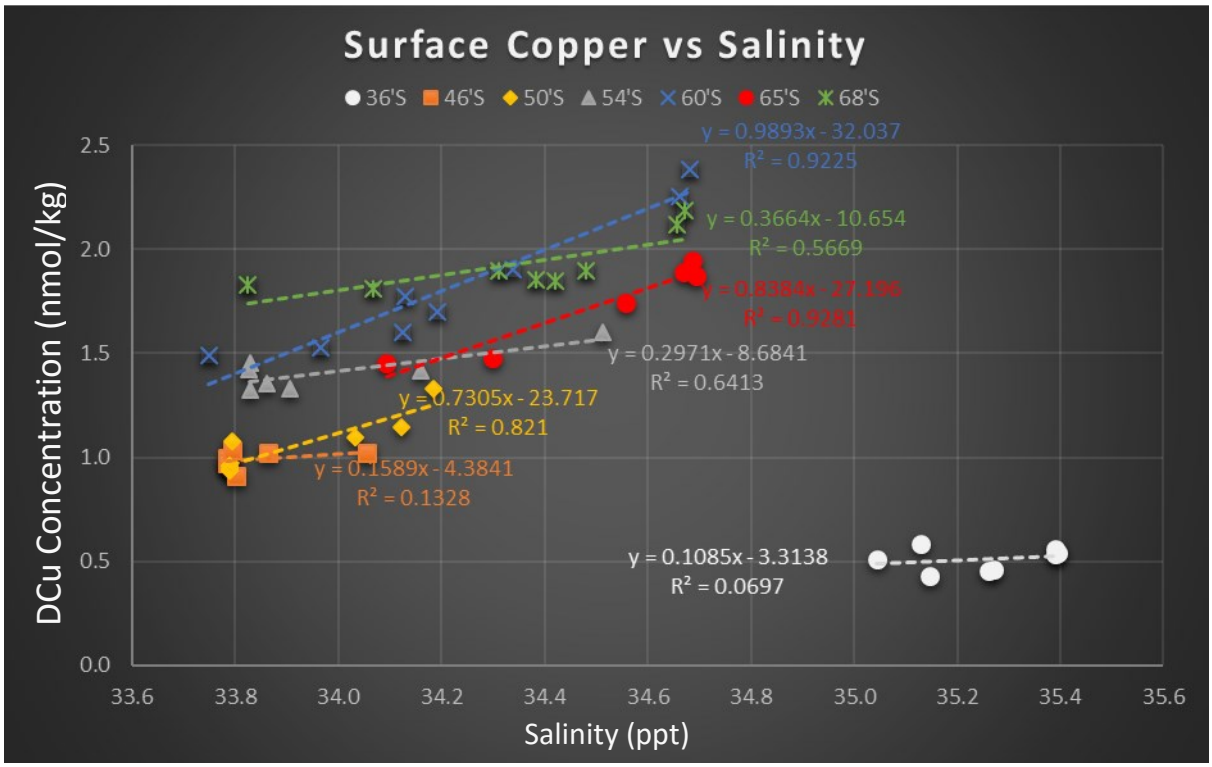

Figure 24 - Relationships between Copper and Salinity in the MLD

The highest trace metal concentration gradients were observed within the mixed layer depth (MLD) whereas the deepwaters were characterised by a much more conservative concentration-depth relationship. Within the MLD, DCu increased relatively uniformly from 0.55 nmol/kg in the STZ (36°S) to 1.86 nmol/kg in the southern extent of the WG (68°S). A similar north-south gradient was displayed by Si and was reflected in the significant correlation between the two on a station-by-station basis (Figure 25) and over the whole dataset where Cu (nM) = 0.011 Si (µM) + 0.851 (R^2 = 0.85, n=98). Contrastingly DZn had its highest MLD concentrations (11.08 nmol/kg) in the STZ whereafter concentrations
dropped rapidly through the SAZ before increasing steadily from 2.00 nmol/kg to 6.84 nmol/kg moving southwards from the PFZ to the WG.

Throughout the PFZ and STZ, DCu increased steadily with depth. In the WG however, DCu seemed to increase more rapidly at shallower depths (> 1000 metres) while displaying very little variation in the deepwaters. This observation was most pronounced at 60°S and 68°S where the difference between the average intermediate and deepwater DCu concentration was as low as 0.09 nmol/kg. In the surface waters, to depths of 500 m, Zn exhibited similar behaviour to that of phosphate with perhaps the exception at 68°S where elevated surface Zn values contributed to the localised decoupling. A distinct difference between Zn:P relationships north and south of the APF is also visible in Figure 26 whereby Zn, in combination with other trace metals such as Fe, appears to be limiting

primary productivity to a greater extent south of the APF as indicated by the high negative intercepts. Vertical concentration gradients of DZn in the intermediate and deepwaters were low throughout the transect although slightly higher in the PFZ compared to the STZ and WG. Both trace metals showed

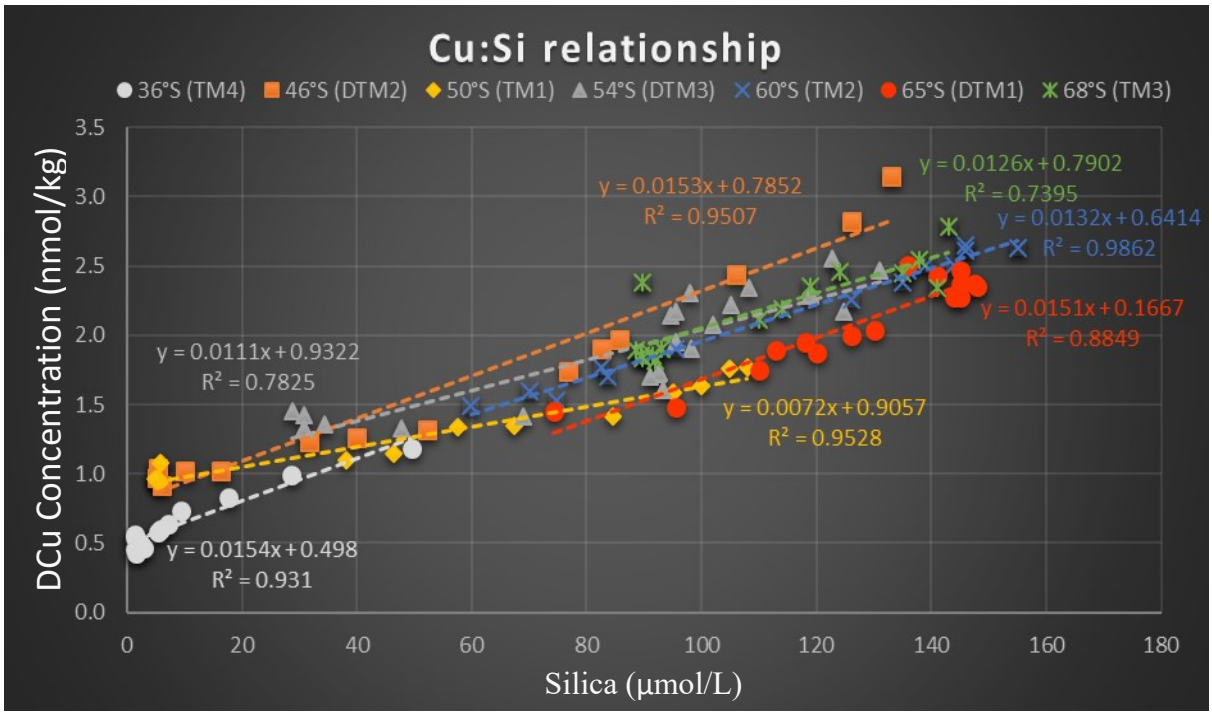

Figure 25 - Relationships between Copper and Silica for the whole water column

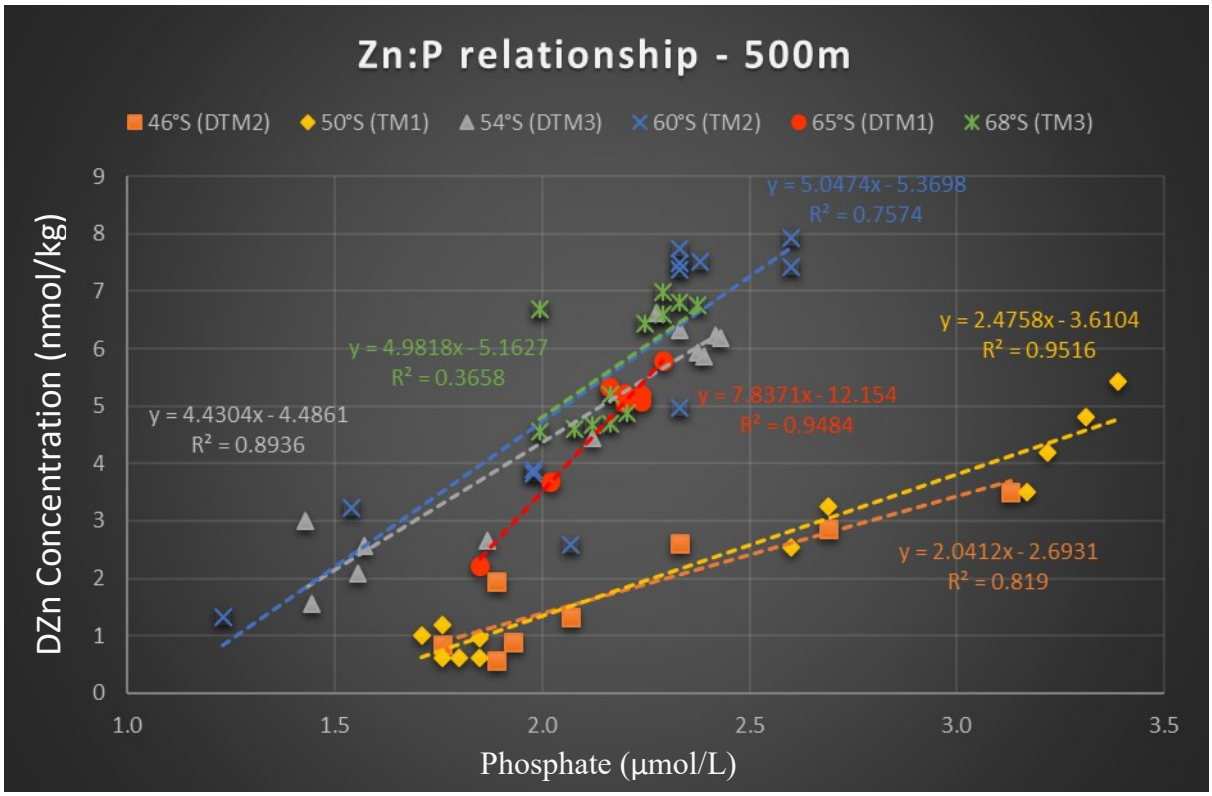

Figure 26 - Relationships between Zinc and Phosphate for the upper water column

localised enrichments at intermediate depths in the northern and southern extent of the WG.

Table 8 – Total (T) and dissolved (D) copper and zinc concentrations according to depth for the seven sample locations along the Bonus Goodhope Line. Tables are in north-south order. Total fraction collected unfiltered in PFA bottles, dissolved fraction collected filtered (0.2 µm) in LDPE bottles. Data and statistics reported here are not corrected for potentially contaminated samples or outliers however references to data in the text are. One standard deviation is reported on duplicate samples. Values highlighted in red are deemed outliers (%RSD > 15%). All concentrations are nmol/kg.

Domain (Station)	Lat/Long	Depth (m)	TCu	DCu	Std Dev.	TZn	DZn	Std Dev.
STZ (TM4)	36˚ 00' S 13˚ 09' E	15	0.54	0.54	0.03	9.36	9.37	0.90
		30	0.55	0.56	0.01	10.33	13.98	2.25
		41	0.53	0.54	0.00	9.32	9.89	0.11
		60	0.50	0.45	0.00	9.49	10.22	0.42
		80	0.46	0.43	0.01	9.71	9.57	0.02
		100	-	0.46	0.02	-	9.04	0.41
		150	0.46	0.51	0.01	8.56	10.86	0.29
		250	0.60	0.58	0.02	8.61	9.44	0.22
		301	0.59	0.60	0.01	8.44	10.02	0.05
		400	0.64	0.63	0.01	9.31	10.65	0.05
		501	0.74	0.73	0.01	8.57	14.43	4.27
		600	0.88	0.83	0.00	9.80	10.26	0.21
		801	1.00	1.00	0.01	10.04	11.92	0.04
		1000	1.27	1.19	0.01	11.53	12.51	0.08
Maximum			1.27	1.19		11.53	14.43	
Minimum			0.46	0.43		8.44	9.04	
Sub-surface (MLD)			0.54	0.55		9.67	11.08	
Surface (500m)			0.56	0.55		9.17	10.68	
Inter (500-1700m)			0.97	0.94		9.99	12.28	
Deep (>1700m)			-	-		-	-	

Domain (Station)	Lat/Long	Depth (m)	TCu	DCu	Std Dev.	TZn	DZn	Std Dev.
PFZ (DTM2)	46˚ 00' S 08˚ 00' E	14	1.09	1.00	0.03	0.90	1.46	0.61
		35	0.99	0.97	0.02	0.86	0.77	0.13
		75	0.98	1.04	0.12	0.76	3.42	2.85
		100	1.12	0.91	0.07	2.59	2.33	0.38
		150	1.10	1.02	0.02	1.95	1.32	0.07
		200	1.08	1.02	0.02	2.69	2.61	0.81
		400	1.26	1.23	0.05	2.31	2.85	0.36
		501	1.43	1.26	0.02	3.81	3.50	0.14
		622	1.36	1.32	0.09	4.88	3.39	0.11
		1000	1.88	1.74	0.03	5.21	4.82	0.00
		1501	2.06	1.90	0.12	4.75	5.01	0.13
		2000	2.15	1.97	0.02	6.65	5.15	0.56
		3000	2.67	2.44	0.05	5.50	5.22	0.08
		4002	2.97	2.82	0.09	5.82	6.14	0.08
		4302	3.95	3.15	0.01	6.97	6.96	0.35
Maximum			3.95	3.15		6.97	6.96	
Minimum			0.98	0.91		0.76	0.77	
Sub-surface (MLD)			1.04	0.98		1.28	2.00	
Surface (500m)			1.13	1.06		1.98	2.28	
Inter (500-1700m)			1.68	1.55		4.66	4.18	
Deep (>1700m)			2.94	2.59		6.23	5.87	

Table 8 continued

Domain (Station)	Lat/Long	Depth (m)	TCu	DCu	Std Dev.	TZn	DZn	Std Dev.
APF (TM1)	50˚ 27' S 02˚ 00' E	16	0.98	0.94	0.05	0.99	1.27	0.31
		31	1.01	0.94	0.06	0.95	0.62	0.03
		40	1.08	0.95	0.03	0.91	0.62	0.00
		60	0.98	0.96	0.07	1.08	1.02	0.13
		78	1.07	0.96	0.01	1.30	0.61	0.01
		100	1.05	1.08	0.02	1.10	1.19	0.14
		150	1.20	1.09	0.00	2.72	2.53	0.02
		198	1.21	1.15	0.02	3.15	3.25	0.10
		251	1.32	1.33	0.01	3.40	3.51	0.02
		303	1.43	1.34	0.02	4.23	4.19	0.07
		400	1.55	1.41	0.05	5.14	4.81	0.18
		500	1.57	1.59	0.04	5.05	5.42	0.20
		599	1.73	1.63	0.03	5.40	6.28	0.84
		800	1.86	1.75	0.01	5.32	5.30	0.03
		1002	1.93	1.77	0.01	5.42	5.35	0.07
Maximum			1.93	1.77		5.42	6.28	
Minimum			0.98	0.94		0.91	0.61	
Sub-surface (MLD)			1.03	0.97		1.06	0.89	
Surface (500m)			1.20	1.14		2.50	2.42	
Inter (500-1700m)			1.84	1.72		5.38	5.64	
Deep (>1700m)			-	-		-	-	

Domain (Station)	Lat/Long	Depth (m)	TCu	DCu	Std Dev.	TZn	DZn	Std Dev.
ACC (DTM3)	54˚ 00' S 00˚ 00.' E	15	1.53	1.45	0.01	2.36	1.55	0.04
		23	1.52	1.42	0.00	5.87	3.01	0.07
		50	1.52	1.32	0.06	2.48	2.09	0.14
		75	1.44	1.35	0.03	2.74	2.55	0.13
		101	1.36	1.33	0.02	2.82	2.65	0.06
		151	1.63	1.41	0.01	4.98	4.44	0.01
		250	1.63	1.60	0.01	6.43	5.93	0.25
		298	1.95	1.72	0.07	6.37	6.22	0.25
		350	1.77	1.73	0.11	6.35	5.87	0.38
		398	1.92	1.70	0.01	6.07	6.18	0.00
		450	1.91	1.90	0.09	6.09	6.32	0.19
		500	0.57	1.95	0.06	6.73	6.61	0.13
		549	2.20	2.07	0.22	6.79	6.57	0.63
		599	2.15	2.14	0.01	7.52	6.68	0.07
		650	2.36	2.17	0.04	6.56	6.42	0.15
		749	2.38	2.21	0.00	6.67	6.48	0.02
		1000	2.30	2.30	0.00	6.71	6.71	0.00
		1250	2.30	2.17	0.01	6.71	6.95	0.00
		1502	2.46	2.28	0.06	7.83	7.15	0.05
		1749	2.44	2.30	0.05	7.74	7.45	0.28
		2001	2.50	2.34	0.01	7.38	7.51	0.13
		2249	2.74	2.55	0.06	7.66	7.66	0.20
		2400	2.92	2.46	0.04	9.18	7.96	0.10
Maximum			2.92	2.55		9.18	7.96	
Minimum			0.57	1.32		2.36	1.55	
Sub-surface (MLD)			1.52	1.40		3.57	2.22	
Surface (500m)			1.56	1.58		4.94	4.45	
Inter (500-1700m)			2.09	2.16		6.94	6.69	
Deep (>1700m)			2.65	2.41		7.99	7.65	

Table 8 continued

Domain (Station)	Lat/Long	Depth (m)	TCu	DCu	Std Dev.	TZn	DZn	Std Dev.
WG (TM2)	60˚ 00' S 00˚ 00' E	16	1.69	1.49	0.02	2.91	1.33	0.06
		41	1.59	1.60	0.03	3.59	3.22	0.29
		58	1.67	1.53	0.04	4.41	2.58	0.13
		60	2.11	1.77	0.04	4.50	3.89	0.04
		79	1.90	1.70	0.01	4.26	3.82	0.02
		100	2.00	1.90	0.08	5.88	4.97	0.15
		150	2.21	2.25	0.01	7.20	7.49	0.00
		199	2.57	2.38	0.06	7.62	7.38	0.18
		251	2.44	2.46	0.06	7.51	7.51	0.15
		300	2.61	1.47	1.03	8.16	7.41	0.42
		399	2.76	2.51	0.06	10.58	7.93	0.11
		500	2.76	2.61	0.01	7.88	7.74	0.07
		599	2.86	2.63	0.04	8.00	7.82	0.16
		800	2.93	2.64	0.01	8.03	7.54	0.05
		1001	2.76	2.95	0.25	7.57	8.72	0.75
Maximum			2.93	2.95	1.03	10.58	8.72	0.75
Minimum			1.59	1.47	0.01	2.91	1.33	0.00
Sub-surface (MLD)			1.64	1.55	0.02	3.25	2.28	0.18
Surface (500m)			2.19	1.97	0.12	6.21	5.44	0.13
Inter (500-1700m)			2.83	2.71	0.08	7.87	7.96	0.26
Deep (>1700m)			-	-	-	-	-	-

Domain (Station)	Lat/Long	Depth (m)	TCu	DCu	Std Dev.	TZn	DZn	Std Dev.
WG (DTM1)	65˚ 00' S 00˚ 00' E	25	1.55	1.29	0.01	2.58	1.02	0.03
		39	1.67	1.45	0.00	3.66	2.21	0.10
		51	1.76	1.48	0.05	4.42	3.68	0.12
		70	1.90	1.74	0.05	5.33	5.22	0.11
		100	2.04	1.89	0.09	5.94	5.78	0.01
		151	1.92	1.95	0.03	4.93	5.08	0.08
		200	2.04	1.87	0.01	5.66	5.05	0.04
		400	2.05	2.00	0.05	5.10	5.20	0.09
		498	2.10	2.03	0.00	5.27	5.33	0.00
		749	2.36	2.50	0.21	5.44	6.05	0.52
		1001	2.57	2.43	0.03	5.82	5.53	0.05
		1251	2.33	2.27	0.07	5.30	5.46	0.10
		1501	2.31	2.28	0.02	5.69	5.35	0.00
		2002	2.18	2.47	0.06	4.88	5.97	0.23
		2501	2.55	2.37	0.01	6.13	6.11	0.05
		3001	2.45	2.35	0.02	5.09	5.63	0.01
		3650	2.52	2.37	0.08	5.25	5.02	0.20
Maximum			2.57	2.50		6.13	6.11	
Minimum			1.55	1.29		2.58	1.02	
Sub-surface (MLD)			1.66	1.41		3.55	2.31	
Surface (500m)			1.89	1.74		4.76	4.29	
Inter (500-1700m)			2.33	2.30		5.50	5.54	
Deep (>1700m)			2.42	2.39		5.34	5.68	

Table 8 continued

Domain (Station)	Lat/Long	Depth (m)	TCu	DCu	Std Dev.	TZn	DZn	Std Dev.
WG (TM3)	67˚ 58' S 00˚ 01' E	15	2.11	1.83	0.11	5.33	4.56	0.28
		30	2.10	1.81	0.05	5.78	4.61	0.12
		40	2.04	1.90	0.01	5.15	5.19	0.08
		60	2.02	1.86	0.02	4.75	17.12	6.23
		80	1.97	1.85	0.01	4.65	4.69	0.07
		99	2.09	1.89	0.02	4.91	4.88	0.08
		150	2.30	2.12	0.05	6.38	6.43	0.15
		201	2.38	2.19	0.04	6.83	6.77	0.04
		250	2.52	2.35	0.01	6.64	6.59	0.01
		301	2.46	2.34	0.01	6.69	6.79	0.03
		400	2.53	2.45	-	6.88	6.99	-
		501	2.62	2.38	0.03	6.74	6.68	0.13
		600	2.69	2.45	0.03	7.06	6.89	0.00
		799	2.82	2.55	0.04	7.54	7.44	0.15
		1000	2.87	2.79	0.21	7.49	7.97	0.72
Maximum			2.87	2.79		7.54	17.12	
Minimum			1.97	1.81		4.65	4.56	
Sub-surface (MLD)			2.05	1.86		5.09	6.84	
Surface (500m)			2.26	2.08		5.89	6.78	
Inter (500-1700m)			2.75	2.54		7.21	7.25	
Deep (>1700m)			-	-		-	-	

4.2. Discussion

4.2.1. Controls of Copper and Zinc distribution

Previous work on DCu in the Southern Ocean includes studies by Boye et al. 2012 and Heller & Croot 2014. Boye reports DCu along the first leg of the transect extending from Cape Town, in a south-west direction through the STZ and ACC, until the SBdy at ~55°S. Heller & Croot report DCu throughout the WG along the Zero Meridian. Multiple cross-over stations allow comparison between the DCu results obtained from this study and the previous work although it must be noted that samples collected in the previous work were collected in 2008, an approximate six-year difference in sample collection period. There was a good general agreement between data from the STZ to the PFZ. In these domains we report DCu ranges from ~0.4 - ~3.0 nmol/kg, slightly greater than the range of ~0.5 - ~2.5 nmol/kg reported by Boye. DCu in the mixed layer showed little variation with values remaining relatively constant at 0.90 nmol/kg until the APF whereas we report slighter lower average DCu values which increase in the mixed layer from 0.75 nmol/kg near the STF to ~1 nmol/kg at the APF. Both studies report consistently positive DCu gradients with depth throughout displaying maximum DCu values in the bottom waters. In the WG, Heller & Croot report DCu surface concentrations ranging between 1-2 nmol/kg which is in good agreement with our results. Strongest concentration gradients were visible in the upper 500 metres of the water column. In the intermediate and deepwaters of the central WG, DCu behaved very conservatively maintaining stable concentrations of ~2.3 nmol/kg until the ocean floor in both datasets.

Like Cu, few previous studies on Zn in the Southern Ocean have been undertaken. This is emphasized by the absence of DZn data for the STZ (section GIPY4) in the GEOTRACES database (www.geotraces.org). Recently however, dissolved Zn data, including a cross-over station at 36°S; 13°E, from the STZ has become available (Wyatt *et al.*, 2014). DZn in the upper 500 metres (9.04 – 10.86 nmol/kg) was comparatively higher than the range of 0.2-0.5 nmol/kg reported by Wyatt. Despite our data not showing a constant concentration increase with depth, both datasets agree on maximum DZn values in the AABW where values were more comparable, ~12 nmol/kg reported here compared to ~9 nmol/kg reported by Wyatt. Croot et al. 2011 sampled the ACC and WG along the Bonus Goodhope Line in 2008 resulting in numerous cross-over stations with which to compare DZn results. Croot reports surface DZn concentrations increasing from < 1.00 nmol/kg in the ACC to ~2.00 nmol/kg in the southern reaches of the WG. Although in good agreement within the ACC, we report comparably higher average DZn MLD concentrations, 2-4 nmol/kg, southward in the WG. Maximum DZn concentrations of ~7.00 nmol/kg were reported in the intermediate waters (500 – 2000 metres) of the WG. This is in accordance with the corresponding maximum DZn concentration of 7.5 nmol/kg

obtained in this study. In both studies, DZn showed more conservative deepwater behaviour in the WG compared to the ACC.

4.2.1.1. Sub-Tropical Zone (STZ)

One station was conducted within the STZ therefore discussion in terms of observed north-south trends in this region is limited. Nevertheless, the results obtained from the STZ have provided some interesting characteristics. In this domain, DZn displayed the greatest concentrations for the whole water column observed along the transect (figure 27). Similar behaviour was observed for Pb and Mn, although Mn only displayed elevated concentrations in the surface waters. Contrastingly Cu exhibited its lowest concentrations for the whole water column observed along the transect (Figure 28), as did the trace elements Co, Ni, and Cd. Fe concentrations were within the range observed during the transect. The Zn:Cu ratio for the STZ was 16.9:1 compared to the average of 2.38:1 and 2.58:1 for the ACC and WG respectively.

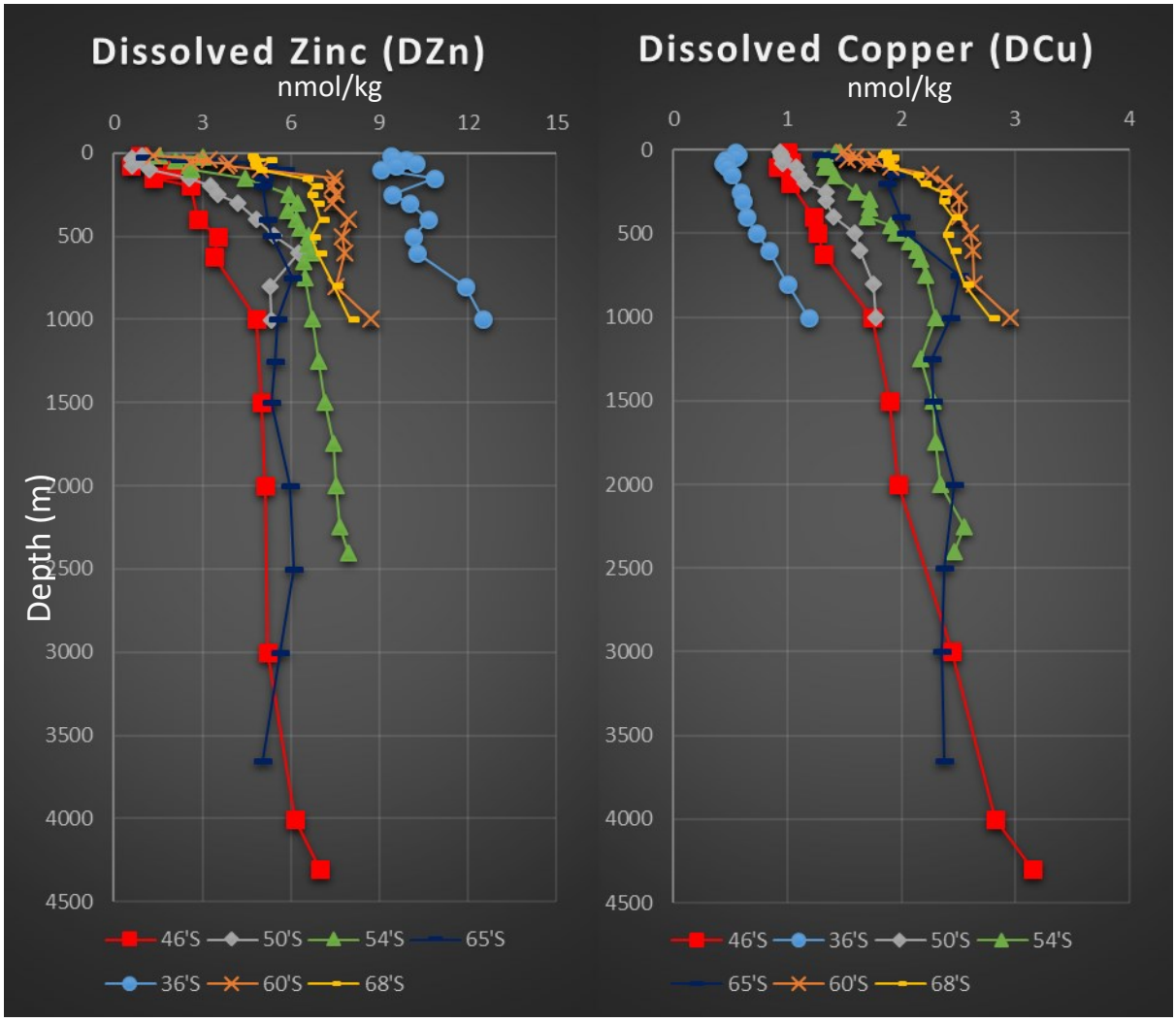

Figure 27 - DZn profiles obtained along the transect. The figure highlights the elevated DZn concentrations in the STZ (36°S).

Figure 28 -DCu profiles obtained along the transect. The figure highlights the low concentrations in the STZ (36°S).

Coincidently, this was the only station where Zn did not significantly ($P > 0.05$) correlate with salinity in the MLD. When taking the whole water column into account, a significant correlation ($P < 0.05$) was found. DCu displayed the same behaviour with salinity in the STZ. This suggests a decoupling between deeper water and near surface DZn and DCu concentrations whereby the latter reflects an external trace metal source. Riverine derived Cu and Zn is thought to be the dominant supply to the oceans (Baars and Croot, 2011). The STZ is proximal to the African continent and so riverine inputs into surface waters is a plausible source yet fails to explain the depleted Cu, as well as Co, Ni and Cd concentrations. Continental erosion as a possible trace metal source results in the same conclusion. The transport and deposition of atmospheric aerosol is also a significant source of trace metals to the surface ocean. As westerly winds predominate, aeolian and volcanic dust originating in southern South America is considered to be the main source of dust inputs into the south east Atlantic. Dry and wet deposition fluxes of a suite of trace metals have been calculated previously for the South Atlantic (Chance, Jickells and Baker, 2015). Using a deposition velocity (V_d) of 0.03 $m.s^{-1}$, values of 0.6 and 0.06 nmol m^{-2} day^{-1} were calculated for Zn and Cu respectively. Importantly, Zn solubility was high (66 – 97%) while Cu showed an extremely low solubility range of < 5%. In the same study, wet deposition was deemed a more significant source of trace metals to the surface ocean. Concentrations of trace metals in rainwater yielded a wet deposition flux of 981 ± 1006 and 35 ± 29 nmol m^{-2} day^{-1} respectively although uncertainty was high as a result of a small sample population. Solubility for these two elements varied between 10 – 90%. All variables considered, the relationship between total flux (wet and dry) of Cu and Zn, as well as other trace metals, agrees with the relative enrichments/depletions observed however cannot account for the magnitude of these differences.

In comparison to the diatom based ACC and WG, the STZ exhibits a cyanobacteria based phytoplankton community assemblage (Figure 20. Viljoen, 2016). Cyanobacteria require Zn for the essential carbon fixation enzyme Carbonic Anhydrase (CA) and for phosphorus acquisition via the enzyme Alkaline Phosphatase (AP) although there is evidence that at least some carbonic anhydrases can be substituted with different metal cofactors such as Co^{2+} and Cd^{2+}(Barnett *et al.*, 2012; Baars *et al.*, 2014). The depletion of DCo (<5 pmol/kg) and DCd (<9 pmol/kg) in the euphotic zone within the STZ suggests that substitution may play a major role in the distribution of DZn here although additional work on Co and Cd speciation as well as the exact substitutive mechanism that cyanobacteria employ is needed to make more concrete conclusions. In addition to possible substitution, cyanobacteria have exceptionally low Zn requirements in contrast to diatoms which have a high Zn requirement. The control cyanobacteria exert via their trace metal uptake ratios could explain the elevated Zn concentrations observed despite low productivity measured at the surface (chl-a = 0.03 µg. L^{-1}). An

important factor to consider is that cyanobacteria usually dominate low Zn areas however, in the STZ, the higher SST and low Si concentrations provide the most likely reasons for cyanobacteria to out compete diatoms.

The distribution of Zn in the deepwaters (> 1750 m) is primarily influenced by the intrusion of NADW and AABW. Additionally, shelf to open ocean mixing, advection of water masses that have been in contact with continental margins and entrainment of shelf inputs from the southern margin of South Africa may well explain the enrichments in the AAIW, UCDW and NADW as well as the relative maxima of Cu observed in the AABW (Boye *et al.*, 2012). Inherently lower Zn values, 4.2 – 4.5 nmol/kg, have been observed for NADW resulting in a decrease in DZn between 1750 – 3000 metres depth (Wyatt *et al.*, 2014). We report values of ~ 10 nmol/kg in NADW however it is important to note that these relatively enhanced values have been extrapolated as a result of samples only being collected from the upper 1000 metres and may deviate slightly from in-situ Zn concentrations. High Zn concentrations averaging 7.2 nmol/kg with local enrichments of up to 8.6 nmol/kg (Croot, Baars and Streu, 2011; Wyatt *et al.*, 2014) compare more closely with our average AABW DZn values of ~11 nmol/kg. These waters coincided with elevated Si concentrations in excess of 100 µM and is in accordance with the resuspension of opal rich sediments from the Cape Basin floor.

4.2.1.2. Antarctic Circumpolar Current (ACC)

The APF, situated within the ACC, serves as the division between oligotrophic waters to the north and the HNLC zone to the south. The meridional distribution of macronutrients exemplifies this control with depleted concentrations observed to the north of the APF and increasingly higher concentrations to the south. Despite the higher availability of macronutrients in the ACC and WG, phytoplankton abundance is still low showing only locally enhanced productivity. Light limitation in combination with lower dissolved trace metal, in particularly Fe, availability in these waters are the underlying cause of this phenomena (Löscher, 1999). For global oceans values of 3.15, 4.59 and 0.54 nmol/kg are reported for Cu, Zn and Fe respectively (Sohrin *et al.*, 2008). Average values in the ACC of 1.74, 1.70 and 0.23 nmol/kg for the three trace metals were obtained in this study and show the limiting nature of micronutrients in the SO compared to global oceans.

Local minima in the vertical profiles of Cu, particularly at 54°S, and Zn were associated with elevated chl-a concentrations at the related depth and indicate uptake by phytoplankton in the euphotic zone. A local DZn sub-surface maximum (~3 nmol/kg) was evident at 54°S and may be attributed to the release of sea ice diatoms from melting sea ice and subsequent remineralisation

releasing Zn (Baars and Croot, 2011). Compared to DCu, DZn showed stronger regeneration rates below the mixed layer, increasing in concentration by roughly three-fold. Maxima associated with regeneration were deepest in the northern ACC and decreased southwards. The deeper remineralisation cycle of Zn with respect to other trace metals has been previously noted in the ACC and has been identified as a key control on the distribution of Zn in the Southern Ocean (Baars *et al.*, 2014). There was no clear zone of regeneration for DCu, instead concentrations increased steadily with depth. DZn profiles displayed smaller concentration gradients in the central deepwaters of the ACC suggesting slow physical mixing in the water column associated with a zone of low current shear where the lateral velocities of the ACC are lowest (Croot, Baars and Streu, 2011).

DCu concentrations in the MLD did not conform to the general north-south increase. Concentrations at 46°S were on average 0.07 nmol/kg higher when compared to 50°S while at 54°S, DCu was even greater than concentrations observed in the northern WG. For all stations in the ACC, DCu did not significantly correlate ($P > 0.05$) with salinity in the MLD which is indicative of an external atmospheric surface input. Back trajectories from the station locations, using the NOAA HYSPLIT atmospheric transport modelling system (Stein *et al.*, 2015), were simulated in order to identify potential source regions for the elevated DCu concentrations observed (Figure 29). Interestingly, the simulation results indicate that dust originating from Patagonia was a probable input source only at 50°S yet concentrations here were still lower compared to 46°S. Enhanced dry deposition fluxes have

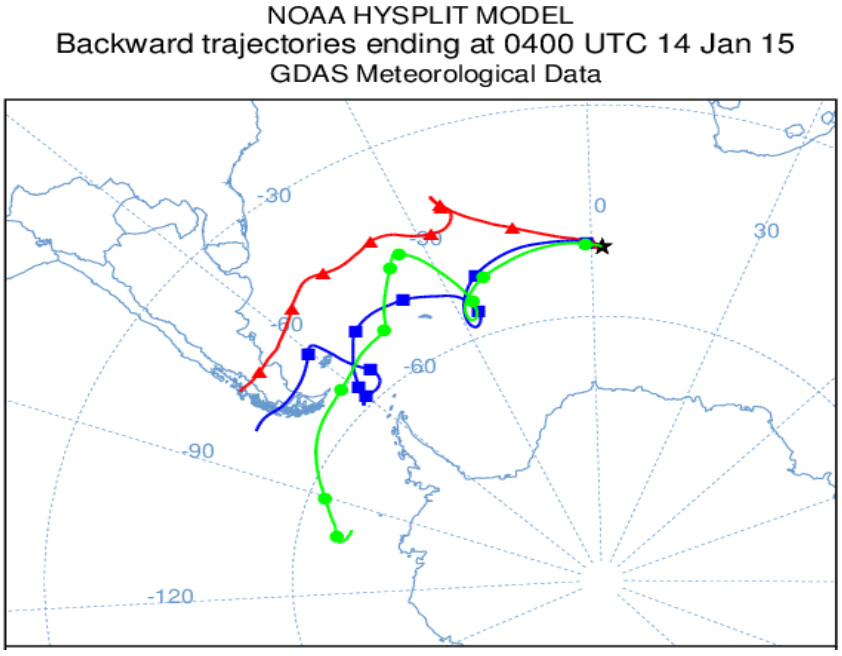

Figure 29 – A 9 day (216 hour) NOAA HYSPLIT backward trajectory beginning at 50°S, the location of TM1. The back trajectory starts on 14/01/2015 at 04h:00 coinciding with our arrival at the sample location. The model illustrates the possible source regions of dust, the Patagonian Desert in the above example, to TM1 at 10 metres (red), 500 metres (blue) and 1000 metres (green).

been reported to be up to 2.8 times greater in the southern ACC compared to the STZ (Boye *et al.*, 2012). A dry deposition Cu flux of 4.3 - 13 pmol/kg has previously been calculated using mean aerosol concentrations in the region and a dry deposition velocity of 0.3 cm s^{-1} (Duce and Tindale, 1991). In terms of bio-availability, this flux may be overestimated as the fraction of aerosol particles that readily dissolve before settling out the photic zone must be taken into account. Dry deposition can therefore only account for a small fraction of the DCu input to surface waters and indicates a larger input from wet deposition sources, such as rain events, which more likely explains the elevated concentrations at 46°S.

Diatoms appear to dominate surface phytoplankton community assemblages accounting for roughly 50% of biomass at 46°% and 54°S (Figure 20. Viljoen, 2016). The other main contributors were Haptophytes (45%) at 46°S and a combination of Haptophytes and dinoflagellates at 54°S (Figure 20. Viljoen, 2016). In the central ACC (50°S), Haptophytes were however more dominant than diatoms contributing 44%, compared to 32% from diatoms, to total biomass. The results from a bioassay experiment conducted at the chl-max (81 m) at 46°S showed a very similarly composed community structure (Figure 30). The presence of dinoflagellates may be important as dinoflagellates and associated bacteria are a known source of organic ligands for copper which decreases the bioavailable fraction of Cu (Baars *et al.*, 2014). Through studies with organic complexing agents, the growth and Cu uptake rates of phytoplankton species has been shown to be related to the free Cu concentration [Cu^{2+}] rather than the total Cu concentration. The presence of organic complexing ligands in seawater

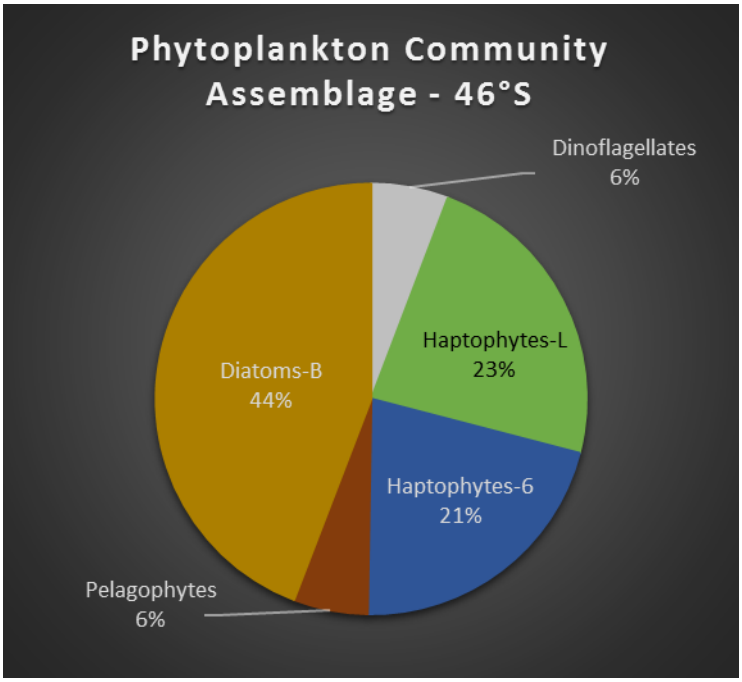

Figure 30 - relative phytoplankton community assemblage obtained from a bioassay experiment conducted at chl-a max (81 m) at 46°S. Data sourced from (Viljoen, 2016)

acts to lower the [Cu^{2+}] reducing toxicity but also potentially limiting phytoplankton growth (Brand, Sunda and Guillard, 1986). Cu deficient cells become less able to transport Fe due to the involvement of copper oxidases in Fe uptake within phytoplankton cells (Heller and Croot, 2014). Additionally, increased [Cu^{2+}] can inhibit the uptake of other trace metals such as Mn. Zn complexation by organic ligands in the SO is deemed insignificant due to the saturation of Zn ligands as a result of relatively high DZn concentrations (Baars and Croot, 2011). The source of organic ligands is unknown although thought to stem from phytoplankton and/or bacteria. Relatively low phytoplankton abundance in the ACC, and hence lower ligand secretion, may contribute to the saturation of ligands in this region. Estuarine marine sediments have also been identified as a possible source for Zn complexing ligands however the long residence time of zinc in oceans (50 000 years) suggests this flux of organic ligands may not be important (Baars and Croot, 2011). Additional sources of copper complexing ligands include hydrothermal vents and ocean floor sediments (Baars *et al.*, 2014). Residence times for Cu in the deepwaters have been estimated at 650 years based on the supply of Cu from sediments and indicate complexation may be a more significant control on Cu compared to Zn (Heller and Croot, 2014). Given the small percentage that dinoflagellates contribute to an already low biomass, it suggests Zn and Cu bio-limitation was unlikely during this expedition. Culture experiments with marine diatoms have indicated two transport systems of Cd, a low-zinc induced system and an Mn uptake system under Zn replete conditions (Boye *et al.*, 2012). A low-zinc transport mechanism - as a result of the low dissolved Zn concentrations centered around the APF – would explain the relative depletion of Mn (Figure 31) and Cd (Figure 32) in the WG surface waters compared to the ACC. See subsequent discussion for the WG for more detail.

Maximum DCu and DZn concentrations of ~2.75 nmol/kg and ~7.50 nmol/kg respectively were observed at intermediate depths in the southern portion of the ACC. Lateral advection of waters from the Drake Passage via the eastwards flowing ACC combined with upwelling of nutrient enriched UCDW south of the APF is a likely cause of these elevated concentrations. Most of the upwelled UCDW is transported northwards via Ekman drift resulting in more widespread enrichments (Coale, Michael Gordon and Wang, 2005). In addition this constant flux may be mediated by sinking biogenic particles out of the AASW as suggested by (Löscher, 1999).

4.2.1.3. Weddell Gyre (WG)

Surface water DCu and DZn concentrations obeyed the north-south increasing trend exhibited through the STZ and ACC. Higher surface concentrations in the WG are partly attributed to ice melt and subsequent input of associated trace metals into the surface waters (Grotti *et al.*, 2001). The major

source for Zn to surface waters in the Southern Ocean is through upwelling and vertical mixing of Zn-rich intermediate and bottom waters. Precipitation, specifically rain, is a small source to the Southern Ocean region with measured fluxes typically low 0.4 – 1mmol $m^{-2}y^{-1}$ (Halstead, Cunninghame and Hunter, 2000). Ice core records from Antarctica also support low Zn fluxes by rainwater (Hong *et al.*, 1998). DFe surface concentrations at 65°S were in excess of 0.2 nmol/kg, the highest observed in the WG. The combination of non-limiting Fe and ice melt resulted in a remarkable diatom bloom at 65°S which was reflected by the extremely high chl-a concentrations, ≤ 3.82 µg/L, in the euphotic zone. As a consequence of the high primary productivity in this location, DCu and DZn exhibited the strongest depletion observed. This was most evident in the vertical profile of DZn which decreased in concentration by a factor of 5.62 nmol/kg, compared to 1.52 for Cu, between 150 metres and surface. The extended Redfield ratio, $(C_{124}N_{16}P_1S_{1:3}K_{1:7}Mg_{0:56}Ca_{0:5})_{1000}Sr_{5:0}Fe_{7:5}Zn_{0:80}Cu_{0:38}Co_{0:19}Cd_{0:21}Mo_{0:03}$ predicts the increased relative uptake of Zn compared to Cu based on the relative trace element composition of planktonic biomass (Ho *et al.*, 2003). Furthermore, Fe-stimulated increases in phytoplankton growth and photosynthetic activity lead to increases in carbonic anhydrase activity and an increased requirement for Zn relative to Cu (Franck *et al.*, 2003).

Distinct local maxima in DZn, and to a lesser degree Cu, were clearly visible at 150 metres depth for stations in the central WG. This behaviour reflects a shallow zone of strong remineralisation of sinking organic material. Shallow remineralisation zones have been previously reported in the central WG and identified as a layer with elevated TCO_2 and reduced oxygen (Baars and Croot, 2011). Temporal and spatial variances in zooplankton grazing mechanisms are thought to play an important role in controlling the recycling of trace metals below the mixed layer. Zooplankton communities dominated by salps, as opposed to copepods (krill), are more likely to result in shallower remineralisation zones because copepods produce more rapidly sinking faecal pellets (Croot, Baars and Streu, 2011).

The highest DZn (~8.7 nmol/kg) and DCu (~2.95 nmol/kg) concentrations observed in the WG were sourced from LCDW at intermediate depths. This water mass also showed elevated silicate concentrations (< 150 µM) during the expedition. Interestingly the close trace metal/Si correlation was lost in the WG bottom waters (AABW) where silicate increased to approximately 175 µM as opposed to DZn and DCu which decreased to > 5 nmol/kg and > 2.5 nmol/kg respectively. Previous expeditions have also noted the decoupling of Zn and Si in the deepwaters owing to a relative decrease in Zn in the AABW (Croot, Baars and Streu, 2011). Bottom water enrichments of silicate in the WG are variable with strong local regeneration from opal rich sediment as well as import of remotely formed

water masses enriched in dissolved silicate. Investigations into the chemical composition of phytoplankton has revealed that zinc is incorporated into diatom frustules and so it seems counter intuitive that upon dissolution of the frustule, a deepwater regeneration for Si, and not Zn, is present (Ellwood and Hunter, 1999). Subsequent culture experiments have revealed that the amount of Zn incorporated into the opal represents only 1 – 3% of the total amount of Zn taken up by the diatom (Ellwood and Hunter, 2000). It was concluded that Zn within diatoms appears to be associated with their cellular organic tissue rather than their exoskeletal, as is Cu. The importance of the Southern Ocean in the oceanic Si cycle is reflected in the WG seafloor being covered in diatom frustules. The downward flux of diatoms, i.e. the silicate pump, may be the main transfer mechanism of trace metals, including Cu and Zn, out of the surface waters.

The WG surface phytoplankton communities were dominantly diatom based, accounting for between 45% and 59% of the biomass, followed by haptophytes making up almost all the rest of the biomass (Figure 20. Viljoen, 2016). Primary productivity, as reflected by chl-a concentrations, was highest in the central and northern WG. It appears a shift in the dominant Cd transport system in diatoms has taken place from a low-zinc transport system in the ACC to an Mn system in the WG.

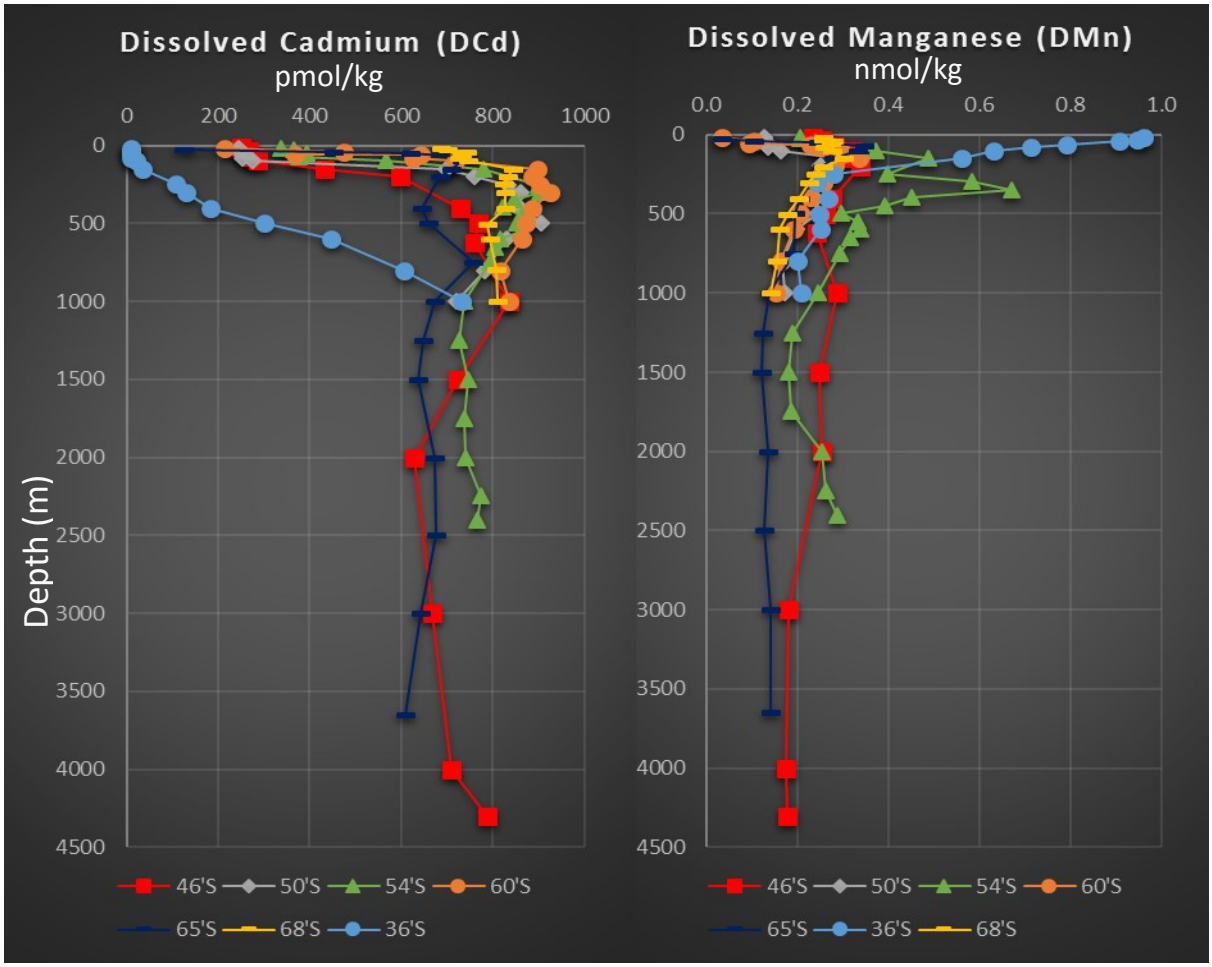

Figure 31 - DCd profiles obtained along the transect

Figure 32 -DMn profiles obtained along the transect

Inspection of the relative Zn (Figure 27), Cd (Figure 31) and Mn (Figure 32) meridional distribution profiles reveals strong depletions of Cd (100-200 pmol/kg) and Mn (< 0.035 nmol/kg) relative to zinc (> 1 nmol/kg), especially in the central and northern surface waters of the WG. These observations were in contrast to the relationships observed between these trace metals in the ACC whereby zinc concentrations (< 1 nmol/kg) were low compared to Mn (> 0.2 nmol/kg) and Cd (250 – 350 pmol/kg). High Zn concentrations have been known to be toxic to marine phytoplankton although studies have shown that Zn toxicity is unlikely at concentrations < 1nmol/kg (Franck *et al.*, 2003). It is possible however that Zn may competitively inhibit Fe uptake, resulting in a higher likelihood for Zn toxicity at the low Fe concentrations (0.11 -0.21 nmol/kg) observed in the WG. Although no work has demonstrated this competitive effect at low Fe concentrations, it has been shown at low Mn concentrations (Sunda, 1991).

4.2.2. Trace Metal – Macronutrient Relationships

It is well established that distributions of both Cu and Zn correlate with the major nutrients NO_3^-, $Si(OH)_4$ and PO_4^{3-} (Baars and Croot, 2011). These correlations result from the strong coupled cycling between these two parameters mediated by phytoplankton utilisation, scavenging and recycling by zooplankton in the surface waters. Investigating trace metal/macronutrient relationships, henceforth referred to as disappearance ratios, provides important clues as to the primary factors driving or limiting primary production in ocean waters.

No significant correlation was found between DCu and PO_4^{3-} or NO_3^- throughout the water column along the Zero Meridian. DCu did however correlate significantly with Si at all sampling stations. These conclusions are in accordance with previous work in the Southern Ocean (Nolting & de Baar 1994; Löscher 1999 & Heller & Croot 2014). Dissolved Zn did not show good correlation with PO_4^{3-} over the whole water column however isolating the upper 500 metres revealed significant correlations in the ACC and WG, with the exception at 68°S where Zn was depleted with respect to PO_4^{3-} according to the equation Zn (nM) = 4.98 PO_4^{3-} (µM) – 5.16 (R^2 = 0.366). A very similar trend between Zn:P disappearance ratios for the whole water column compared to the upper 500 metres was found in a previous study (Croot, Baars and Streu, 2011). In the same study, Croot found a significant correlation between Zn and Si for the entire dataset with an overall relation of Zn (nM) = 0.039 Si (µM) + 0.437 (R^2 = 0.821, n=121). The equivalent relation in this study was Zn (nM) = 0.043 Si (µM) + 1.021 (R^2 = 0.80, n=98), also identifying a significant correlation and indicating that Si was more limiting in this study. The overall Zn:Si correlation was less than the corresponding Cu:Si correlation (Cu (nM) = 0.011 Si (µM) + 0.851 (R^2 = 0.85, n=98)). For separate stations, Zn:Si slopes were relatively

constant (0.037 – 0.068) while intercepts varied from -1.94 at 68°S to 1.16 at 46°S. Slope and intercept values for the surface waters (< 500 m) varied little from their whole water column counterparts. Calculated disappearance ratios for Cu and Zn with respect to Si and PO_4^{3-} are compared to the scarcely available data in literature.

4.2.2.1. Cu:Si

Table 9 presents comparisons between Cu:Si disappearance ratios obtained from this study and from three other datasets for the whole water column at selected locations encompassing the whole transect. Meridionally, average Cu:Si ratios showed a slight north-south increase with slopes ranging from 0.013 nM/ µM in the STZ to 0.015 nM/ µM in the WG. A similar north-south trend was found by Löscher 1999 and Heller & Croot 2014 although larger slopes (0.020-0.022 nM/ µM) were reported. Boye et al. 2012 however observed a north-south decrease in Cu:Si slope values which may be attributed to differences in sample collection season. Samples were collected in Spring, coinciding with the diatom bloom in the PFZ (Löscher, 1999), mid-summer (this study) and in the post diatom bloom late summer (Boye *et al.*, 2012) resulting in a decrease of the Cu:Si ratio in the PFZ relative to the other domains as the season progresses. The seasonal decrease of the Cu/Si ratio over the diatom productive season is probably due to preferential Si uptake by diatoms in the upper water column and Cu scavenging in deeper waters, as well as to a longer retention of Cu compared to Si during dissolution of the diatom frustules in the sediments (Löscher, 1999). Si was found to be depleted throughout the STZ, SAZ and PFZ with MLD values < 5 µM throughout. Si depletion has resulted in the higher slope value obtained here compared to the global average (Table 9). On a regional scale one would expect greater Cu:Si ratios when compared to literature however low Si concentrations were mediated by lower relative DCu MLD concentrations. The comparatively low Cu:Si slopes observed in the ACC and WG from this study coincided with depleted surface Fe stocks of < 1.00 nmol/kg however the relationship between the uptake of Cu and Fe by diatoms could not be observed in the HNLC surface waters where Cu concentrations increased southwards, in contrast to Fe. Differences in biogeochemical cycling of Fe and Cu, especially due to external sources and mixed layer recycling processes, as well as particle reactivity may cause the different trends observed in surface waters of the HNLC area (Chever *et al.*, 2010).

Table 9 - Obtained Cu:Si disappearance ratios from this study as well as Löscher 1999; Boye et al. 2012 and Heller & Croot 2014 at multiple locations within each biogeochemical domain.

Region	Depth (m)	Slope	Intercept	R^2	n	References
STZ (36°S - 42°S)	10-4000	0.011	0.84	0,81	45	Boye et al. (2012)
	15-1000	0.013	0.64	0.99	14	This study
	10-4400	0.015	0.68	0.92	24	Heller and Croot (2015)

N-ACC (42°S - 48°S)	39 - 3153	0.018	0.94	0.98	12	Löscher (1999)
	14-4302	0.015	0.79	0.96	15	This study
S-ACC (50°S - 55°S)	10-3500	0.013	0.71	0.81	26	Heller and Croot (2015)
	500-3153	0.013	1.31	0.96	12	Löscher (1999)
	15-2400	0.011	0.93	0.78	38	This study
WG (58°S - 68°S)	25-5300	0.020	0.79	0.82	45	Heller and Croot (2015)
	500-3712	0.022	0.51	0.91	9	Löscher (1999)
	15-3650	0.015	0.64	0.89	47	This study
ACC & WG	10-4000	0.007	0.77	0.90	135	Boye et al. (2012)
Global	10-5000	0.007	0.83	0.73	-	Boye et al. (2012)

The influence of seasonality on trace metal/ macronutrient ratios has been shown to exert an important control (Ellwood, Boyd and Sutton, 2008), however, perhaps even more important, is the control exerted by phytoplankton community assemblage (Arrigo, 1999). High diatom production plays an important role in the cycling of Cu and Si. Table 10 shows the change in Cu:Si ratios through the MLD and into the intermediate waters. Locations have AASW comprising their upper ~200 m with UCDW underlying. The corresponding phytoplankton assemblages are compiled in Figure 20 (Viljoen, 2016), together with surface chl-a concentrations, and highlight the dominance of diatoms throughout. Differences in slopes at each depth are caused by different input and output fluxes of trace metals and macronutrients. Highest Cu:Si slopes coincided with elevated diatom production reflecting the greater degree to which Si was preferentially taken up. At all stations, Cu:Si decreased through the MLD and, with the exception at 65°S, decreased across the MLD boundary. This decrease is attributed to (1) preferential Si uptake by diatoms in surface waters; (2) the release of Cu and Si from sinking diatom frustules according to the ratio in which they were taken up i.e. Si > Cu; (3) Cu scavenging below the mixed layer; (4) longer retention of Cu during the dissolution of diatoms in sediment. This cycle is summarised in Figure 33. The increase in Cu:Si slopes below the mixed layer is due to a localised absence of Si regeneration in the UCDW.

Table 10 - Cu:Si ratios showing decreasing slope values through the MLD and into intermediate waters for all stations in the ACC and WG.

Water mass	Depth (m)	Cu:Si (nM/μM)					
		46°S	50°S	54°S	60°S	65°S	68'S
AASW	15	0.190	0.169	0.050	0.025	0.020	0.020
	40	0.189	0.173	0.043	0.023	0.020	0.020
	100	0.148	0.186	0.028	0.020	0.017	0.021
	150	0.101	0.029	0.020	0.018	0.017	0.019
	200	0.062	0.025	0.017	0.018	0.016	0.019
UCDW	300-1000	0.019	0.011	0.015	0.008	0.035	0.004

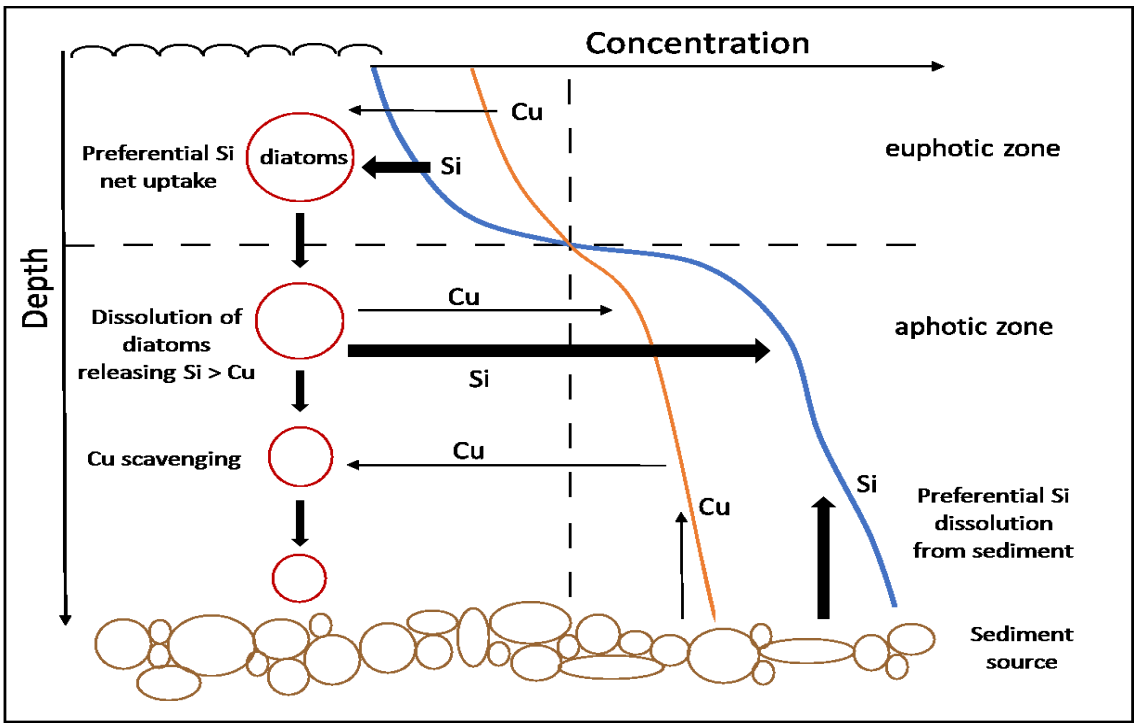

Figure 33 - Cu:Si cycling in high diatom production regions as seen locally in the ACC and WG. The thickness of the arrows represents the relative importance of the flux. The vertical dashed line represents a conservative profile of a constant Cu:Si concentration, without the influence of diatoms and hydrography. Figure adapted from (Löscher, 1999).

4.2.2.2. Zn:P

Zn:P disappearance ratios in the upper water column (<500 m) showed an overall increasing trend southwards from a minimum slope value of 2.73 nM/ µM found at the APF (50°S) to a maximum slope value of 6.86 nM/ µM at 65°S in the WG. A similar southward increasing behaviour, with a Zn:P slope range of 1.80 – 7.00 nM/ µM, was observed along the Zero Meridian by Croot et al. 2011. These observations are shown in Figure 34 (left) and highlight the close correlation between the two studies. Analysis of the PO_4^{3-} distribution in Figure 19 (middle) reveals little variation in the deepwaters, most notably south of the APF. Zn on the other hand showed moderate deepwater variations which explains the lack of significant correlation for Zn:P over the whole water column. A number of processes are suggested to be possible reasons for the observed Zn:P increase along the transect.

I. Biodilution is a term used to describe the relative uptake rates of micronutrients with respect to macronutrients at varying phytoplankton growth rates whereby slow growth rates favour higher trace metal: macronutrient ratios (Croot, Baars and Streu, 2011). This process is unlikely responsible for the observed increase in Zn:P ratios as CO_2 limiting phytoplankton growth rates is unlikely in the Southern Ocean. Temperature has also been shown to exert a strong influence on phytoplankton growth rates however cells growing south of the APF are well adapted and optimised for these conditions (Eppley 1972).

II. The effect of Fe limitation on Zn:P ratios has previously been investigated during the Southern Ocean Iron Experiment (SOFeX) (Twining, Baines and Fisher, 2004). Results indicated that Zn:P ratios were elevated when Fe was limiting diatom growth making Fe limitation a strong candidate for controlling disappearance ratios between Zn and PO_4^{3-}.

III. N:P ratios in the Southern Ocean have been shown to vary from the Redfield ratio of 16:1 according to the dominant phytoplankton community whereby values lower than 16 are associated with diatom blooms and values greater than 16 are associated with *Phaeocystis* blooms (De Baar *et al.*, 1997; Arrigo, 1999). Calculated N:P ratios were < 15 at all stations in accordance with diatoms dominating the phytoplankton community assemblage at all stations shown in Figure 20 (Viljoen, 2016). An N:P ratio of 14.5 has been previously reported for the South Atlantic sector of the SO (Frew *et al.*, 2001). There was also a north-south N:P ratio increase similar to that of Zn:P yet less significant. It has been postulated that N:P and Zn:P ratios are interlinked however no laboratory data investigating this hypothesis in polar phytoplankton species is currently available (Croot, Baars and Streu, 2011).

IV. Irradiance has also been shown in laboratory studies to influence the Zn:P ratio of phytoplankton with the Zn:P ratio in several phytoplankton species increasing significantly with decrease in irradiance (Finkel *et al.*, 2006). Irradiance invariably decreases southward and suggests a significant role in the observed southward Zn:P ratio increase. Irradiance has also been shown in laboratory studies to influence the Zn:P ratio of phytoplankton (Finkel et al., 2006) with the Zn:P ratio in several phytoplankton species increasing significantly with decrease in irradiance. The photoperiod is also important as a related study using the diatom *Thalassiosira pseudona* gave an increase in the Zn:P ratio with a decrease in the photoperiod (Sunda and Huntsman, 2005). This was ascribed, in part, to an increased cellular requirement for Zn to support enhanced carbonic anhydrase (CA) fixation of carbon and a reduced growth rate. However, in the same study a reduction in the light intensity resulted in a reduced cellular Zn requirement, which was possibly linked to a decrease in the growth rate with resulting lower demand for CA and other Zn enzymes.

Considering the above processes, it would suggest that trace metal and/or light limitation is the critical factor controlling the observed Zn:P ratios in the Southern Ocean

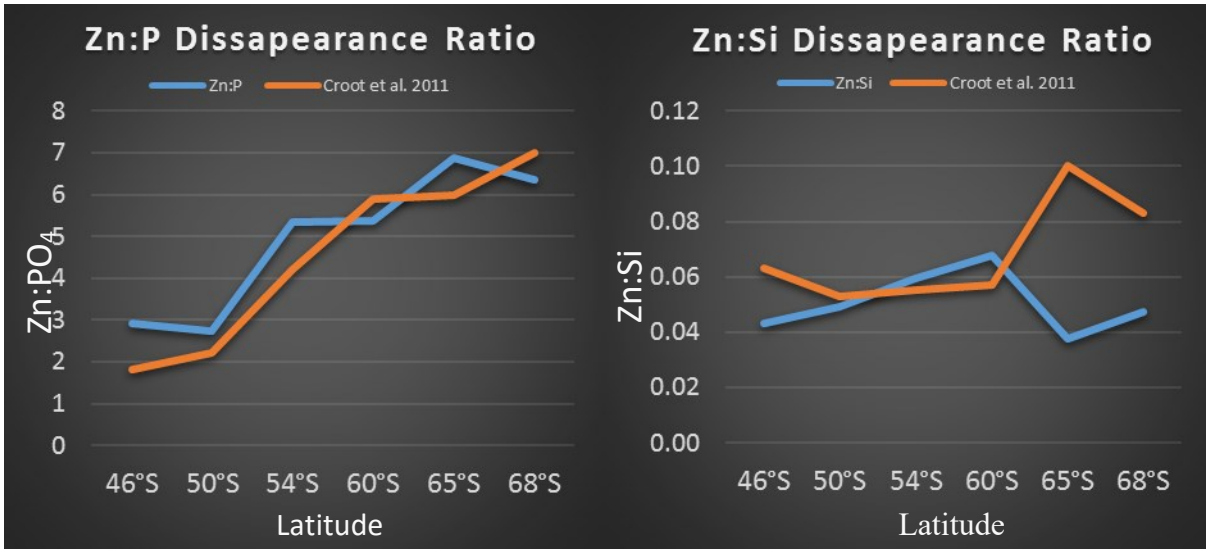

Figure 34 - observed surface N-S Zn:P disappearance ratios (left) and Zn:Si disappearance ratios (right) compared with (Croot, Baars and Streu, 2011)

4.2.2.3. Zn:Si

Zn and Si were strongly correlated throughout the study region in both the surface waters and whole water column. Disappearance ratios varied only fractionally between 0.04 and 0.07 nM/µM (Figure 34 right). The Zn:Si slope range fell between the ranges of 0.033 – 0.038 nM/µM (Löscher, 1999) and 0.05 - 0.10 nM/µM (Croot, Baars and Streu, 2011) and compared well with slope values of 0.059 nM/µM obtained in the Drake Passage (Croot, Baars and Streu, 2011). The major difference in these findings occurred at 65°S and 68°S where Croot attributed a large increase in slope value to the presence of a phytoplankton bloom present during their occupation. Interestingly, a diatom bloom was present at the surface during our occupation at 65°S and 68°S yet the opposite Zn:Si trend was observed whereby values dropped significantly to the lowest ratios recorded. From a temporal perspective, a greater utilization of Zn over the later part of the phytoplankton growth season has been observed previously (Croot et al. 2011). This observation does not hold for our comparison as samples were collected during late summer on both expeditions. In addition, because the Zn:P relationships are in good agreement between the two studies, it suggests Si is exerting a strong control over the differences between the Zn:Si ratios. Results from a bioassay experiment performed at 65°S reveal a significantly different subsurface phytoplankton community assemblage. The bioassay was conducted at the chl-a max (40 m) and indicates a shift away from a diatom based surface assemblage to a Haptophyte dominated assemblage (Figure 35). Laboratory work has demonstrated that the haptophyte (type H), *Phaeocystis*, and diatoms prefer Zn to satisfy their growth requirement while the haptophyte (type 6), *Emiliana Huxleyi*, prefers Co (Sunda and Huntsman, 2000). It follows that higher DZn/DCo ratios favour the growth of diatoms and *Phaeocystis* while becoming disadvantageous to the

growth of *Emiliana Huxleyi*. Calculated DZn/DCo ratios of 0.30 and 0.15 at 65°S (diatom and *Phaeocystis* dominated) and 46°S (greater contribution from *Emiliana Huxleyi*) are in agreement with the laboratory work. The shift in phytoplankton community structure has led to large deeper water Si gradients compared to Zn which ultimately resulted in the observed variations between disappearance ratios.

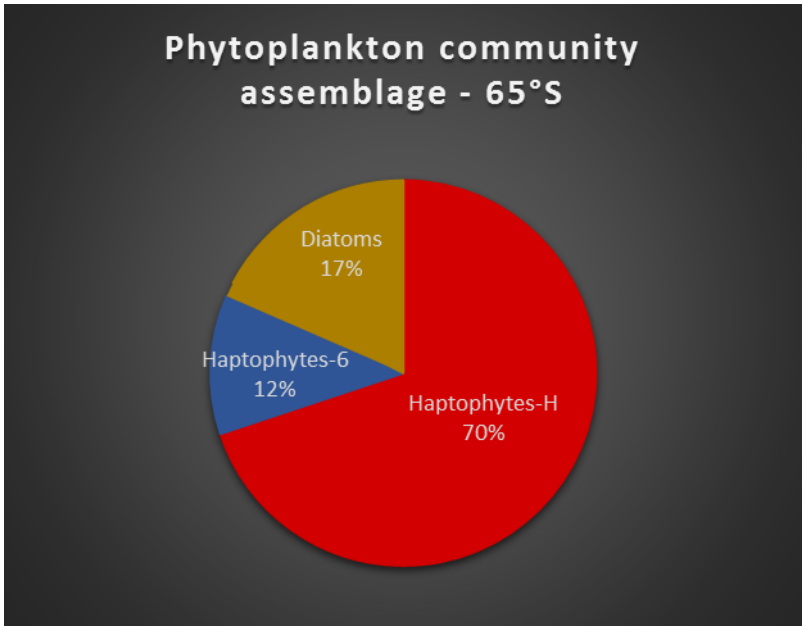

Figure 35 - relative phytoplankton community assemblage obtained from a bioassay experiment conducted at chl-a max (40 m) at 65°S. Data sourced from (Viljoen, 2016).

The Biodilution effect, used to explain the southward increase in Zn:P ratios, may not hold as an explanation for the observed Zn:Si southward increase. The silica content of phytoplankton cells is known to be dependent on Fe availability with faster growing cells, under Fe replete conditions, being more weakly silicified compared to slower growing cells (Croot, Baars and Streu, 2011). Zn may be required for Si uptake resulting in a narrow range of Zn:Si values in the open ocean as seen in Figure 34 (right) where Zn:Si ratios are relatively constant throughout the ACC and northern WG. It is not clear why Zn and Si should be so highly correlated in the ocean. Evidence points toward a connection in the uptake of diatoms however the physiology behind this link is poorly understood.

Zn:Si ratios in deep waters have been used in paleo oceanographic studies as a proxy for the Zn environment for benthic forams and subsequently utilised as a water mass tracer. Due to the lack of global deepwater Zn data, a global deepwater ratio of 0.052 nM/µM has been measured with Si concentrations (Marchitto, Curry and Oppo, 2000). A deepwater (> 1750 m) Zn:Si ratio of 0.052 nM/µM calculated for this study indicates that this ratio is accurate in estimating deep water Zn values.

5. Conclusion

The research described in this thesis serves a dual purpose. Firstly, to report on the process undertaken in order to validate an improved seawater collection and subsequent ICP-MS based analytical technique for the simultaneous quantification of a suite of trace elements (Mn, Fe, Co, Ni, Cu, Zn, Cd, Pb) for their total (unfiltered) and dissolved (<0.2µm) fractions. The method is based on the established protocols defined by the International GEOTRACES programme, from whom we are seeking accreditation. Secondly, to employ the validated analytical technique to measure the concentrations of dissolved copper (DCu) and zinc (DZn) in the Atlantic sector of the Southern Ocean

Seawater sample collection was performed at multiple locations along the Bonus Goodhope Line (BGH) during the 2014/2015 austral summer using a vertical profile sampling technique. Included in the sampling schedule was a baseline station, as required by GEOTRACES, in order to affect an intercalibration through analysis. Samples were analysed for their dissolved Iron (DFe) content at the University of Plymouth (UK) and compared to the results obtained using the facilities at the Department of Earth Science, Stellenbosch University. When compared to results received from the intercalibration, concentrations reported here were slightly higher in the surface waters yet displayed excellent agreement in the intermediate and deepwaters. Differences in the surface waters were attributed to differences in sample resolution. Sampled depths were also predetermined to coincide with those of Klunder et al. 2011 who reported DFe concentrations at the same location. Comparison with this dataset yielded the absence of a concentration peak (1.82 nmol/kg) between 250 and 450 metres depth while deepwater concentrations were substantially higher. Differences in sample collection period and variability in hydrothermal vent outputs from the ocean floor respectively, accounted for these observed dissimilarities. The results of the intercalibration provide sufficient evidence to conclude an effective and contamination free vertical profile sample collection protocol.

A coupled pre-concentration and ICP-MS based analytical technique was employed for the selective removal of trace element ions from the seawater matrix prior to measurement. Certified reference material (SAFe, GEOTRACES and NASS-5) was analysed prior to seawater samples to assess the accuracy, reproducibility and repeatability of the analytical method. Results for the SAFe D1 and D2 standards revealed a good agreement between obtained and certified values perhaps with the exception of Fe for the D1 standard. The reported value of 1.00 ± 0.21 nmol/kg was substantially greater than the 0.67 ± 0.04 nmol/kg consensus value. This is suggestive of possible contamination, most likely sourced from atmospheric deposition entering the sample while on the ICP-MS sample rack. Co and Cu were underestimated by ~ 32% and ~12% respectively. This was expected as, unlike

samples contributing to the consensus values, UV oxidation was not performed prior to preconcentration and ICP-MS analysis. The range of underestimation was within the limits attained by Milne et al. 2010.

Detection limits calculated were well below the average mean trace metal concentrations in the ocean as reported by Sohrin et al. 2008, with the exception of Co which was only marginally below. After a 40 times preconcentration however, all trace elements were at least an order of magnitude above their respective detection limits. Procedural blanks were > 0.52% of the mean open ocean concentration for Ni, Cu, Zn, Cd and Pb. Significant blanks were observed for Mn, Fe and Co and attributed to accumulating atmospheric fallout while sitting uncapped (approx. 2 hrs) on the ICP-MS sample rack. This behaviour did not affect seawater samples as they were left uncapped on the sample rack for a maximum of 6 mins.

To monitor in-run ICP-MS precision and instrumental drift, two internal control standards were inserted into the sequence at set intervals. Firstly, a large volume SU TM4 control standard was created from seawater collected at sample station TM4 (36°S; 13°E). Initially this standard was preconcentrated and analysed without acidification however after results showed a lack of precision, most notably for Fe, it was decided to acidify the standard to that of the seawater samples (pH of 1.7). Formulation of our own consensus value was achieved by multiple analyses (n=10) of the sample. The lack of precision was improved substantially after acidification. Secondly a quality control standard was analysed after every 6 seawater samples and compared to its certified value. Results for the SU TM4 control showed excellent in-run repeatability however significant inter-analysis differences, particularly for Fe, were observed. The quality control standards were slightly underestimated for all analyses except for DTM3 (54°S; 0°) which displayed remarkable accuracy and precision. The results of the internal standards highlight the importance of consistent ICP-MS calibration as it was established that variations in calibration contributed significantly to the inter-analysis variability in elemental concentrations.

Through analysis of certified reference material and internal control standards, the seaFAST-pico SC-4 DX module has demonstrated its ability to simultaneously preconcentrate a suite of trace elements. The utilisation of a polyaminocarboxylic acid, containing both EDTA and IDA, functional group immobilised on the resin column has allowed the selective removal of trace elements from their seawater matrix at a relatively large pH range while displaying an excellent exclusion ability for alkali and alkaline earth metals which contribute to ICP-MS interference. The seawater collection protocol combined with the ICP-MS based analytical technique have proved successful in yielding reliable, accurate and precise trace metal datasets.

The vertical distributions of the total and dissolved fractions of the bio-active trace metals copper and zinc are reported from multiple locations in the Atlantic sector of the Southern Ocean. Samples were collected along the Bonus Goodlhope Line during the 2014/2015 austral summer and represent seawater from contrasting biogeochemical domains. Data are reported in conjunction with other measured biological parameters including macronutrient ($Si(OH)_4$, PO_4^{3-} and NO_3^-) distributions, temperature, salinity and phytoplankton abundance and community assemblages. This provided a unique opportunity to study the factors controlling trace metal distributions and ultimately provide insights regarding the role of the Southern Ocean in the global carbon cycle.

Dissolved copper (DCu) displayed typical nutrient behaviour throughout the transect consistent with sub nanomolar surface concentrations increasing steadily until maxima of between 2 and 3 nmol/kg in the AABW were observed. Dissolved zinc (DZn) concentrations ranged between approximately 1 and 12 nmol/kg and exhibited characteristic nutrient behaviour although intermediate and deepwater distributions were more conservative compared to copper. Both hypotheses were therefore accepted. Local DZn and, to a lesser extent DCu, minima were observed at stations coinciding with elevated productivity (chl-a) owing to biological utilization. Sub-surface DCu and DZn maxima resulted from remineralisation of sinking organic matter from AASW. The incorporation of zinc and silica into diatom opal resulted in a deeper regeneration cycle compared to copper and other macronutrients. The downward flux of diatoms i.e. the silicate pump, is the primary transfer mechanism of DCu and DZn from surface waters in the Southern Ocean. Concentration gradients in intermediate and deep waters were maintained by lateral advection of waters from the Drake Passage and upwelling of nutrient rich UCDW and AABW south of the APF.

DCu displayed the lowest observed concentrations throughout the water column in the STZ. Contrastingly DZn displayed the highest observed concentrations in the STZ. The lack of a significant correlation with salinity in the surface waters for both trace metals suggests an external surface input however possible sources such as riverine inflow, aeolian dust deposition and erosion from the African continental shelf fail to explain the enrichment of Zn simultaneously with the depletion of copper. It appears the resident phytoplankton community, composed of > 90% cyanobacteria, plays a primary role in controlling distributions in the STZ via their exceptionally low zinc requirement.

DCu and DZn displayed a general north-south increase in average MLD and whole water column concentrations although zinc showed some deviation from this trend in the surface waters of the WG. Dry and wet atmospheric deposition inputs were thought to be minor with a greater influx of trace metals sourced from melting sea ice in the southern ACC and WG surface waters. The macronutrients, most notably Si, mirrored this behaviour resulting in significant correlations between

Si and both trace metals over the whole water column. An overall Cu:Si relationship of Cu (nM) = 0.011 Si (µM) + 0.851 (R^2 = 0.85, n=98) was obtained for this study. In the ACC and WG, decreasing Cu:Si ratios through the water column were as a result of the control exerted by the dominant diatom community whereby preferential Si uptake in surface waters resulted in preferential Si release during diatom frustule dissolution in deeper waters. The role of phytoplankton governing trace metal: macronutrient ratios was also observed in the central WG where a shift from a diatom based surface assemblage to a haptophyte based community structure at the chl-a max resulted in a significant decrease in Zn:Si based on different nutritive requirements. Additionally, the relative depletions of DMn and DCd with respect to DZn points toward a shift in the dominant Cd transport system in diatoms from a low-zinc induced system in the ACC to a Mn uptake system in the WG. Despite this, the overall Zn:Si relation of Zn (nM) = 0.043 Si (µM) + 1.021 (R^2 = 0.80, n=98) compared well with the relation of Zn (nM) = 0.039 Si (µM) + 0.437 (R^2 = 0.821, n=121) (Croot, Baars and Streu, 2011). The calculated Zn:Si deepwater ratio of 0.052 nM/µM has validated the inferred ratio of 0.052 nM/µM used as a proxy for benthic foram environments. Additional factors were also observed to influence the relationship between trace metals and macronutrients. For example, the north-south increase in surface Zn:P disappearance ratios were attributed to a combination of light and trace metal limitation.

The APF exerted a strong control over nutrient distributions separating the oligotrophic waters to the north and the HNLC waters to the south. With ample macronutrient availability in the HNLC region of the Southern Ocean, yet relatively low phytoplankton abundance, it is clear that trace metal availability contributes substantially to limiting primary production and subsequently the efficiency of the biological carbon pump.

6. References

Achterberg, E. P. and Braungardt, C. (1999) 'Stripping voltammetry for the determination of trace metal speciation and in-situ measurements of trace metal distributions in marine waters', *Analytica Chimica Acta*, 400, pp. 381–397.

Achterberg, E. P., Braungardt, C. B., Sandford, R. C. and Worsfold, P. J. (2001) 'UV digestion of seawater samples prior to the determination of copper using flow injection with chemiluminescence detection', *Advances in Marine Biology*, 440, pp. 27–36.

Alberto C. Nav (2012) 'A perspective on the future of physical', *Philosophical Transactions of the Royal Society*, 370, pp. 5480–5511. doi: 10.1098/rsta.2012.0400.

Andersson, P., Codispoti, L., Croot, P., Francois, R., Lohan, M. and Obata, H. (2014) *Sampling and Sample-handling Protocols for GEOTRACES Cruises*.

Arrigo, K. R. (1999) 'Phytoplankton Community Structure and the Drawdown of Nutrients and CO2 in the Southern Ocean', *Science*, 283(5400), pp. 365–367. doi: 10.1126/science.283.5400.365.

De Baar, H. J. W., Van Leeuwe, M. A., Scharek, R., Goeyens, L., Bakker, K. M. J. and Fritsche, P. (1997) 'Nutrient anomalies in Fragilariopsis kerguelensis blooms, iron deficiency and the nitrate/phosphate ratio (A. C. Redfield) of the Antarctic Ocean', *Deep-Sea Research Part II: Topical Studies in Oceanography*, 44(1–2), pp. 229–260. doi: 10.1016/S0967-0645(96)00102-6.

Baars, O., Abouchami, W., Galer, S., Boye, M. and Croot, P. (2014) 'Dissolved cadmium in the Southern Ocean: Distribution, speciation, and relation to phosphate', *Limnol. Oceanogr*, 59(2), pp. 385–399. doi: 10.4319/lo.2014.59.2.0385.

Baars, O. and Croot, P. L. (2011) 'The speciation of dissolved zinc in the Atlantic sector of the Southern Ocean', *Deep-Sea Research Part II: Topical Studies in Oceanography*. Elsevier, 58(25–26), pp. 2720–2732. doi: 10.1016/j.dsr2.2011.02.003.

Barnett, J. P., Millard, A., Ksibe, A. Z., Scanlan, D. J., Schmid, R. and Blindauer, C. A. (2012) 'Mining genomes of marine cyanobacteria for elements of zinc homeostasis', *Frontiers in Microbiology*, 3(APR), pp. 1–21. doi: 10.3389/fmicb.2012.00142.

Biller, D. V. and Bruland, K. W. (2012) 'Analysis of Mn, Fe, Co, Ni, Cu, Zn, Cd, and Pb in seawater using the Nobias-chelate PA1 resin and magnetic sector inductively coupled plasma mass spectrometry (ICP-MS)', *Marine Chemistry*. Elsevier B.V., 130–131, pp. 12–20. doi: 10.1016/j.marchem.2011.12.001.

Bown, J., Boye, M., Baker, A., Duvieilbourg, E., Lacan, F., Le Moigne, F., Planchon, F., Speich, S. and Nelson, D. M. (2011) 'The biogeochemical cycle of dissolved cobalt in the Atlantic and the Southern Ocean south off the coast of South Africa', *Marine Chemistry*. Elsevier B.V., 126(1–4), pp. 193–206. doi: 10.1016/j.marchem.2011.03.008.

Boye, M., Wake, B. D., Lopez Garcia, P., Bown, J., Baker, A. R. and Achterberg, E. P. (2012) 'Distributions of dissolved trace metals (Cd, Cu, Mn, Pb, Ag) in the southeastern Atlantic and the Southern Ocean', *Biogeosciences*, 9(8), pp. 3231–3246. doi: 10.5194/bg-9-3231-2012.

Brand, L. E., Sunda, W. G. and Guillard, R. R. L. (1986) 'Reduction of marinephytoplankton reproduction rates by copper and cadmium', *Journal of Experimental Marine Biology and Ecology*, 96(3), pp. 225–250.

Bruland, K. W., Franks, R. P., Knauer, G. A. and Martin, J. H. (1979) 'Sampling and analytical methods

for the determination of copper, cadmium, zinc, and nickel at the nanogram per liter level in sea water', *Analytica Chimica Acta*, 105(C), pp. 233–245. doi: 10.1016/S0003-2670(01)83754-5.

Chance, R., Jickells, T. D. and Baker, A. R. (2015) 'Atmospheric trace metal concentrations, solubility and deposition fluxes in remote marine air over the south-east Atlantic', *Marine Chemistry*. The Authors, 177, pp. 1–12. doi: 10.1016/j.marchem.2015.06.028.

Chever, F., Bucciarelli, E., Sarthou, G., Speich, S., Arhan, M., Penven, P. and Tagliabue, A. (2010) 'Physical speciation of iron in the Atlantic sector of the Southern Ocean along a transect from the subtropical domain to the Weddell Sea Gyre', *Journal of Geophysical Research: Oceans*, 115(10), pp. 1–15. doi: 10.1029/2009JC005880.

Coale, K. H. and Bruland, K. W. (1990) 'Spatial and temporal variability in copper complexation in the North Pacific', *Deep Sea Research*, 37(2), pp. 317–336.

Coale, K. H., Michael Gordon, R. and Wang, X. (2005) 'The distribution and behavior of dissolved and particulate iron and zinc in the Ross Sea and Antarctic circumpolar current along 170°W', *Deep Sea Research Part I: Oceanographic Research Papers*, 52(2), pp. 295–318. doi: 10.1016/j.dsr.2004.09.008.

Croot, P. L., Baars, O. and Streu, P. (2011) 'The distribution of dissolved zinc in the Atlantic sector of the Southern Ocean', *Deep Sea Research Part II: Topical Studies in Oceanography*. Elsevier, 58(25–26), pp. 2707–2719. doi: 10.1016/j.dsr2.2010.10.041.

Duce, R. a and Tindale, N. W. (1991) 'Atmospheric transport of iron and its deposition in the ocean', *Limnology and Oceanography*, 36(8), pp. 1715–1726. doi: 10.4319/lo.1991.36.8.1715.

Ellwood, M. J. and Van den Berg, C. M. G. (2001) 'Determination of organic complexation of cobalt in seawater by cathodic stripping voltammetry', *Marine Chemistry*, 75(1–2), pp. 33–47. doi: 10.1016/S0304-4203(01)00024-X.

Ellwood, M. J., Boyd, P. W. and Sutton, P. (2008) 'Winter-time dissolved iron and nutrient distributions in the Subantarctic Zone from 40-52S; 155-160E', *Geophysical Research Letters*, 35(11), pp. 2–7. doi: 10.1029/2008GL033699.

Ellwood, M. J. and Hunter, K. A. (1999) 'Determination of the Zn/Si ratio in diatom opal: A method for the separation, cleaning and dissolution of diatoms', *Marine Chemistry*, 66(3–4), pp. 149–160. doi: 10.1016/S0304-4203(99)00037-7.

Ellwood, M. J. and Hunter, K. A. (2000) 'The incorporation of zinc and iron into the frustule of the marine diatom Thalassiosira pseudonana', *Limnology and Oceanography*, 45(7), pp. 1517–1524. doi: 10.4319/lo.2000.45.7.1517.

F. M. M. Morel, R, J. . R., Roberts, S. B., Chamberlain, C. P., Lee, J. G. and Lee, D. (1994) 'Zinc and carbon co-limitation of marine phytoplankton', *Nature*, 369, pp. 740–742.

Finkel, Z. V., Quigg, A., Raven, J. a., Reinfelder, J. R., Schofield, O. E. and Falkowski, P. G. (2006) 'Irradiance and the elemental stoichiometry of marine phytoplankton', *Limnol. Oceanogr.*, 51(October 2015), pp. 2690–2701. doi: 10.4319/lo.2006.51.6.2690.

Franck, V. M., Bruland, K. W., Hutchins, D. A. and Brzezinski, M. A. (2003) 'Iron and zinc effects on silicic acid and nitrate uptake kinetics in three high-nutrient, low-chlorophyll (HNLC) regions', *Marine Ecology Progress Series*, 252(3), pp. 15–33. doi: 10.3354/meps252015.

Frew, R., Bowie, A., Croot, P. and Pickmere, S. (2001) 'Macronutrient and trace-metal geochemistry of an in situ iron-induced Southern Ocean bloom', *Deep-Sea Research Part II: Topical Studies in Oceanography*, 48(11–12), pp. 2467–2481. doi: 10.1016/S0967-0645(01)00004-2.

Gibberd, M. J., Kean, E., Barlow, R., Thomalla, S. and Lucas, M. (2013) 'Phytoplankton

chemotaxonomy in the Atlantic sector of the Southern Ocean during late summer 2009', *Deep-Sea Research Part I: Oceanographic Research Papers*. Elsevier, 78, pp. 70–78. doi: 10.1016/j.dsr.2013.04.007.

Gladyshev, S., Arhan, M., Sokov, A. and Speich, S. (2008) 'A hydrographic section from South Africa to the southern limit of the Antarctic Circumpolar Current at the Greenwich meridian', *Deep-Sea Research Part I: Oceanographic Research Papers*, 55(10), pp. 1284–1303. doi: 10.1016/j.dsr.2008.05.009.

Grotti, M., Soggia, F., Abelmoschi, M. L., Rivaro, P., Magi, E. and Frache, R. (2001) 'Temporal distribution of trace metals in Antarctic coastal waters'.

Halstead, M. J. R., Cunninghame, R. G. and Hunter, K. A. (2000) 'Wet deposition of trace metals to a remote site in Fiordland, New Zealand', *Atmospheric Environment*, 34(4), pp. 665–676. doi: 10.1016/S1352-2310(99)00185-5.

Hassler, C. S., Sinoir, M., Clementson, L. A. and Butler, E. C. V (2012) 'Exploring the link between micronutrients and phytoplankton in the Southern Ocean during the 2007 austral summer', *Frontiers in Microbiology*, 3(JUL), pp. 1–26. doi: 10.3389/fmicb.2012.00202.

Heller, M. I. and Croot, P. L. (2014) 'Copper speciation and distribution in the Atlantic sector of the Southern Ocean', *Marine Chemistry*. Elsevier B.V., 173(February 2008), pp. 253–268. doi: 10.1016/j.marchem.2014.09.017.

Ho, T.-Y., Quigg, A., Finkel, Z. V., Milligan, A. J., Wyman, K., Falkowski, P. G. and Morel, F. M. M. (2003) 'The elemental composition of some marine phytoplankton', *Journal of Phycology*, 39(6), pp. 1145–1159. doi: 10.1111/j.0022-3646.2003.03-090.x.

Ho, T. Y., Chien, C. Te, Wang, B. N. and Siriraks, A. (2010) 'Determination of trace metals in seawater by an automated flow injection ion chromatograph pretreatment system with ICPMS', *Talanta*. Elsevier B.V., 82(4), pp. 1478–1484. doi: 10.1016/j.talanta.2010.07.022.

Hong, S., Boutron, C. F., Edwards, R. and Morgan, V. I. (1998) 'Heavy metals in antarctic ice from Law Dome: initial results.', *Environmental research*, 78(2), pp. 94–103. doi: 10.1006/enrs.1998.3849.

Jerez Veguería, S. F., Godoy, J. M., De Campos, R. C. and Gonçalves, R. A. (2013) 'Trace element determination in seawater by ICP-MS using online, offline and bath procedures of preconcentration and matrix elimination', *Microchemical Journal*. Elsevier B.V., 106, pp. 121–128. doi: 10.1016/j.microc.2012.05.032.

Kingston, H. M., Barnes, I. L., Brady, T. J., Rains, T. C. and Champ, M. A. (1978) 'Separation of eight transition elements from alkali and alkaline earth elements in estuarine and seawater with chelating resin and their determination by graphite furnace atomic absorption spectrometry', *Analytical Chemistry*, 50(14), pp. 2064–2070. doi: 10.1021/ac50036a031.

Klunder, M. B., Laan, P., Middag, R., De Baar, H. J. W. and Van Ooijen, J. C. (2011) 'Dissolved iron in the Southern Ocean (Atlantic sector)', *Deep-Sea Research Part II*. Elsevier, 58(25–26), pp. 2678–2694. doi: 10.1016/j.dsr2.2010.10.042.

Lagerstrom, M. E., Field, M. P., Seguret, M., Fischer, L., Hann, S. and Sherrell, R. M. (2013) 'Automated on-line flow-injection ICP-MS determination of trace metals (Mn, Fe, Co, Ni, Cu and Zn) in open ocean seawater: Application to the GEOTRACES program', *Marine Chemistry*, 155(July), pp. 71–80. doi: 10.1016/j.marchem.2013.06.001.

Lee, J., Boyle, E. A., Echegoyen-Sanz, Y., Fitzsimmons, J. N., Zhang, R. and Kayser, R. A. (2011) 'Analysis of trace metals (Cu, Cd, Pb, and Fe) in seawater using single batch nitrilotriacetate resin extraction and isotope dilution inductively coupled plasma mass spectrometry.', *Analytica chimica*

acta. Elsevier B.V., 686(1–2), pp. 93–101. doi: 10.1016/j.aca.2010.11.052.

Lohan, M. C., Aguilar-Islas, A. M., Franks, R. P. and Bruland, K. W. (2005) 'Determination of iron and copper in seawater at pH 1.7 with a new commercially available chelating resin, NTA Superflow', *Analytica Chimica Acta*, 530(1), pp. 121–129. doi: 10.1016/j.aca.2004.09.005.

Löscher, B. M. (1999) 'Relationship among Ni, Cu, Zn, and major nutrients in the Southern Ocean', *Marine Chemistry*, 67, pp. 67–102.

Marchitto, T. M., Curry, W. B. and Oppo, D. W. (2000) 'Zinc concentrations in benthic foraminifera reflect seawater chemistry', *Paleoceanography*, 15(3), pp. 299–306. doi: 10.1029/1999PA000420.

Mclaren, J. W., Mykytiuk, A. P., Willie, S. N. and Berman, S. S. (1985) 'Determination of Trace Metals in Seawater by Inductively Coupled Plasma Mass Spectrometry with Preconcentration on', *Analytical Chemistry*, (57), pp. 2907–2911. doi: 10.1021/ac00291a037.

Milne, A., Landing, W., Bizimis, M. and Morton, P. (2010) 'Determination of Mn, Fe, Co, Ni, Cu, Zn, Cd and Pb in seawater using high resolution magnetic sector inductively coupled mass spectrometry (HR-ICP-MS)', *Analytica Chimica Acta*. Elsevier B.V., 665(2), pp. 200–207. doi: 10.1016/j.aca.2010.03.027.

Minami, T., Konagaya, W., Zheng, L., Takano, S., Sasaki, M., Murata, R., Nakaguchi, Y. and Sohrin, Y. (2015) 'An off-line automated preconcentration system with ethylenediaminetriacetate chelating resin for the determination of trace metals in seawater by high-resolution inductively coupled plasma mass spectrometry', *Analytica Chimica Acta*. Elsevier B.V., 854, pp. 183–190. doi: 10.1016/j.aca.2014.11.016.

Moffett, J. W. and Dupont, C. (2007) 'Cu complexation by organic ligands in the sub-arctic NW Pacific and Bering Sea', *Deep-Sea Research Part I: Oceanographic Research Papers*, 54(4), pp. 586–595. doi: 10.1016/j.dsr.2006.12.013.

Moffett, J. W. and Ho, J. (1996) 'Oxidation of cobalt and manganese in seawater via a common microbially catalyzed pathway', *Geochimica et Cosmochimica Acta*, 60(18), pp. 3415–3424. doi: 10.1016/0016-7037(96)00176-7.

Le Moigne, F. A. C., Boye, M., Masson, A., Corvaisier, R., Grossteffan, E., Gueneugues, A. and Pondaven, P. (2013) 'Description of the biogeochemical features of the subtropical southeastern Atlantic and the Southern Ocean south of South Africa during the austral summer of the International Polar Year', *Biogeosciences*, 10(1), pp. 281–295. doi: 10.5194/bg-10-281-2013.

Nolting, R. F. and de Baar, H. J. W. (1994) 'Behaviour of nickel, copper, zinc and cadmium in the upper 300m of a transect in the Southern Ocean (57°-62°S, 49°W)', *Marine Chemistry*, 45, pp. 225–242.

Pollard, R. T., Lucas, M. I. and Read, J. F. (2002) 'Physical controls on biogeochemical zonation in the Southern Ocean', *Deep-Sea Research Part II: Topical Studies in Oceanography*, 49(16), pp. 3289–3305. doi: 10.1016/S0967-0645(02)00084-X.

Popova, E. E., Ryabchenko, V. A. and Fasham, M. J. R. (2000) 'Biological pump and vertical mixing in the Southern Ocean: Their impact on atmospheric CO2', *Global Biogeochemical Cycles*, 14(1), pp. 477–498. doi: 10.1029/1999GB900090.

Quéroué, F., Townsend, A., van der Merwe, P., Lannuzel, D., Sarthou, G., Bucciarelli, E. and Bowie, A. (2014) 'Advances in the offline trace metal extraction of Mn, Co, Ni, Cu, Cd, and Pb from open ocean seawater samples with determination by sector field ICP-MS analysis', *Analytical Methods*, 6(9), p. 2837. doi: 10.1039/c3ay41312h.

Rahmi, D., Zhu, Y., Fujimori, E., Umemura, T. and Haraguchi, H. (2007) 'Multielement determination of trace metals in seawater by ICP-MS with aid of down-sized chelating resin-packed minicolumn for preconcentration', *Talanta*, 72(2), pp. 600–606. doi: 10.1016/j.talanta.2006.11.023.

Reid, P. C., Fischer, A. C., Lewis-Brown, E., Meredith, M. P., Sparrow, M., Andersson, A. J., Antia, A., Bates, N. R., Bathmann, U., Beaugrand, G., Brix, H., Dye, S., Edwards, M., Furevik, T., Gangstø, R., Hátún, H., Hopcroft, R. R., Kendall, M., Kasten, S., Keeling, R., Le Quéré, C., Mackenzie, F. T., Malin, G., Mauritzen, C., Ólafsson, J., Paull, C., Rignot, E., Shimada, K., Vogt, M., Wallace, C., Wang, Z. and Washington, R. (2010) *Impacts of the oceans on climate change*, *Advances in Marine Biology*. doi: 10.1016/S0065-2881(09)56001-4.

Richard W. Eppley (1972) 'Temperature and phytoplankton growth in sea', *Fishery Bulletin*, 70(4), pp. 1063–1085.

Saito, M. A. and Moffett, J. W. (2001) 'Complexation of cobalt by natural organic ligands in the Sargasso sea as determined by a new high-sensitivity electrochemical cobalt speciation method suitable for open ocean work', *Marine Chemistry*, 75(1–2), pp. 49–68. doi: 10.1016/S0304-4203(01)00025-1.

Saito, M. A. and Moffett, J. W. (2002) 'Temporal and spatial variability of cobalt in the Atlantic Ocean', *Geochimica et Cosmochimica Acta*, 66(11), pp. 1943–1953. doi: 10.1016/S0016-7037(02)00829-3.

Smetacek, V., De Baar, H. J. W., Bathmann, U. V., Lochte, K. and Rutgers Van Der Loeff, M. M. (1997) 'Ecology and biogeochemistry of the Antarctic Circumpolar Current during austral spring: A summary of Southern Ocean JGOFS cruise ANT X/6 of R.V. Polarstern', *Deep-Sea Research Part II: Topical Studies in Oceanography*, 44(1–2), pp. 1–21. doi: 10.1016/S0967-0645(96)00100-2.

Sohrin, Y., Urushihara, S., Nakatsuka, S., Kono, T., Higo, E., Minami, T., Norisuye, K. and Umetani, S. (2008) 'Multielemental determination of GEOTRACES key trace metals in seawater by ICPMS after preconcentration using an ethylenediaminetriacetic acid chelating resin', *Analytical Chemistry*, 80(16), pp. 6267–6273. doi: 10.1021/ac800500f.

Stein, A. F., Draxler, R. R., Rolph, G. D., Stunder, B. J. B., Cohen, M. D. and Ngan, F. (2015) 'Noaa's hysplit atmospheric transport and dispersion modeling system', *Bulletin of the American Meteorological Society*, 96(12), pp. 2059–2077. doi: 10.1175/BAMS-D-14-00110.1.

Sunda, W. (1991) 'Trace metal interactions with marine phytoplankton', *Biological Oceanography*, 6(June 2015), pp. 411–442. doi: 10.1080/01965581.1988.10749543.

Sunda, W. G. and Huntsman, S. A. (2000) 'Effect of Zn, Mn, and Fe on Cd accumulation in phytoplankton: Implications for oceanic Cd cycling', *Limnology and Oceanography*, 45(7), pp. 1501–1516. doi: 10.4319/lo.2000.45.7.1501.

Sunda, W. G. and Huntsman, S. A. (2005) 'Effect of CO 2 supply and demand on zinc uptake and growth limitation in a coastal diatom', *Limnology and Oceanography*, 50(4), pp. 1181–1192. Available at: http://www.jstor.org/stable/10.2307/3597397%5Cnpapers2://publication/uuid/17E0C4E2-A77E-4E49-90E1-C3255D7A7DE3.

Tabachnick, B. G. and Fidell, L. S. (2007) *Using multivariate statistics*, *Harper Collins Publishers*. doi: 10.1037/022267.

Twining, B. S., Baines, S. B. and Fisher, N. S. (2004) 'Element stoichiometries of individual plankton cells collected during the Southern Ocean Iron Experiment (SOFeX)', *Limnology and Oceanography*, 49(6), pp. 2115–2128. doi: 10.4319/lo.2004.49.6.2115.

Viljoen, J. J. (2016) *Phytoplankton Pigment Analysis and CHEMTAX determination of phytoplankton community structure in the Southern Ocean*.

Wang, B.-S., Lee, C.-P. and Ho, T.-Y. (2014) 'Trace metal determination in natural waters by automated solid phase extraction system and ICP-MS: the influence of low level Mg and Ca.', *Talanta*. Elsevier, 128, pp. 337–44. doi: 10.1016/j.talanta.2014.04.077.

Williams, R. G. and Follows, M. J. (2011) 'Biological Fundamentals', *Ocean Dynamic and the Carbon Cycle: Principles and Mechanisms*, pp. 93–124.

Wyatt, N. J., Milne, A., Woodward, E. M. S., Rees, A. P., Browning, T. J., Bouman, H. A., Worsfold, P. J. and Lohan, M. C. (2014) 'Biogeochemical cycling of dissolved zinc along the GEOTRACES South Atlantic transect GA10 at 40°S', *Global Biogeochemical Cycles*, 28(1), pp. 44–56. doi: 10.1002/2013GB004637.

7. Appendix

A. Complete Total and Dissolved Trace Metal Dataset

Table A1 - Total (T) and dissolved (D) concentrations for a suite of trace metals according to depth for the seven sample locations along the Bonus Goodhope Line. Tables are in north-south order. Total fraction collected unfiltered in PFA bottles, dissolved fraction collected filtered (0.2 µm) in LDPE bottles. Data and statistics reported here are not corrected for potentially contaminated samples or outliers however references to data in the text are. One standard deviation is reported on duplicate samples. Values highlighted in red are deemed outliers (%RSD > 15%). Concentrations are nmol/kg except trace metals with a (*) which are in pmol/kg.

Domain (Station)	Lat/Long	Depth (m)	TMn	DMn	Std Dev.	TFe	Dfe	Std Dev.	TCo*	DCo	Std Dev.	TNi	DNi	Std Dev.
STZ (TM4)	36˚ 00' S 13˚ 09' E	15	1.01	0.96	0.04	0.26	0.17	0.01	18.02	7.66	2.52	2.46	2.37	0.03
		30	1.04	0.95	0.00	0.22	0.27	0.09	18.35	6.69	1.40	2.44	2.39	0.02
		41	1.03	0.91	0.03	0.29	0.20	0.05	21.20	4.10	0.02	2.46	2.34	0.03
		60	0.85	0.79	0.03	0.39	0.18	0.00	19.57	7.00	0.76	2.45	2.36	0.05
		80	0.80	0.71	0.00	0.34	0.17	0.04	19.68	8.09	0.21	2.70	2.60	0.00
		100	-	0.63	0.03	-	0.13	0.01	-	11.33	1.30	-	2.45	0.03
		150	0.58	0.56	0.00	0.32	0.25	0.06	13.90	11.16	0.50	2.74	3.03	0.02
		250	0.41	0.28	0.00	1.18	0.35	0.01	20.03	18.43	0.16	3.34	3.25	0.08
		301	0.35	0.24	0.01	1.33	0.36	0.00	19.34	18.42	0.46	3.41	3.43	0.06
		400	0.41	0.27	0.00	1.10	0.39	0.00	23.32	22.15	0.11	3.82	3.81	0.06
		501	0.37	0.25	0.00	1.12	0.41	0.01	27.37	27.25	1.69	4.37	4.29	0.04
		600	0.38	0.25	0.00	2.04	0.59	0.01	34.47	31.06	0.01	5.22	4.79	0.02
		801	0.28	0.20	0.00	1.35	0.56	0.02	33.60	34.24	0.68	5.45	5.59	0.04
		1000	0.31	0.21	0.00	1.64	0.64	0.04	35.42	32.75	0.25	6.18	6.14	0.05
Maximum			1.04	0.96		2.04	0.64		35.42	34.24		6.18	6.14	
Minimum			0.28	0.20		0.22	0.13		13.90	4.10		2.44	2.34	
Sub-surface (MLD)			1.02	0.94		0.26	0.21		19.19	6.15		2.45	2.37	
Surface (500m)			0.68	0.59		0.66	0.26		20.08	12.93		3.02	2.94	
Inter (500-1700m)			0.34	0.23		1.54	0.55		32.71	31.32		5.30	5.20	
Deep (>1700m			-	-		-	-		-	-		-	-	

Table A1 continued

Domain (Station)	Lat/Long	Depth (m)	TCu	DCu	Std Dev.	TZn	DZn	Std Dev.	TCd*	DCd	Std Dev.	TPb*	DPb	Std Dev.
STZ (TM4)	36˚ 00' S 13˚ 09' E	15	0.54	0.54	0.03	9.36	9.37	0.90	16.57	11.43	2.78	17.60	16.84	0.45
		30	0.55	0.56	0.01	10.33	13.98	2.25	18.60	8.68	0.09	19.64	17.92	0.06
		41	0.53	0.54	0.00	9.32	9.89	0.11	16.57	8.40	0.05	18.32	16.97	0.09
		60	0.50	0.45	0.00	9.49	10.22	0.42	17.42	8.62	0.02	16.92	16.43	0.29
		80	0.46	0.43	0.01	9.71	9.57	0.02	23.23	10.25	0.24	16.31	15.83	0.11
		100	-	0.46	0.02	-	9.04	0.41	-	21.47	0.38	-	17.03	0.41
		150	0.46	0.51	0.01	8.56	10.86	0.29	29.70	33.41	1.63	15.29	17.22	0.05
		250	0.60	0.58	0.02	8.61	9.44	0.22	107.27	106.50	2.87	20.07	19.49	0.28
		301	0.59	0.60	0.01	8.44	10.02	0.05	117.62	128.62	5.55	20.10	20.62	0.24
		400	0.64	0.63	0.01	9.31	10.65	0.05	180.52	181.83	3.21	18.07	17.91	0.17
		501	0.74	0.73	0.01	8.57	14.43	4.27	297.46	299.39	1.31	15.64	15.18	0.08
		600	0.88	0.83	0.00	9.80	10.26	0.21	448.65	445.76	6.28	16.11	15.16	0.08
		801	1.00	1.00	0.01	10.04	11.92	0.04	584.19	604.57	6.39	14.73	15.71	0.29
		1000	1.27	1.19	0.01	11.53	12.51	0.08	711.01	732.09	1.59	13.58	12.92	0.20
Maximum			1.27	1.19		11.53	14.43		711.01	732.09		20.10	20.62	
Minimum			0.46	0.43		8.44	9.04		16.57	8.40		13.58	12.92	
Sub-surface (MLD)			0.54	0.55		9.67	11.08		17.25	9.50		18.52	17.24	
Surface (500m)			0.56	0.55		9.17	10.68		82.49	74.42		17.79	17.40	
Inter (500-1700m)			0.97	0.94		9.99	12.28		510.33	520.45		15.02	14.74	
Deep (>1700m			-	-		-	-		-	-		-	-	

Table A1 continued

Domain (Station)	Lat/Long	Depth (m)	TMn	DMn	Std Dev.	TFe	Dfe	Std Dev.	TCo*	DCo	Std Dev.	TNi	DNi	Std Dev.
PFZ (DTM2)	46˚ 00' S 08˚ 00' E	14	0.29	0.23	0.00	0.71	0.38	0.03	49.22	33.34	0.94	5.59	5.07	0.02
		35	0.28	0.25	0.02	0.70	0.39	0.07	37.85	33.35	1.64	5.40	5.30	0.05
		75	0.24	0.28	0.02	0.56	0.61	0.24	48.84	35.47	2.21	5.08	5.36	0.01
		100	0.34	0.32	0.00	0.66	0.40	0.01	41.72	33.37	5.08	5.90	5.09	0.50
		150	0.33	0.31	0.00	0.62	0.47	0.07	40.02	37.59	0.59	5.77	5.51	0.01
		200	0.35	0.34	0.01	1.11	0.51	0.00	44.81	38.84	0.30	5.63	5.65	0.01
		400	0.26	0.27	0.02	1.31	0.68	0.02	43.16	37.73	1.15	6.16	6.30	0.29
		501	0.31	0.26	0.01	1.19	0.80	0.14	44.02	38.39	1.41	6.35	6.22	0.18
		622	0.27	0.24	0.02	1.20	0.61	0.03	35.76	33.05	1.55	5.97	6.11	0.44
		1000	0.37	0.29	0.01	1.46	0.87	0.05	36.79	32.42	0.36	7.26	6.77	0.03
		1501	0.32	0.25	0.01	1.85	1.04	0.10	34.68	30.87	1.90	6.96	6.63	0.34
		2000	0.37	0.25	0.00	1.66	0.98	0.03	33.68	27.52	1.14	6.60	6.27	0.09
		3000	0.25	0.18	0.00	1.67	0.95	0.10	21.90	18.34	0.79	6.68	6.47	0.17
		4002	0.45	0.17	0.00	4.32	0.86	0.06	22.24	13.29	0.73	6.75	6.68	0.24
		4302	1.08	0.18	0.01	11.83	0.84	0.08	28.95	13.27	0.46	8.39	7.26	0.03
Maximum			1.08	0.34		11.83	1.04		49.22	38.84		8.39	7.26	
Minimum			0.24	0.17		0.56	0.38		21.90	13.27		5.08	5.07	
Sub-surface (MLD)			0.29	0.27		0.66	0.44		44.41	33.88		5.49	5.20	
Surface (500m)			0.30	0.28		0.86	0.53		43.71	36.01		5.73	5.56	
Inter (500-1700m)			0.32	0.26		1.42	0.83		37.81	33.68		6.64	6.43	
Deep (>1700m			0.54	0.20		4.87	0.91		26.69	18.10		7.10	6.67	

Table A1 continued

Domain (Station)	Lat/Long	Depth (m)	TCu	DCu	Std Dev.	TZn	DZn	Std Dev.	TCd*	DCd	Std Dev.	TPb*	DPb	Std Dev.
PFZ (DTM2)	46˚ 00' S 08˚ 00' E	14	1.09	1.00	0.03	0.90	1.46	0.61	348.07	249.01	0.57	11.42	11.34	0.80
		35	0.99	0.97	0.02	0.86	0.77	0.13	324.63	268.11	4.70	12.69	11.53	0.27
		75	0.98	1.04	0.12	0.76	3.42	2.85	321.00	269.61	13.40	10.17	16.82	5.71
		100	1.12	0.91	0.07	2.59	2.33	0.38	368.12	286.60	31.76	15.65	10.82	0.71
		150	1.10	1.02	0.02	1.95	1.32	0.07	457.45	431.72	0.84	19.71	12.31	0.14
		200	1.08	1.02	0.02	2.69	2.61	0.81	584.55	597.62	8.41	14.58	14.05	0.02
		400	1.26	1.23	0.05	2.31	2.85	0.36	711.69	727.69	30.50	14.10	15.50	1.28
		501	1.43	1.26	0.02	3.81	3.50	0.14	799.08	769.51	8.35	16.89	15.87	0.37
		622	1.36	1.32	0.09	4.88	3.39	0.11	727.83	760.55	46.08	13.94	13.43	0.75
		1000	1.88	1.74	0.03	5.21	4.82	0.00	891.60	836.17	6.13	14.21	13.55	0.81
		1501	2.06	1.90	0.12	4.75	5.01	0.13	752.50	722.64	37.87	13.71	13.00	1.06
		2000	2.15	1.97	0.02	6.65	5.15	0.56	644.25	629.05	12.17	18.18	11.70	0.21
		3000	2.67	2.44	0.05	5.50	5.22	0.08	683.01	667.70	14.40	8.59	8.37	0.05
		4002	2.97	2.82	0.09	5.82	6.14	0.08	706.93	708.84	19.89	11.16	9.87	0.00
		4302	3.95	3.15	0.01	6.97	6.96	0.35	894.34	787.23	0.87	10.44	7.46	0.28
Maximum			3.95	3.15		6.97	6.96		894.34	836.17		19.71	16.82	
Minimum			0.98	0.91		0.76	0.77		321.00	249.01		8.59	7.46	
Sub-surface (MLD)			1.04	0.98		1.28	2.00		340.46	268.33		12.48	12.63	
Surface (500m)			1.13	1.06		1.98	2.28		489.33	449.98		14.40	13.53	
Inter (500-1700m)			1.68	1.55		4.66	4.18		792.75	772.22		14.69	13.96	
Deep (>1700m			2.94	2.59		6.23	5.87		732.13	698.20		12.10	9.35	

Table A1 continued

Domain (Station)	Lat/Long	Depth (m)	TMn	DMn	Std Dev.	TFe	Dfe	Std Dev.	TCo*	DCo	Std Dev.	TNi	DNi	Std Dev.
APF (TM1)	50˚ 27' S 02˚ 00' E	16	0.21	0.13	0.01	0.20	0.23	0.01	24.40	20.30	0.83	4.89	4.98	0.23
		31	0.20	0.12	0.01	0.19	0.11	0.01	23.63	21.69	2.63	5.10	5.03	0.27
		40	0.22	0.13	0.00	0.19	0.11	0.01	30.17	22.64	0.40	5.34	5.11	0.09
		60	0.22	0.14	0.01	0.17	0.08	0.00	25.67	23.13	0.94	4.94	5.25	0.29
		78	0.26	0.14	0.00	0.36	0.15	0.07	27.41	23.01	0.59	5.27	5.21	0.06
		100	0.27	0.16	0.00	0.50	0.22	0.08	26.07	24.55	0.24	5.08	5.61	0.11
		150	0.31	0.29	0.00	0.56	0.21	0.02	33.21	32.51	0.24	5.80	5.65	0.03
		198	0.28	0.25	0.00	0.48	0.20	0.01	31.63	31.14	0.02	5.56	5.78	0.12
		251	0.26	0.25	0.00	0.52	0.34	0.10	30.20	31.73	0.38	5.76	6.07	0.00
		303	0.27	0.24	0.00	0.67	0.29	0.00	31.46	30.73	0.11	6.15	6.19	0.07
		400	0.28	0.24	0.00	0.84	0.34	0.01	30.59	27.74	1.06	6.22	6.12	0.26
		500	0.27	0.24	0.01	0.91	0.41	0.01	27.32	28.89	0.46	6.24	6.65	0.21
		599	0.27	0.20	0.00	0.80	0.38	0.01	26.22	28.96	0.34	6.39	6.33	0.02
		800	0.19	0.17	0.01	0.95	0.43	0.01	29.38	27.56	0.29	6.31	6.28	0.13
		1002	0.21	0.17	0.00	0.89	0.55	0.02	26.67	26.51	0.34	6.16	6.17	0.04
Maximum			0.31	0.29		0.95	0.55		33.21	32.51		6.39	6.65	
Minimum			0.19	0.12		0.17	0.08		23.63	20.30		4.89	4.98	
Sub-surface (MLD)			0.23	0.14		0.27	0.15		26.22	22.55		5.10	5.20	
Surface (500m)			0.25	0.19		0.47	0.23		28.48	26.50		5.53	5.64	
Inter (500-1700m)			0.22	0.18		0.88	0.45		27.42	27.68		6.29	6.26	
Deep (>1700m			-	-		-	-		-	-		-	-	

Table A1 continued

Domain (Station)	Lat/Long	Depth (m)	TCu	DCu	Std Dev.	TZn	DZn	Std Dev.	TCd*	DCd	Std Dev.	TPb*	DPb	Std Dev.
APF (TM1)	50˚ 27' S 02˚ 00' E	16	0.98	0.94	0.05	0.99	1.27	0.31	307.27	245.60	11.16	5.56	5.32	0.23
		31	1.01	0.94	0.06	0.95	0.62	0.03	313.74	248.25	20.44	5.94	5.81	0.53
		40	1.08	0.95	0.03	0.91	0.62	0.00	330.08	247.15	3.44	6.83	5.86	0.00
		60	0.98	0.96	0.07	1.08	1.02	0.13	320.40	257.46	16.12	5.71	5.61	0.40
		78	1.07	0.96	0.01	1.30	0.61	0.01	367.56	253.52	1.21	6.46	5.96	0.10
		100	1.05	1.08	0.02	1.10	1.19	0.14	343.06	275.90	4.30	6.70	7.01	0.08
		150	1.20	1.09	0.00	2.72	2.53	0.02	724.62	698.59	4.03	9.65	9.43	0.00
		198	1.21	1.15	0.02	3.15	3.25	0.10	728.29	758.77	10.08	11.49	11.96	0.74
		251	1.32	1.33	0.01	3.40	3.51	0.02	768.60	831.51	2.83	9.38	10.33	0.08
		303	1.43	1.34	0.02	4.23	4.19	0.07	859.34	861.58	14.65	10.77	10.96	0.19
		400	1.55	1.41	0.05	5.14	4.81	0.18	882.56	859.94	28.78	10.60	10.17	0.22
		500	1.57	1.59	0.04	5.05	5.42	0.20	836.28	905.86	25.43	9.68	10.48	0.34
		599	1.73	1.63	0.03	5.40	6.28	0.84	834.32	830.61	1.39	9.42	8.53	0.08
		800	1.86	1.75	0.01	5.32	5.30	0.03	782.81	783.03	0.96	9.22	8.72	0.01
		1002	1.93	1.77	0.01	5.42	5.35	0.07	729.21	721.36	6.89	9.00	8.81	0.02
Maximum			1.93	1.77		5.42	6.28		882.56	905.86		11.49	11.96	
Minimum			0.98	0.94		0.91	0.61		307.27	245.60		5.56	5.32	
Sub-surface (MLD)			1.03	0.97		1.06	0.89		330.35	254.65		6.20	5.93	
Surface (500m)			1.20	1.14		2.50	2.42		565.15	537.01		8.23	8.24	
Inter (500-1700m)			1.84	1.72		5.38	5.64		782.11	778.33		9.21	8.69	
Deep (>1700m			-	-		-	-		-	-		-	-	

Table A1 continued

Domain (Station)	Lat/Long	Depth (m)	TMn	DMn	Std Dev.	TFe	Dfe	Std Dev.	TCo*	DCo	Std Dev.	TNi	DNi	Std Dev.
ACC (DTM3)	53˚ 59' S 00˚ 00' E	15	0.27	0.20	0.00	0.47	0.24	0.02	28.41	23.56	0.90	5.74	5.42	0.07
		23	0.31	0.21	0.00	0.55	0.12	0.01	31.36	25.68	0.28	5.71	5.78	0.06
		50	0.34	0.24	0.00	2.34	0.33	0.15	32.28	24.46	0.63	5.95	5.41	0.21
		75	0.32	0.24	0.02	1.08	0.30	0.08	29.60	24.43	0.79	5.39	5.23	0.02
		101	0.41	0.37	0.01	0.18	0.21	0.04	29.25	27.77	0.37	5.25	5.50	0.08
		151	0.53	0.49	0.02	0.32	0.27	0.05	36.54	32.47	0.05	6.02	5.68	0.04
		250	0.40	0.40	0.01	0.60	0.41	0.04	30.12	31.96	0.42	5.81	6.04	0.05
		298	0.68	0.58	0.02	2.19	1.22	0.00	35.36	31.77	1.20	6.76	6.31	0.27
		350	0.67	0.67	0.04	2.71	1.82	0.02	39.08	29.79	1.47	5.98	6.13	0.34
		398	0.50	0.45	0.02	1.63	0.92	0.01	30.46	28.51	0.64	6.34	6.10	0.02
		450	0.32	0.34	0.05	0.89	0.44	0.06	28.03	28.30	0.63	6.26	6.74	0.40
		500	0.29	0.30	0.02	0.26	3.43	2.98	22.98	28.87	1.10	6.18	6.59	0.17
		549	0.38	0.33	0.00	2.00	0.94	0.01	31.45	28.05	2.39	6.86	6.86	0.71
		599	0.35	0.34	0.00	0.81	0.55	0.02	25.31	25.28	0.03	6.79	6.99	0.03
		650	0.34	0.32	0.00	0.92	0.53	0.02	30.82	24.78	0.06	7.12	6.94	0.12
		749	0.32	0.29	0.00	0.77	0.46	0.02	23.79	22.89	0.25	6.95	6.79	0.00
		1000	0.27	0.24	0.00	0.64	0.64	0.00	19.87	18.21	0.00	6.45	6.45	0.00
		1250	0.27	0.19	0.00	0.64	0.43	0.01	16.55	18.21	0.00	6.45	6.24	0.00
		1502	0.23	0.18	0.01	0.99	0.49	0.08	18.21	16.55	0.00	6.33	6.18	0.14
		1749	0.25	0.19	0.00	0.96	0.48	0.01	16.55	15.73	0.83	6.08	6.10	0.15
		2001	0.33	0.25	0.01	0.86	0.57	0.01	14.90	14.90	0.00	6.05	6.06	0.04
		2249	0.32	0.26	0.01	0.99	0.56	0.02	38.08	14.90	0.00	6.61	6.29	0.21
		2400	0.40	0.29	0.02	1.53	0.59	0.01	21.52	14.90	0.00	6.77	6.27	0.14
Maximum			0.68	0.67		2.71	3.43		39.08	32.47		7.12	6.99	
Minimum			0.23	0.18		0.18	0.12		14.90	14.90		5.25	5.23	
Sub-surface (MLD)			0.30	0.22		1.12	0.23		30.68	24.57		5.80	5.54	
Surface (500m)			0.42	0.37		1.10	0.81		31.12	28.13		5.95	5.91	
Inter (500-1700m)			0.31	0.27		0.88	0.93		23.62	22.86		6.64	6.63	
Deep (>1700m			0.33	0.25		1.08	0.55		22.76	15.11		6.38	6.18	

Table A1 continued

Domain (Station)	Lat/Long	Depth (m)	TCu	DCu	Std Dev.	TZn	DZn	Std Dev.	TCd*	DCd	Std Dev.	TPb*	DPb	Std Dev.
ACC (DTM3)	54˚ 00' S 00˚ 00' E	15	1.53	1.45	0.01	2.36	1.55	0.04	426.89	337.32	2.64	5.26	4.94	0.05
		23	1.52	1.42	0.00	5.87	3.01	0.07	533.96	364.28	2.15	5.26	5.14	0.08
		50	1.52	1.32	0.06	2.48	2.09	0.14	514.70	393.04	23.23	5.23	4.96	0.47
		75	1.44	1.35	0.03	2.74	2.55	0.13	406.89	375.99	3.22	7.34	7.27	0.10
		101	1.36	1.33	0.02	2.82	2.65	0.06	596.36	566.16	9.66	5.10	5.47	0.02
		151	1.63	1.41	0.01	4.98	4.44	0.01	848.85	778.08	11.97	6.99	6.70	0.16
		250	1.63	1.60	0.01	6.43	5.93	0.25	856.73	899.14	5.79	8.56	8.58	0.05
		298	1.95	1.72	0.07	6.37	6.22	0.25	927.65	903.99	46.65	8.72	8.22	0.40
		350	1.77	1.73	0.11	6.35	5.87	0.38	802.50	847.38	48.15	8.07	8.31	0.46
		398	1.92	1.70	0.01	6.07	6.18	0.00	848.66	822.10	1.40	8.49	8.33	0.03
		450	1.91	1.90	0.09	6.09	6.32	0.19	814.46	864.45	23.68	9.45	9.80	0.46
		500	0.57	1.95	0.06	6.73	6.61	0.13	838.34	851.31	20.41	7.52	7.64	0.60
		549	2.20	2.07	0.22	6.79	6.57	0.63	812.36	861.39	75.35	7.06	7.67	0.91
		599	2.15	2.14	0.01	7.52	6.68	0.07	784.47	816.38	1.52	7.72	7.60	0.07
		650	2.36	2.17	0.04	6.56	6.42	0.15	810.81	803.75	17.95	8.54	9.65	0.42
		749	2.38	2.21	0.00	6.67	6.48	0.02	799.48	793.21	4.91	8.46	8.25	0.01
		1000	2.30	2.30	0.00	6.71	6.71	0.00	737.72	737.72	0.00	6.12	6.12	0.00
		1250	2.30	2.17	0.01	6.71	6.95	0.00	737.72	726.00	7.38	6.12	5.41	0.24
		1502	2.46	2.28	0.06	7.83	7.15	0.05	747.26	746.40	17.36	5.18	4.71	0.00
		1749	2.44	2.30	0.05	7.74	7.45	0.28	738.59	738.15	19.53	4.71	4.47	0.24
		2001	2.50	2.34	0.01	7.38	7.51	0.13	759.42	741.19	6.08	4.24	5.18	0.47
		2249	2.74	2.55	0.06	7.66	7.66	0.20	759.42	772.87	18.66	6.12	5.89	0.24
		2400	2.92	2.46	0.04	9.18	7.96	0.10	824.51	765.49	7.81	5.18	4.71	0.00
Maximum			2.92	2.55		9.18	7.96		927.65	903.99		9.45	9.80	
Minimum			0.57	1.32		2.36	1.55		406.89	337.32		4.24	4.47	
Sub-surface (MLD)			1.52	1.40		3.57	2.22		491.85	364.88		5.25	5.01	
Surface (500m)			1.56	1.58		4.94	4.45		701.33	666.94		7.17	7.11	
Inter (500-1700m)			2.09	2.16		6.94	6.69		783.52	792.02		7.09	7.13	
Deep (>1700m			2.65	2.41		7.99	7.65		770.48	754.42		5.06	5.06	

Table A1 continued

Domain (Station)	Lat/Long	Depth (m)	TMn	DMn	Std Dev.	TFe	Dfe	Std Dev.	TCo*	DCo	Std Dev.	TNi	DNi	Std Dev.
WG (TM2)	59˚ 59' S 00˚ 00' E	16	0.17	0.03	0.00	0.34	0.13	0.00	27.61	14.48	0.48	6.18	5.98	0.04
		41	0.17	0.10	0.00	0.25	0.46	0.01	22.36	20.48	0.20	5.64	6.09	0.08
		58	0.18	0.09	0.01	0.64	0.26	0.03	21.97	16.33	1.30	6.03	5.89	0.07
		60	0.31	0.23	0.00	2.02	0.19	0.00	34.09	24.12	0.07	6.33	6.17	0.01
		79	0.29	0.25	0.00	0.20	0.14	0.03	23.45	20.43	0.86	6.21	6.02	0.02
		100	0.31	0.29	0.01	0.26	0.33	0.02	22.36	23.27	0.50	6.35	6.16	0.18
		150	0.29	0.34	0.01	0.35	0.25	0.00	18.88	20.94	0.03	6.11	6.73	0.04
		199	0.28	0.28	0.01	0.44	0.24	0.01	19.77	19.24	0.63	6.92	6.83	0.20
		251	0.25	0.26	0.00	0.34	0.23	0.01	17.25	17.26	0.67	6.48	6.80	0.05
		300	0.26	0.26	0.01	0.31	0.16	0.12	19.79	17.22	-	6.79	5.85	1.11
		399	0.24	0.23	0.00	0.41	0.33	0.02	16.74	14.97	0.13	7.10	6.73	0.10
		500	0.20	0.21	0.00	0.33	0.30	0.01	16.17	14.03	0.33	6.71	6.73	0.11
		599	0.19	0.19	0.00	0.36	0.30	0.01	13.96	14.12	1.21	6.91	6.71	0.08
		800	0.18	0.16	0.00	0.47	0.31	0.01	12.83	11.09	0.38	7.00	6.73	0.08
		1001	0.15	0.15	0.00	0.45	0.38	0.03	10.89	12.32	0.66	6.51	7.28	0.30
Maximum			0.31	0.34	0.01	2.02	0.46	0.12	34.09	24.12	1.30	7.10	7.28	1.11
Minimum			0.15	0.03	0.00	0.20	0.13	0.00	10.89	11.09	0.03	5.64	5.85	0.01
Sub-surface (MLD)			0.17	0.07	0.00	0.30	0.30	0.00	24.99	17.48	0.34	5.91	6.04	0.06
Surface (500m)			0.25	0.21	0.00	0.49	0.25	0.02	21.70	18.56	0.47	6.40	6.33	0.17
Inter (500-1700m)			0.18	0.18	0.00	0.40	0.32	0.01	13.46	12.89	0.64	6.78	6.86	0.14
Deep (>1700m			-	-	-	-	-	-	-	-	-	-	-	-

Table A1 continued

Domain (Station)	Lat/Long	Depth (m)	TCu	DCu	Std Dev.	TZn	DZn	Std Dev.	TCd*	DCd	Std Dev.	TPb*	DPb	Std Dev.
WG (TM2)	60˚ 00' S 00˚ 00' E	16	1.69	1.49	0.02	2.91	1.33	0.06	433.35	215.16	1.23	4.89	3.85	0.01
		41	1.59	1.60	0.03	3.59	3.22	0.29	546.35	473.32	5.55	4.92	4.85	0.10
		58	1.67	1.53	0.04	4.41	2.58	0.13	497.95	368.77	5.95	5.05	4.20	0.14
		60	2.11	1.77	0.04	4.50	3.89	0.04	684.08	641.89	5.47	6.08	5.53	0.01
		79	1.90	1.70	0.01	4.26	3.82	0.02	685.51	624.72	2.41	5.16	4.82	0.05
		100	2.00	1.90	0.08	5.88	4.97	0.15	739.67	719.12	18.61	5.90	5.67	0.05
		150	2.21	2.25	0.01	7.20	7.49	0.00	807.37	896.40	0.21	7.19	7.23	0.09
		199	2.57	2.38	0.06	7.62	7.38	0.18	897.46	884.64	25.79	7.04	6.58	0.13
		251	2.44	2.46	0.06	7.51	7.51	0.15	844.17	902.36	22.71	6.17	6.18	0.20
		300	2.61	1.47	1.03	8.16	7.41	0.42	904.00	924.64	6.41	6.29	5.95	0.26
		399	2.76	2.51	0.06	10.58	7.93	0.11	935.37	886.59	7.69	7.86	6.17	0.18
		500	2.76	2.61	0.01	7.88	7.74	0.07	869.65	872.39	2.32	5.78	5.75	0.07
		599	2.86	2.63	0.04	8.00	7.82	0.16	883.42	862.76	12.91	5.50	5.27	0.15
		800	2.93	2.64	0.01	8.03	7.54	0.05	869.04	816.70	5.08	6.07	5.56	0.06
		1001	2.76	2.95	0.25	7.57	8.72	0.75	776.73	834.42	7.32	5.62	6.27	0.07
Maximum			2.93	2.95	1.03	10.58	8.72	0.75	935.37	924.64	25.79	7.86	7.23	0.26
Minimum			1.59	1.47	0.01	2.91	1.33	0.00	433.35	215.16	0.21	4.89	3.85	0.01
Sub-surface (MLD)			1.64	1.55	0.02	3.25	2.28	0.18	489.85	344.24	3.39	4.90	4.35	0.06
Surface (500m)			2.19	1.97	0.12	6.21	5.44	0.13	737.08	700.83	8.69	6.03	5.56	0.11
Inter (500-1700m)			2.83	2.71	0.08	7.87	7.96	0.26	849.71	846.57	6.91	5.74	5.71	0.09
Deep (>1700m			-	-	-	-	-	-	-	-	-	-	-	-

Table A1 continued

Domain (Station)	Lat/Long	Depth (m)	TMn	DMn	Std Dev.	TFe	Dfe	Std Dev.	TCo*	DCo	Std Dev.	TNi	DNi	Std Dev.
WG (DTM1)	65˚ 00' S 00˚ 00' E	25	0.18	0.03	0.00	0.75	0.21	0.02	31.79	9.46	0.12	5.04	4.65	0.01
		39	0.23	0.10	0.00	0.45	0.19	0.06	28.96	13.36	7.87	5.30	4.73	0.51
		51	0.33	0.24	0.01	0.23	0.23	0.05	28.75	24.01	0.95	5.45	4.96	0.20
		70	0.38	0.35	0.00	0.26	0.49	0.19	29.88	26.09	0.38	5.68	5.69	0.16
		100	0.34	0.33	0.01	0.90	0.29	0.01	28.35	24.12	0.70	5.96	5.76	0.25
		151	0.29	0.28	0.00	0.73	0.35	0.01	27.95	23.16	0.22	5.63	5.71	0.03
		200	0.26	0.25	0.00	0.75	0.36	0.06	22.31	20.87	0.16	5.67	5.55	0.02
		400	0.21	0.21	0.01	0.59	0.39	0.08	72.38	17.15	0.01	5.19	5.49	0.09
		498	0.21	0.19	0.00	0.39	0.40	0.08	18.24	16.40	0.03	5.52	5.56	0.03
		749	0.18	0.19	0.02	0.88	0.47	0.04	30.24	18.41	1.72	5.68	6.51	0.61
		1001	0.20	0.14	0.00	1.29	0.43	0.03	20.97	14.84	0.45	6.17	5.71	0.04
		1251	0.16	0.12	0.00	1.41	0.47	0.01	15.06	12.84	0.37	5.41	5.44	0.15
		1501	0.17	0.12	0.01	1.13	0.62	0.06	13.82	13.76	0.18	5.35	5.30	0.13
		2002	0.14	0.13	0.01	0.79	0.56	0.04	16.76	14.77	0.50	4.88	5.67	0.16
		2501	0.18	0.13	0.00	1.22	0.50	0.00	29.33	14.24	0.54	5.59	5.60	0.04
		3001	0.19	0.14	0.00	1.40	0.53	0.05	18.85	13.75	0.41	5.25	5.40	0.07
		3650	0.25	0.14	0.01	2.70	0.51	0.02	36.83	12.66	0.61	5.23	5.03	0.20
Maximum			0.38	0.35		2.70	0.62		72.38	26.09		6.17	6.51	
Minimum			0.14	0.03		0.23	0.19		13.82	9.46		4.88	4.65	
Sub-surface (MLD)			0.25	0.13		0.48	0.21		29.84	15.61		5.26	4.78	
Surface (500m)			0.27	0.22		0.56	0.32		32.07	19.40		5.49	5.35	
Inter (500-1700m)			0.19	0.15		1.02	0.48		19.67	15.25		5.63	5.70	
Deep (>1700m			0.19	0.14		1.53	0.53		25.44	13.85		5.24	5.43	

Table A1 continued

Domain (Station)	Lat/Long	Depth (m)	TCu	DCu	Std Dev.	TZn	DZn	Std Dev.	TCd*	DCd	Std Dev.	TPb*	DPb	Std Dev.
WG (DTM1)	65˚ 00' S 00˚ 00' E	25	1.55	1.29	0.01	2.58	1.02	0.03	480.92	124.69	3.79	5.55	3.80	0.16
		39	1.67	1.45	0.00	3.66	2.21	0.10	700.56	452.78	1.46	6.87	5.00	0.04
		51	1.76	1.48	0.05	4.42	3.68	0.12	702.95	619.91	19.97	7.22	6.08	0.30
		70	1.90	1.74	0.05	5.33	5.22	0.11	761.33	737.80	1.98	7.62	9.05	0.47
		100	2.04	1.89	0.09	5.94	5.78	0.01	758.66	731.83	26.79	10.64	8.95	0.29
		151	1.92	1.95	0.03	4.93	5.08	0.08	674.98	710.07	2.62	7.58	7.15	0.07
		200	2.04	1.87	0.01	5.66	5.05	0.04	683.25	684.35	0.48	7.25	6.25	0.27
		400	2.05	2.00	0.05	5.10	5.20	0.09	616.51	645.97	12.24	5.39	5.89	0.32
		498	2.10	2.03	0.00	5.27	5.33	0.00	647.75	657.97	3.62	7.13	6.67	0.10
		749	2.36	2.50	0.21	5.44	6.05	0.52	657.33	757.20	62.38	8.11	7.43	0.69
		1001	2.57	2.43	0.03	5.82	5.53	0.05	702.53	672.09	4.82	7.65	5.77	0.11
		1251	2.33	2.27	0.07	5.30	5.46	0.10	660.92	648.19	26.14	6.25	5.13	0.19
		1501	2.31	2.28	0.02	5.69	5.35	0.00	637.99	635.51	13.40	5.02	5.53	0.17
		2002	2.18	2.47	0.06	4.88	5.97	0.23	576.54	671.69	11.44	4.44	4.69	0.00
		2501	2.55	2.37	0.01	6.13	6.11	0.05	650.61	675.45	1.86	6.91	5.37	0.03
		3001	2.45	2.35	0.02	5.09	5.63	0.01	635.00	642.59	12.42	7.53	6.29	0.21
		3650	2.52	2.37	0.08	5.25	5.02	0.20	577.32	607.83	20.31	8.55	6.24	0.57
Maximum			2.57	2.50		6.13	6.11		761.33	757.20		10.64	9.05	
Minimum			1.55	1.29		2.58	1.02		480.92	124.69		4.44	3.80	
Sub-surface (MLD)			1.66	1.41		3.55	2.31		628.14	399.13		6.55	4.96	
Surface (500m)			1.89	1.74		4.76	4.29		669.66	596.15		7.25	6.54	
Inter (500-1700m)			2.33	2.30		5.50	5.54		661.31	674.19		6.83	6.10	
Deep (>1700m			2.42	2.39		5.34	5.68		609.87	649.39		6.86	5.65	

Table A1 continued

Domain (Station)	Lat/Long	Depth (m)	TMn	DMn	Std Dev.	TFe	Dfe	Std Dev.	TCo*	DCo	Std Dev.	TNi	DNi	Std Dev.
WG (TM3)	67˚ 58' S 00˚ 01' E	15	0.30	0.26	0.01	0.98	0.11	0.00	45.17	30.05	1.65	6.48	6.02	0.30
		30	0.31	0.26	0.01	0.71	0.10	0.00	39.42	29.23	1.85	6.68	6.00	0.09
		40	0.30	0.28	0.00	0.21	0.10	0.01	67.48	28.20	0.53	6.51	6.31	0.08
		60	0.38	0.27	0.01	6.36	0.34	0.10	38.89	33.13	4.32	6.62	6.21	0.04
		80	0.29	0.26	0.00	0.32	0.10	0.01	33.87	27.79	0.49	6.55	6.23	0.09
		99	0.28	0.28	0.00	0.87	0.13	0.00	47.83	28.12	0.18	6.73	6.23	0.09
		150	0.29	0.30	0.01	0.93	0.24	0.00	33.66	25.65	0.21	6.60	6.57	0.16
		201	0.26	0.26	0.00	0.63	0.24	0.02	27.62	23.35	0.18	6.90	6.58	0.12
		250	0.25	0.24	0.00	0.74	0.28	0.01	23.83	21.73	0.11	6.88	6.61	0.00
		301	0.22	0.22	0.00	0.92	0.27	0.00	65.59	20.80	0.08	6.92	6.79	0.01
		400	0.21	0.20	-	0.41	0.34	-	19.51	19.63	-	6.68	6.88	-
		501	0.20	0.18	0.01	0.58	0.27	0.00	24.05	17.91	0.12	6.75	6.39	0.01
		600	0.19	0.16	0.00	0.68	0.31	0.00	47.48	17.96	0.52	6.69	6.40	0.08
		799	0.17	0.15	0.01	1.19	0.33	0.01	36.71	16.53	0.70	6.84	6.60	0.15
		1000	0.16	0.14	0.00	1.15	0.37	0.01	47.29	15.58	0.67	6.86	7.04	0.33
Maximum			0.38	0.30		6.36	0.37		67.48	33.13		6.92	7.04	
Minimum			0.16	0.14		0.21	0.10		19.51	15.58		6.48	6.00	
Sub-surface (MLD)			0.31	0.27		1.58	0.15		45.44	29.42		6.59	6.17	
Surface (500m)			0.27	0.25		1.14	0.21		38.91	25.47		6.69	6.40	
Inter (500-1700m)			0.18	0.16		0.90	0.32		38.88	17.00		6.78	6.61	
Deep (>1700m			-	-		-	-		-	-		-	-	

Table A1 continued

Domain (Station)	Lat/Long	Depth (m)	TCu	DCu	Std Dev.	TZn	DZn	Std Dev.	TCd*	DCd	Std Dev.	TPb*	DPb	Std Dev.
WG (TM3)	67˚ 58' S 00˚ 01' E	15	2.11	1.83	0.11	5.33	4.56	0.28	744.36	685.82	35.13	6.12	5.82	0.25
		30	2.10	1.81	0.05	5.78	4.61	0.12	766.49	701.32	15.37	6.56	5.78	0.14
		40	2.04	1.90	0.01	5.15	5.19	0.08	770.07	742.68	4.42	7.30	7.05	0.10
		60	2.02	1.86	0.02	4.75	17.12	6.23	727.42	732.23	5.30	6.10	5.93	0.08
		80	1.97	1.85	0.01	4.65	4.69	0.07	714.56	725.38	11.01	6.42	6.29	0.05
		99	2.09	1.89	0.02	4.91	4.88	0.08	730.94	744.93	10.48	5.99	6.17	0.09
		150	2.30	2.12	0.05	6.38	6.43	0.15	810.73	844.73	18.37	6.36	6.37	0.11
		201	2.38	2.19	0.04	6.83	6.77	0.04	830.66	831.88	13.74	6.86	7.12	0.01
		250	2.52	2.35	0.01	6.64	6.59	0.01	835.75	824.07	6.53	6.05	6.19	0.01
		301	2.46	2.34	0.01	6.69	6.79	0.03	788.65	826.52	5.00	6.22	6.56	0.01
		400	2.53	2.45	-	6.88	6.99	-	790.99	827.15	-	5.75	6.16	-
		501	2.62	2.38	0.03	6.74	6.68	0.13	795.23	787.07	14.89	6.78	5.51	0.21
		600	2.69	2.45	0.03	7.06	6.89	0.00	799.71	793.63	9.96	7.11	6.98	0.04
		799	2.82	2.55	0.04	7.54	7.44	0.15	820.58	807.59	18.61	6.47	6.37	0.23
		1000	2.87	2.79	0.21	7.49	7.97	0.72	812.89	809.61	0.33	5.47	5.26	0.06
Maximum			2.87	2.79		7.54	17.12		835.75	844.73		7.30	7.12	
Minimum			1.97	1.81		4.65	4.56		714.56	685.82		5.47	5.26	
Sub-surface (MLD)			2.05	1.86		5.09	6.84		742.31	722.06		6.41	6.17	
Surface (500m)			2.26	2.08		5.89	6.78		775.49	772.82		6.37	6.25	
Inter (500-1700m)			2.75	2.54		7.21	7.25		807.10	799.47		6.46	6.03	
Deep (>1700m			-	-		-	-		-	-		-	-	

B. SU TM4 Control Results

Table B1 - results of all un-acidified TM4 control standards analysed. Values coloured red indicate results greater than 1 S.D. from the mean. Values coloured in red and bolded indicate values greater than 2 S.D. from the mean. Values with a strikethrough are values greater than 3 S.D. from the mean and are deemed outliers.

Un-acidified TM4		**Mn**	**Fe**	**Co**	**Ni**	**Cu**	**Zn**	**Cd**	**Pb**
Analysis ID	*Sample ID*	*nmol/kg*	*nmol/kg*	*pmol/kg*	*nmol/kg*	*nmol/kg*	*nmol/kg*	*pmol/kg*	*pmol/kg*
2015 initial test	TM4_1	0.19	0.12	17.85	5.13	0.52	4.27	560.88	6.45
	TM4_2	0.18	0.10	17.50	5.13	0.51	4.32	560.79	6.25
DTM1	TM4_1	0.19	***0.44***	16.59	4.52	0.51	4.58	533.72	7.16
	TM4_2	0.20	0.13	15.59	4.14	***0.39***	5.24	516.45	7.16
DTM 2	TM4_1	***0.23***	0.27	***20.59***	5.49	0.61	4.79	656.87	8.93
	TM4_2	***0.23***	0.23	18.94	5.45	***0.63***	4.63	640.62	9.20
	TM4_3	0.19	0.19	15.10	4.51	0.56	4.03	569.87	8.39
	TM4_4	***0.23***	0.22	19.06	5.10	0.52	4.07	605.38	9.09
2016 initial test	TM4_1	0.18	0.14	15.53	4.40	0.52	4.76	546.10	7.22
	TM4_2	0.17	0.14	13.43	4.14	0.49	4.40	511.54	5.59
	TM4_3	0.18	0.14	14.10	4.17	0.54	4.59	512.29	6.37
	TM4_4	0.18	0.08	13.81	4.41	0.53	4.72	555.30	5.67
2016 stds analysis	TM4_1	0.18	0.20	14.61	4.67	0.50	5.25	568.56	~~***17.80***~~
	TM4_2	0.16	0.15	13.56	4.87	0.53	4.71	543.02	7.08
	TM4_3	0.15	0.05	12.45	4.01	0.41	4.09	***479.91***	4.73
	TM4_4	0.16	0.06	14.73	4.80	0.50	4.91	587.14	5.78
2016 second stds analysis	TM4_1	0.20	0.09	16.57	4.88	0.51	5.10	613.32	5.76
	TM4_2	0.19	0.08	15.47	4.86	0.50	5.06	597.74	5.80
	TM4_3	0.20	~~***0.60***~~	14.75	4.89	0.54	5.06	590.06	5.94
	TM4_4	0.21	0.10	15.45	4.80	0.47	5.04	595.51	5.55
	TM4_5	0.19	0.06	15.31	4.84	0.48	5.03	597.56	5.68
DTM 3	TM4_1	0.18	0.08	16.60	5.35	0.57	5.74	***690.91***	8.30
	TM4_2	0.17	0.06	12.79	4.39	0.41	4.53	544.53	5.22
	TM4_3	0.17	0.05	15.39	5.04	0.50	5.01	631.13	6.01
	TM4_4	0.18	0.09	15.49	5.12	0.51	5.47	648.34	6.04
	TM4_5	0.16	0.03	14.90	5.19	0.50	5.38	601.46	6.12
	TM4_6	0.17	0.06	14.90	4.75	0.47	5.59	618.81	5.65
	TM4_7	0.17	0.08	13.24	4.67	0.45	5.40	591.04	5.18

Table B2 - results of all acidified TM4 control standards analysed. Values coloured red indicate results greater than 1 S.D. from the mean. Values coloured in red and bolded indicate values greater than 2 S.D. from the mean. Values with a strikethrough are values greater than 3 S.D. from the mean and are deemed outliers.

Acidified		**Mn**	**Fe**	**Co**	**Ni**	**Cu**	**Zn**	**Cd**	**Pb**
Analysis ID	*Sample ID*	*nmol/kg*	*nmol/kg*	*pmol/kg*	*nmol/kg*	*nmol/kg*	*nmol/kg*	*pmol/kg*	*pmol/kg*
test	TM4A_1	0.27	0.33	18.56	5.97	1.62	5.93	644.34	6.89
	TM4A_2	0.27	0.33	18.39	5.89	1.60	5.85	625.54	6.97
	TM4A_3	0.26	0.34	18.13	5.88	1.60	5.91	636.02	6.82
	TM4A_4	0.26	0.32	17.58	5.73	1.55	5.75	627.77	6.57
	TM4A_5	0.26	0.33	19.38	5.84	1.58	5.91	639.75	6.75
	TM4A_6	**~~0.29~~**	**~~0.42~~**	19.23	5.77	1.55	5.81	622.85	6.92
	TM4A_7	0.26	0.33	18.75	5.73	1.55	5.79	615.83	6.77
	TM4A_8	0.26	0.34	16.98	5.83	1.60	5.82	624.43	6.89
	TM4A_9	0.26	0.31	17.44	5.57	1.50	5.74	603.50	6.57
	TM4A_10	0.25	**~~0.37~~**	17.81	5.75	1.54	5.75	610.71	6.68
DTM3 - Winter	TM4A_1	0.26	0.29	20.65	6.10	1.64	5.86	637.46	6.71
	TM4A_2	0.26	0.26	20.49	6.05	1.64	5.63	638.80	6.60
	TM4A_3	0.25	0.27	19.88	5.83	1.64	5.57	629.67	6.52
	TM4A_4	0.26	0.28	20.46	5.96	1.68	5.80	649.51	6.68
	TM4A_5	0.26	0.29	20.81	6.19	1.67	5.85	650.03	6.81
	TM4A_6	0.26	0.27	20.64	6.05	1.66	5.68	645.77	6.60
	TM4A_7	0.26	0.27	19.98	5.87	1.67	5.68	645.45	6.60
	TM4A_8	0.26	0.25	19.70	5.65	1.60	5.66	630.48	6.42
TM1	TM4A_1	0.23	0.28	16.77	5.71	1.57	**~~7.03~~**	603.10	6.89
	TM4A_2	0.25	0.25	16.85	5.62	1.53	5.44	598.77	6.67
	TM4A_3	0.24	0.26	17.68	5.72	1.57	5.53	607.41	6.24
	TM4A_4	0.26	0.27	16.45	5.81	1.56	5.65	621.58	6.40
	TM4A_5	**~~0.21~~**	0.32	22.58	6.21	**~~1.95~~**	**~~6.88~~**	624.92	**5.97**
	TM4A_6	**~~0.21~~**	0.32	21.79	5.96	1.64	5.65	631.72	6.09
DTM2 - Winter	TM4A_1	0.26	0.29	22.66	5.94	1.61	5.78	624.52	6.37
	TM4A_2	0.24	0.29	23.62	5.93	1.65	5.62	616.92	6.27
	TM4A_3	0.26	0.30	23.32	6.34	1.76	5.99	667.36	6.76
	TM4A_4	0.25	0.33	21.23	5.86	1.63	5.57	625.87	6.34
	TM4A_5	0.24	0.30	21.17	5.65	1.58	5.47	608.35	6.07
TM1 - Winter	TM4A_1	0.26	0.28	24.34	6.04	1.67	6.08	663.14	6.92
	TM4A_2	0.25	0.27	23.23	6.06	1.66	5.86	626.56	6.65
	TM4A_3	0.26	0.30	22.80	5.99	1.65	6.06	650.87	6.57
	TM4A_4	0.26	0.31	22.75	6.06	1.71	6.09	653.18	**~~7.83~~**
	TM4A_5	0.27	0.31	23.51	6.09	1.69	6.14	662.44	6.83
	TM4A_6	0.27	0.31	22.48	6.07	1.65	5.94	665.85	6.71
	TM4A_7	0.28	0.34	24.23	**~~6.80~~**	**1.85**	6.35	**~~710.81~~**	**7.33**
	TM4A_8	0.25	0.30	22.23	5.90	1.59	5.68	625.40	6.33

Table B2 cont. - results of all acidified TM4 control standards analysed. Values coloured red indicate results greater than 1 S.D. from the mean. Values coloured in red and bolded indicate values greater than 2 S.D. from the mean. Values with a strikethrough are values greater than 3 S.D. from the mean and are deemed outliers.

Acidified		**Mn**	**Fe**	**Co**	**Ni**	**Cu**	**Zn**	**Cd**	**Pb**
Analysis ID	*Sample ID*	*nmol/kg*	*nmol/kg*	*pmol/kg*	*nmol/kg*	*nmol/kg*	*nmol/kg*	*pmol/kg*	*pmol/kg*
DTM1 Soluble	TM4A_1	0,26	0,25	17,53	6,12	1,65	5,68	651,56	6,49
	TM4A_2	0,26	0,27	18,60	5,91	1,68	5,82	661,11	6,77
	TM4A_3	0,25	0,23	16,74	5,68	1,62	5,52	639,40	6,47
	TM4A_4	0,25	0,25	16,38	5,64	1,65	5,62	633,62	6,71
DTM2 - soluble	TM4A_4	0,25	0,25	16,38	5,64	1,65	5,62	633,62	6,71
	TM4A_5	0,25	0,24	16,22	5,85	1,62	5,46	631,49	6,32
	TM4A_6	0,27	0,29	17,70	6,20	1,69	5,80	652,75	6,65
	TM4A_7	0,25	0,28	15,95	5,77	1,59	5,40	629,99	6,38
DTM3 - soluble	TM4A_2	0,25	0,24	17,40	5,97	1,64	5,68	635,78	6,66
	TM4A_3	0,26	0,23	18,28	5,91	1,67	5,72	644,75	6,66
	TM4A_4	0,26	0,28	17,81	6,10	1,73	5,94	674,22	6,75
	TM4A_5	0,25	0,27	17,00	5,74	1,65	5,74	635,79	6,42
	TM4A_6	0,26	0,29	17,50	6,06	1,69	5,92	652,08	6,49

C. Cleaning Protocols

GO-FLO Bottles:

Modifications to the GO-FLO bottles were as follows:

- The O-rings on the inside of the GO-FLO bottles were replaced with Viton O-rings.
- Stainless steel bands were replaced by heavy duty plastic cable ties.

Cleaning Protocol

- Fill GoFlo bottle with a pre-made mixture of 500ml iso-2-propanol to 10L milli-Q water. Allow 12 hours for iso-2-propanol to leach the organic material from the inside of the GoFlo bottles.
- Rinse GoFlo bottles thoroughly 3 times with milli-Q.
- Fill GoFlo with a 0.3M mixture of 10.2M HCl and milli-Q and allow to stand for 1 day (minimum).
- 24 hours prior to sampling stations a soak station is conducted where GO-FLO bottles are deployed and retrieved filled with seawater. GO-FLO bottles are then stored, containing the seawater, and allowed to condition. The contents are released before deployment at the sampling station.

PFA and LDPE Sampling Bottles:

Pre-cruise cleaning was performed following the stepwise procedure outlined in the GEOTRACES cookbook.

- The bottles may need to be rinsed with methanol or acetone to release oils from manufacturing.
- Soak bottles for one week in an alkaline detergent (e.g. Micro, Decon).
- Rinse 7x with Ultra-High Purity Water (UHPW e.g. Milli-Q)

- Fill bottles with 6M HCl (reagent grade) and submerge in a 2M HCl (reagent grade) bath for one month.
- Rinse 4x with UHPW under clean air.
- Fill bottles with 1 M HCl (Suprapur) for at least one month) for storage in double ziplocked bags.

Falcon Tube Cleaning:

- Place opened Falcon tubes and caps, into a 2M bath of 32% reagent grade (RG) HCl for 3 weeks
- Rinse 3 X with UHPW (Milli-Q).
- Fill 14ml Falcon tube with Suprapur HCl (1M) and cap.
- Place into 0.1M Suprapur (30%) HCl bath – leave for 2 weeks.
- Vials can remain filled with 0.1M Suprarpur (30%) HCl until needed.

Notes:

1) In future the method should follow ship protocol for cleaning of sampling bottles.

2) All sampling beakers, containers, vials, probes and the rinse station should be cleaned according to protocols prior to sample handling.

Suprapur Storage Acid Step:

- Decant 1M HCl contents into chemical waste bin taking care not to make contact between waste bin and bottle
- Rinse bottle 3 times with Milli-Q taking time to rinse the lid and neck of the bottle. Fill roughly half bottle with Milli-Q
- Pipette 4ml of Suprapur HCl into bottle for a final concentration of 0.1M
- Fill remaining volume of bottle with Mill-Q

- Double zip lock bag the bottle (one person drops bottle into the first zip-lock bag held by second person).

Notes:

1) Care must be taken to clean the pipette tip before use.

   I. Rinse 3 times with acid (HCl).

   II. Rinse 3 times with Milli-Q 1.

   III. Rinse 3 times with Milli-Q 2.

Filtration for Total Trace Metal Fraction:

At all stations, all GO-FLO bottle exteriors were rinsed with milli-Q paying particular attention to the taps. The taps were always rinsed last.

Responsibilities: Dirty Hand (DH), Trace Metal Sampler (TMS), Acidifier (AF)

- DH takes double ziplocked 125 ml PFA bottles from black plastic bag, removes the outer ziplock bag and places it in the fumehood. (DH doesn't touch the inner ziplock)
- The acidifier opens the inner ziplock bag and TMS takes the bottle out. (acidifier doesn't touch the bottle)
- TMS empties the storage acid from the PFA bottle into the drain in the GoFlo container.
- TMS proceeds to fill the PFA sample bottle with roughly 25ml for rinsing. A 30 cm tube is inserted into the tap of the GoFlo and sampling is done through this tube. When sampling make sure the lid of the bottle never touches the tube. Repeat this 3 times making sure the lid and neck of the bottle is thoroughly rinsed.
- Once rinsing is complete fill the sample bottle till the neck (125ml) close lid tightly and place in the fumehood.

- Acidifier places the bottle into its inner ziplock bag and seals
- Acidifier then places the ziplock bag into the outer ziplock bag which is held by the DH.
- The DH applies the pre-written label to the outer ziplock bag

Filtration for Dissolved Trace Metals:

The protocol for dissolved trace element sampling is the same as for total trace element sub-sampling except for the following additional apparatus:

- Acropak 0.2 µm filter with particulate shield around the tap. This attaches to the 30 cm tubing from the GO-FLO tap.
- Connecter tubing from the nitrogen line (mounted onto the back wall of the container) to the top of the GO-FLO bottle where it screws in. When the nitrogen line is turned on, this tubing facilitates the pressurizing of the GO-FLO with nitrogen. This pressure increases flow rate of seawater through the filter and ultimately speeds up the sampling process.

Notes:

1) Take care to avoid outside contamination from falling particles by making sure the sample bottle opening is under the filter shield during filtering.
2) Whenever sampling from a new GoFlo bottle, let water run for at least 30 seconds through the Satro Bran filter with nitrogen assistance to flush the seawater from the previous GoFlo bottles through the filter. In addition to this, rinse the inside of the filters shield by holding the filter upright and allowing a small volume of water to collect in it. Swoosh it around a few times and discard. Repeat this 3 times.

D. Pre-Concentration Method

Sample Decant:

- Acid filled, 0.1M, Falcon tube (14ml) is rinsed 10 times with Milli-Q, capped loosely and placed in vial rack to dry.
- Sample decanter prepares to decant 125ml bottle (PFA x 1 Total, LDPE x 2 Dissolved) under laminar flow hood.
- Sample decanter decants approximately 3ml of sample into Falcon tube held by sample receiver.
- Sample receiver caps Falcon tube and thoroughly shakes the contents to "condition" the vile.
- Sample receiver discards contents and falcon tube is filled to 12.5ml with sample.
- Falcon tube is capped tightly by sample receiver who places it in the correct origin location in the sampling vial rack.

TM4 Control Protocol:

- Each batch of samples included several samples with TM4 – large volume available – contents as a control.
- Prepare according to same procedure as Station Sample.

MES Protocol:

- Batch samples included several 0.5ppb multi element standard (MES) spikes.
- The spike was added to seawater from Trace Metal Station 4 (TM4).

Run Procedure:

- Falcon tubes are filled with required samples (see decant procedure).

- Each tube is assigned an origin and destination number on the sampling rack.
- 6 x Sample filled Falcon tubes are opened (If lids are kept make sure it is in numerical order else cross contamination can occur should the samples need to be closed, new clean lids are also an option).
- Change gloves.
- 6 x Destination, empty, Falcon tubes are opened (keep lids in zip-lock bag). It is essential to ensure each vile is dry, else dilution and possibly contamination will occur.

Capping of Pre-Concentrated Samples:

- Put on clean gloves
- Seal falcon tube with lid
- Label falcon tube
- Repeat steps for six falcon tubes

Notes:

It is essential to balance practicality and sample handling as this process can become time consuming (20min per sample). Only six Falcon tubes were opened at any time. This was done to minimise contamination risk and ensure that evaporation of concentrated samples did not concentrate the samples further.

E. Parameters for Method Validation

In any method validation exercise there are certain key parameters that are essential in proving the reliability of the method in question. These parameters are listed and defined below to eliminate any possible confusion as a result of definitions varying depending on the scientific field at hand.

Calibration

Instrument calibration is the essential first step in analytical methods. It is a set of operations that establish the relationship between the output of the ICP-MS setup and the accepted values of the calibration standards. While the calibration standards have known theoretical values, various factors such as the specific analyte being measured, interference effects caused by other components of the sample matrix or random experimental errors require that we calibrate the instrument for the specific analyte and measurement conditions used in the particular analysis. This involves the preparation of a set of standards containing known analyte concentrations, measuring the instrument response for each standard and establishing a relationship between the two. This relationship formula is then applied to measurements of test samples, correcting any inaccuracies or biases present. The standard concentrations should be evenly spaced and cover the range of concentrations encountered during the analysis of test samples.

Limit of Detection

The point at which a measured value is larger than the uncertainty associated with it. It is the lowest concentration of analyte that can be detected but not necessarily quantified. The limit of detection is quantified as three times the standard deviation of the calibration blank.

Accuracy

The extent to which the test results generated by the method and the true value agree. Accuracy in this study is quantified in two ways. Firstly, comparing the trace metal data obtained from this method with an established method. This approach assumes that the uncertainty of the reference method is known. Secondly, accuracy can be assessed by analysing standards with known concentrations e.g. SAFe, GEOTRACES and NASS-5 certified reference material.

Precision

Refers to the scatter of dispersion of a set about its mean value. Repeatability and reproducibility are the two most common measures of precision. Repeatability describes the variability to be expected when a method is performed by a single analyst on the same equipment over a short timescale i.e. when a seawater sample is analysed in duplicate. Reproducibility describes the sort of variability to be expected when samples are analysed by a number of laboratories for comparative purposes. Precision is usually stated in terms of Standard Deviation (SD) or Relative Standard Deviation (RSD).

Stability

System stability is determined by replicate analysis of the same sample at different time and is considered appropriate when the calculated RSD does not exceed a certain percentage of the system precision.

Sensitivity

A measure of the ease with which the instrument responds to changes brought about by a number of factors. It is effectively the gradient of the response curve.